

HDIA **JOURNAL**

The Journal of the Homeland Defense & Security
Information Analysis Center

Volume 5 Issue 4 Winter 2018/2019

PRESERVING WARFIGHTER HEARING

**OPTICAL COHERENCE TOMOGRAPHY LEADS
TO NOVEL AND IMPROVED THERAPIES**



DISTRIBUTION A: APPROVED FOR PUBLIC RELEASE; DISTRIBUTION IS UNLIMITED



Volume 5 • Issue 4 • Winter 2018/2019

Director: **Stuart Stough**

The Journal of the Homeland Defense & Security Information Analysis Center (HDIAC) is published quarterly by the HDIAC staff. HDIAC is a DoD sponsored Information Analysis Center (IAC) with policy oversight provided by the Under Secretary of Defense for Research and Engineering (USD (R&E)), and administratively managed by the Defense Technical Information Center (DTIC). HDIAC is operated by Information International Associates (IIa) in Oak Ridge, Tenn. Reference herein to any specific commercial products, processes or services by trade name, trademark, manufacturer or otherwise, does not necessarily constitute or imply its endorsement, recommendation or favoring by the United States government or HDIAC. The views and opinions of authors expressed herein do not necessarily state or reflect those of the United States government or HDIAC and shall not be used for advertising or product endorsement purposes.

Copyright 2019 by IIa. This Journal was developed by IIa under HDIAC contract FA8075-13-D-0001. The government has unlimited free use of and access to this publication and its contents in both print and electronic versions. Subject to the rights of the government, this document (print and electronic versions) and the contents contained within it are protected by U.S. copyright law and may not be copied, automated, resold or redistributed to multiple users without the written permission of HDIAC. If automation of the technical content for other than personal use, or for multiple simultaneous user access to the Journal, is desired, please contact HDIAC at 865-535-0088 for written approval.

ISSN 2578-0832 (print)

ISSN 2578-0840 (online)

ON THE COVER

Photo illustration created by HDIAC and adapted from U.S. Marines photo by Cpl. Gabino Perez (Available for viewing at <https://www.marines.mil/Photos/igphoto/2002059236/>), U.S. Army photo by Sgt. Justin Geiger (Available for viewing at <http://www.eucom.mil/media-library/Article/35827/us-soldiers-hone-explosive-capabilities-at-saber-strike-17>), and Adobe Stock.



Alternative Energy



Cultural Studies



Biometrics



Homeland Defense & Security



CBRN Defense



Medical



Critical Infrastructure Protection



Weapons of Mass Destruction

Table of Contents



03 Message from the Director



04 Thin-Film Perovskite Solar Cells for Powering Submerged Unmanned Underwater Vehicles

Colin Bailie & John Love



10 3D-Printed Lattice Batteries: Ultralight Energy Storage for Powering the Warfighter

Rahul Panat, Jonghyun Park, M. Sadeq Saleh, & Jie Li



16 Cognitive Protection Systems for the Internet of Things

Josh Siegel



21 Advancing Space Situational Awareness for National Security

Chad Pyle



26 Modeling and Simulation for Genomic Security

Corey Hudson & Glory Aviña



31 Electronic Stickers for Wireless Physiological Monitoring in a Tactical Environment

Carmel Majidi



35 Reviving Dormant Nerves After Spinal Cord Injury

Bo Chen & Zhigang He



37 Preserving Warfighter Hearing: Optical Coherence Tomography Leads to Novel and Improved Therapies

Patricia M. Quiñones, Brian E. Applegate, & John S. Oghalai

Contact

HDIAC Headquarters

104 Union Valley Road
Oak Ridge, TN 37830 • 865-535-0088

Fatena Casey, Technical Office Manager
Joel Hewett, Subject Matter Expert
David McCarville, Social & Multi-Media Editor
Amanda Andrews, Editor
Tim Gould, Graphic Designer

Emese Horvath

Contracting Officer Representative

DoD Information Analysis Centers

8745 John J. Kingman Road
Fort Belvoir, VA 22060
571-448-9753
emese.i.horvath.civ@mail.mil

Follow us on Social Media



DoD_HDIAC



HDIAC Outreach



DoDHDIAAC



HDIAC



dod_hdac



Message from the Director



Stuart Stough
HDIAC Director

The Homeland Defense & Security Information Analysis Center (HDIAC) collaborates with recognized experts to address the scientific and technical (S&T) needs of the Homeland Defense and Security (HDS) community. Through our Technical Inquiry Service, HDIAC provides up to four free hours of research within our eight focus areas: Alternative Energy, Biometrics, CBRN Defense, Critical Infrastructure Protection, Cultural Studies, Homeland Defense and Security, Medical, and Weapons of Mass Destruction. This technical analysis supports research and development (R&D) efforts across industry, academia, and the government.

Over the past several months, HDIAC completed notable Technical Inquiries for the U.S. Department of Homeland Security, the National Institute of Standards and Technology, Consolidated Nuclear Security (Y-12 National Security Complex), United States Special Operations Command, and others. These research efforts addressed novel S&T and R&D advancements in the fields of Biometrics,

Cultural Studies, and Weapons of Mass Destruction.

Through these Technical Inquiries, HDIAC identified several emerging facial recognition technologies capable of functioning in various modalities, ranges, spectrums, and environments. HDIAC also provided information regarding research efforts using social science modelling to enhance situational awareness in unstable regions where nefarious activities, such as smuggling and terrorism, occur. Additionally, HDIAC explored Department of Defense (DoD) requirements regarding novel protective coatings for corrosion prevention.

Members of the HDIAC Subject Matter Expert (SME) Network contribute their expertise to Technical Inquiries, as well as HDIAC Journal articles, Tech Talks, conference presentations, and webinars. SMEs support the HDIAC mission by sharing R&D results and their skills and capabilities, which are used to meet DoD gaps and requirements. In turn, SMEs learn about emerging trends within the HDS Community of Practice through HDIAC products and services, and HDIAC provides analytical support to strengthen their research needs.

For example, SMEs from the Intelligence Advanced Research Projects Activity and U.S. Army Research Laboratory recently provided an in-depth analysis of their novel research and technologies in the form of webinars hosted by HDIAC. These webinars centered on innovative developments in the use of active infrared spectroscopy for safe standoff detection of chemical residues and novel technology to perform biometric face recognition at night-time, respectively.

Recent HDIAC research trends include chemical detection at a distance, such as opioid detection for use by law enforce-

ment and in border protection, and biometric identification, including post-mortem and through-windshield iris recognition.

If your agency's R&D requirements align with at least one of our eight focus areas, we invite you to collaborate with HDIAC. Joining the HDIAC SME Network enables your participation in HDIAC services, including authorship in the HDIAC Journal and contributions to Technical Inquiries. You may also submit a Technical Inquiry to acquire preliminary information that may support your research needs.

Specifically, in the past quarter HDIAC replied to a Technical Inquiry from U.S. Air Force Headquarters regarding the concentration of an agent used for chemical/biological decontamination. According to the customer, HDIAC's recommendation could result in cost savings, while ensuring the safety of both personnel and equipment.

If your information request requires more than four hours of research, HDIAC offers additional technical services, including a Core Analysis Task (CAT). The HDIAC CAT is a pre-awarded, pre-competed contract vehicle that allows work to begin in as little as six weeks after a statement of work is approved. The HDIAC CAT may range from 40 hours to 1 year of work, up to \$500,000. HDIAC supports projects up to TS/SCI level clearance.

If you would like to submit a Technical Inquiry or require additional information about the HDIAC CAT, please visit www.hdiac.org.

THIN-FILM PEROVSKITE SOLAR CELLS FOR POWERING SUBMERGED UNMANNED UNDERWATER VEHICLES

**Colin D. Baillie
& John A. Love**

Unmanned underwater vehicles (UUVs) have been used in marine exploration for several decades, prompting the development of improved control, sensing, and automation systems [1]. These advances, in turn, have opened up the possibility of much wider uses for UUVs, including specialized military operations, such as subsurface sea mine detection and disposal. The breadth of potential applications for these vehicles is likely to grow as the technology continues to advance. However, these increasingly challenging tasks will also require improvements in the power systems used to drive a UUV and its onboard equipment [2].

An ideal UUV would be capable of operating independently on long-range and long-duration missions without recourse to an onshore base facility or support craft. Such a UUV would display low-detectability visible and radar signatures, and be powered by air-independent propulsion to avoid generating detectable acoustic noise when underway.

Battery banks are effective sources of power for such propulsion, but without a power source capable of independently recharging, mission duration and distance are limited. Onboard diesel generators require too much space and weight, and the air intake and exhaust ports not only make a UUV vulnerable to visual detection, but also produce acoustic vibration during operation.

The installation of photovoltaic solar panels on top of a UUV could provide a method for air-independent recharging of battery banks. Because solar panels are inherently solid-state systems with no moving parts, they can generate zero acoustic noise while operating. Although solar panels have been demonstrated as a power system for UUVs previously (in conjunction with lithium batteries) [3, 4], these panels must be surfaced and fully above the water line to effectively charge the batteries. An ideal UUV-solar array design could power a UUV without the need to breach the water surface, thus maintaining minimal visual detectability.

Metal-halide perovskite photovoltaic solar cells provide differentially improved performance at converting water-penetrating visi-

ble light into usable electric power. Covering the top of a UUV with perovskite solar arrays could (a) power a UUV almost indefinitely; (b) minimize space and weight requirements; (c) maximize mission time to recharge time; and (d) avoid acoustic and visual detectability by providing power with no moving parts.

Underwater, Land, and Space

Most solar technologies have been designed and optimized to work either on land or in outer space. In space, solar cells are exposed to high-energy radiation, and some materials have better radiation hardness than others. Solar radiation in outer space strikes solar panels at a constant spectrum and intensity. Within the atmosphere, solar cells are exposed to a wide variety of regional climates and variable weather.

When exposed to the sun on land, solar cells generally function between 20 and 100 percent of standard AM1.5G solar intensity (“full sunlight” in Figure 1), and the sun radiates at a fairly consistent spectrum (except on overcast days). As a result, current solar cells are optimized to work in a variety of climates and absorb full-spectrum sunlight.



Underwater design considerations are far different. As Figure 1 illustrates, water is a strong filter of both ultraviolet and infrared light. At just 1 m below the surface, only visible light remains; at 10 m underwater, red light is filtered out as well; and at a depth of 100 m, green light is also filtered out (absorption of water is derived from Pegau, Gray, & Zaneveld [5]). A light-emitting diode (LED) shining at 1,000 lux—the high intensity commonly used for product displays in retail stores—is also shown for reference in Figure 1.

Underwater solar cells should be optimized for absorbing and converting visible light into electrical energy, and they should be optimized to function at a different light intensity range than terrestrial- or spaced-based arrays.

The energy conversion performance of land-based solar cells deteriorates rapidly as solar intensity dips below 20 percent of full sunlight. The solar intensity between 1 m and 100 m underwater is just 40 percent to 3 percent of what it is at the surface, presenting a far different design criterion for underwater collection.

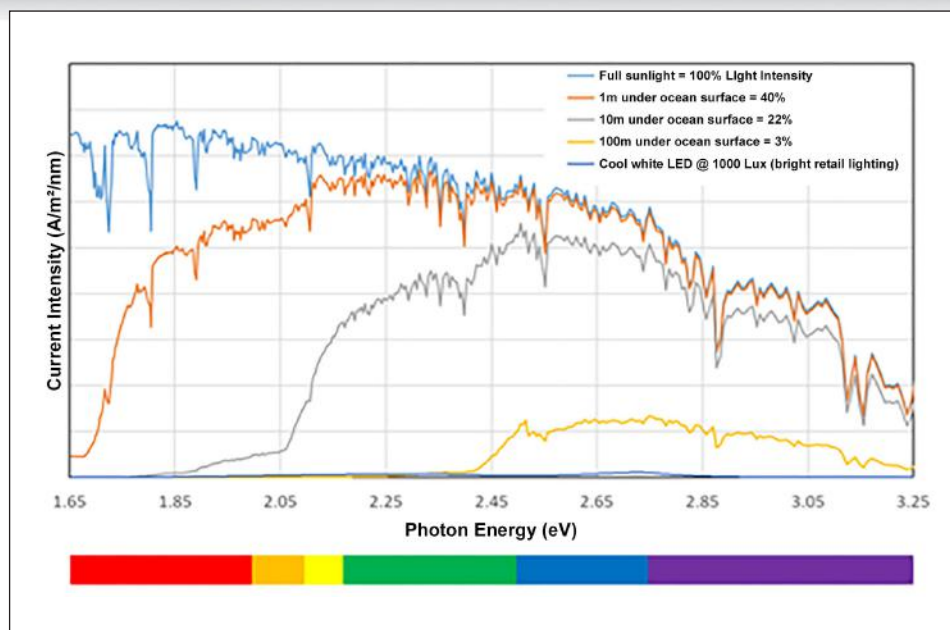


Figure 1. Progression of the underwater spectrum. Below the 1 m depth band, only visible light penetrates.

The oceans also present a different environmental profile for solar panel operation. Ocean temperatures vary between room temperature (~77 degrees Fahrenheit) and freezing, depending on depth and location. This is a fairly narrow operating range. So-

lar panels perform better in cool temperatures—one benefit of operating in the cool marine environment. As a result, the main environmental consideration for underwater operation is the corrosiveness of saltwater. This requires a specific packaging design.

Therefore, an underwater solar cell should be optimized for (a) visible light, (b) lower light intensities than on land, and (c) resistance to saltwater corrosion.

Solar Power Conversion Efficiency

Solar cells operate with two essential components: a light-absorbing material, and two electrical conductors (wires) to transfer the electricity out of the solar cell. A solar cell is defined by its power conversion efficiency (PCE), which can be described as the power supplied by the device (the current and voltage at the maximum power point, J_{MPP} , V_{MPP} , respectively) divided by the total power available in the incident light.

Another way to define the PCE is as a combination of the open circuit voltage (V_{OC}), the short circuit current (J_{SC}), and the fill factor (FF), which is simply a measure of the squareness of the JV curve, or the extent to which the photocurrent depends on the applied voltage. The secondary definition of PCE can be useful, as it demonstrates the need to increase the open circuit voltage and

fill factor in order to boost conversion efficiency and, thus, electrical power output.

$$PCE = \frac{P_{output,max}}{P_{incident}} = \frac{J_{MPP} \cdot V_{MPP}}{P_{incident}} = \frac{J_{SC} \cdot V_{OC} \cdot FF}{P_{incident}}$$

The JSC is directly related to the number of absorbed photons and the quantum efficiency with which they are converted to electricity. It is bounded by the bandgap, or absorption range, of the light-absorbing material. A larger bandgap results in a narrower absorption range. The V_{OC} is also related to the bandgap of the absorbing material, leading to a trade-off between broad absorption and high voltage. A larger bandgap leads to a higher V_{OC} . For land-optimized light absorbers, which take advantage of the wide solar spectrum, the narrow spectrum of visible light underwater limits their utility. Higher bandgap materials which absorb *only* the visible spectrum, but give higher V_{OC} , should be used underwater.

A separate problem is the lower solar intensity available underwater and the resultant lower FF . Wafer silicon-based light absorbers are often hampered by material properties and defects that become a problem at

low light intensity. These problems manifest as a reduction in both V_{OC} and FF through a process called *leakage current* or *shunt conductance*. Leakage current can be conceptualized as water spilling over the sides of a hydroelectric dam: when the turbines are running at full capacity, the leaking water is an inconsequential loss; but, if the turbines were to suddenly operate at 1 percent capacity, there would be as much water leaking out as flowing through the turbines, thus reducing their efficiency. Thin-film solar cells have material and design properties that enable higher performance in low-light environments [6, 7].

To optimize the underwater solar cell for visible light, a larger bandgap absorbing material should be used to maximize V_{OC} . To optimize for low light intensity, a thin-film solar cell should be used to minimize leakage current.

Metal-halide Perovskite Solar Cells

Metal-halide perovskite technology has been developing rapidly in university labs for the last several years, and represents a promising approach for the efficient conversion of visible light into electrical power [8, 9]. These materials adopt the perovskite crystal structure and follow the chemical formula ABX_3 , where A is a cation or mixture of cations—most often Cs^+ , formamidinium, or methyl ammonium; B is Pb^{2+} ; and X represents a halide or a mixture of halides—typically Br or I . The absorption edge of these materials can fall between 1.55 and 2.25 eV (800–550 nanometers [nm]), and can be tuned via composition, specifically by varying the Br - and I - content. The perovskite crystal structure is shown in Figure 2.

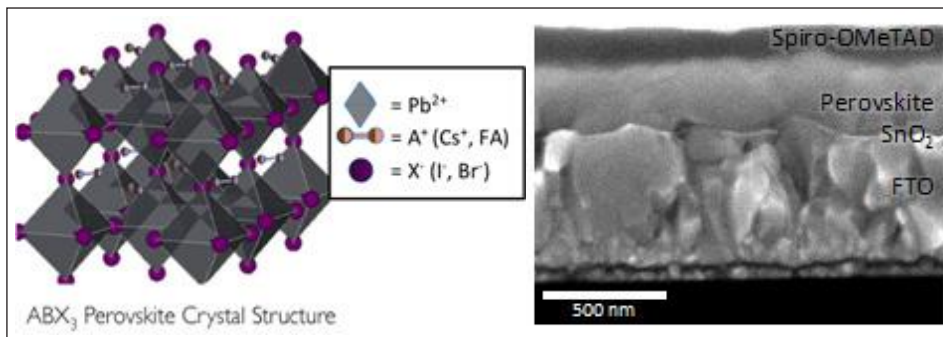


Figure 2. (Left) Crystal structure of a lead halide perovskite. (Right) SEM micrograph showing thin film device architecture.

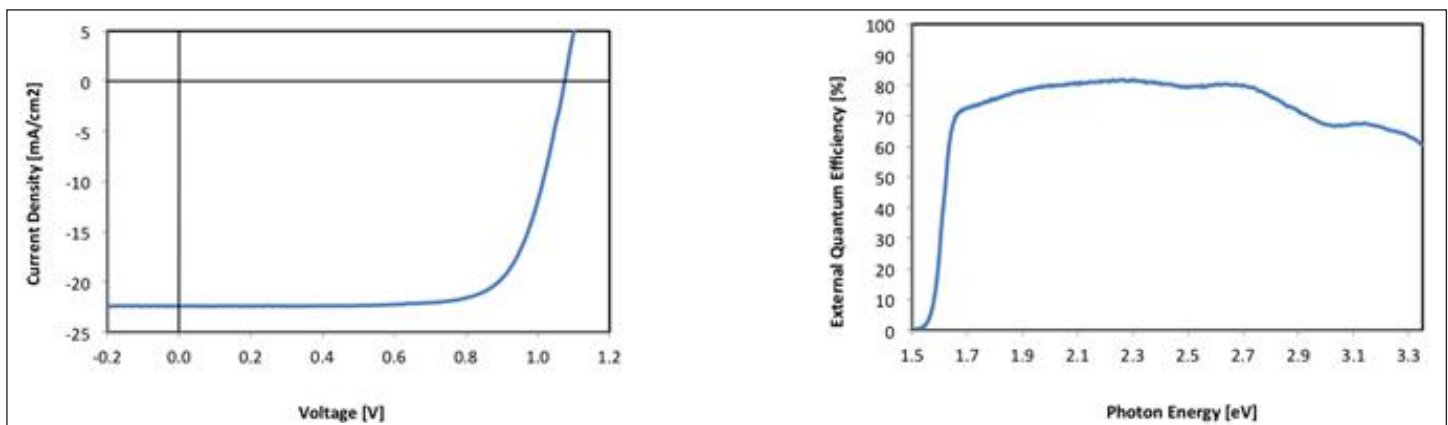


Figure 3. (Left) Current voltage characteristics of a lead halide solar cell. (Right) External quantum efficiency as a function of illumination wavelength.

A perovskite solar cell is a thin film structure, with the light-absorbing perovskite material measuring around 500 nm thick. The entire structure, with electrical conductors included, is about 1 micron wide—about 1/100th the width of a human hair. Researchers are developing perovskite solar cells for land-based solar applications either as a stand-alone material or paired with commercialized technologies such as silicon to boost their power output.

These laboratory solar cells have lived up to performance expectations, reaching parity with other thin film technologies, both (a) as a standalone material, and (b) in its function as a combination of perovskite and silicon [10, 11].

Tandem PV has developed an advanced perovskite solar cell and tested it in conditions representative of modern indoor lighting, using both LED and fluorescent lights. The spectrum of indoor lighting is not dissimilar to the spectrum underwater, and the intensity of lighting indoors is also similar to the light level found hundreds of meters underwater (see Figure 1).

In tests of indoor lighting conditions, the perovskite solar cell has demonstrated a conversion efficiency of 25 to 30 percent when placed underneath a white LED at intensities relevant to underwater operation (see Figure 4). This technology has a theoretical efficiency limit of nearly 50 percent under a visible spectrum.

An important example of the difference between silicon and perovskite solar cells can be seen in Table 1. Silicon converts full sunlight into electricity at about the same efficiency it does visible light, but its overall power production range falls sharply once only visible light is available. Perovskite solar cells are far better at converting visible light into usable energy, producing nearly the same power 1 m underwater as on land. The power generation differences between the two technologies only increase as the water depth increases, and light intensity decreases.

Perovskites as Power Sources for UUVs

On a UUV, the top surface of the submersible can be oriented to constantly face the sun. Typically, around six hours of sunlight are available every day for peak solar power

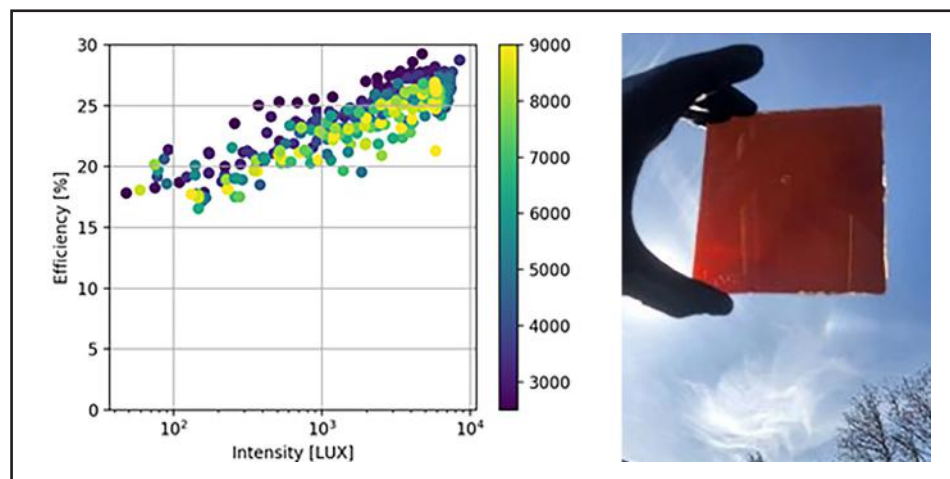


Figure 4. (Left) Efficiency of Tandem PV's perovskite solar technology as a function of light intensity and color temperature of the illumination source (indicated by the color bar, in degrees Kelvin). For reference, the light intensity at a depth of 100 m on the lux scale would be around 10,000 lux. (Right) Photo of a Tandem PV perovskite cell.

Distance under ocean surface	Jsc mA/cm ²	Voc V	FF	Power per m ² (W)
Si – Full sunlight (AM1.5G)	40	.60	.8	192
Si – 1 m underwater	20	.57	.8	91.2
Pero – Full sunlight (AM1.5G)	22	1.10	.72	194
Pero – 1 m underwater	19	1.10	.8	167

Table 1. Expected solar cell parameters for generic silicon and lead halide perovskite devices in direct sunlight and calculated for 1 m under the surface of the ocean.

Distance under ocean surface	Perovskite panel, 1m ²	Perovskite array, 10m ²	Perovskite array, 100m ²
1m	143 W	1,430 W	14,300 W
10m	69 W	690 W	6,900 W
100m	8.6 W	86 W	860 W
1,000m	1 W	10 W	100 W

Table 2. Expected peak power output of perovskite solar arrays depending on coverage area and water depth. Calculated based off Tandem PV solar cell results under simulated light.

production. Depending on the power requirements of the submersible, daylight hours can be used for recharging, while night hours are used for missions. If power requirements are easily met, missions can be run during daylight hours as well, with the solar panels generating power while underway.

The expected peak power output of a perovskite solar array on top of a UUV as a function of coverage area and water depth is presented in Table 2. As long as the sun

is shining, an appreciable amount of power is likely to be generated by the solar panels even if submerged to a depth of 100 m (see Table 2). Further determination of operation duty cycle (mission time vs. recharge time) is pending an engineering investigation of power needs, surface area available, and water depth of missions and recharging depth.

Unlike other electricity generation sources such as diesel and fuel cells, no fuel is stored or consumed by solar panels, enabling indef-

inate UUV missions without the need to return for refueling. Removing the need to carry fuel on board creates space and weight savings that can be used for other purposes such as additional sensing and communication equipment.

Conclusion

Metal-halide perovskite solar cells are uniquely well-suited to convert light into electrical power in a marine environment. Continued improvements in manufacturing protocols and device design will push the power density of this technology even higher. While there is limited publicly available information on UUVs and power requirements, one example is the solar-powered auton-

ous underwater vehicle (SAUV) from Falmouth Scientific [12]; when outfitted with 1 m² of silicon-based solar panels, this small craft can operate indefinitely, but it requires resurfacing and recharging during daylight hours.

Perovskite solar panels, on the other hand, may allow such a craft to operate continuously without refueling, recharging, or surfacing. Solar technologies have additional advantages over traditional fuel sources as they require no moving parts and are air independent, to avoid detectable acoustic noise.

Further development of perovskite solar cells for underwater applications should

involve field testing of perovskite cells underwater at various depths; engineering of packaging for the solar cells compatible with long-term ocean use; a study of the power requirements for UUVs and the anticipated energy generated by the solar panels during missions; and design of the perovskite solar array to conform to UUV shape, size, and weight requirements.

Acknowledgements

This work was partially funded by a small business innovation research grant from the National Science Foundation, and performed in collaboration with the Joint Center for Artificial Photosynthesis at the Lawrence Berkeley National Laboratory.

References

- Gafurov, S. A., & Klochkov, E. V. (2015). Autonomous unmanned underwater vehicles development tendencies. *Procedia Engineering*, 106, 141–148. doi:10.1016/j.proeng.2015.06.017
- Wang, X., Shang, J., Luo, Z., Tang L., Zhang, X., & Li, J. (2012). Reviews of power systems and environmental energy conversion for unmanned underwater vehicles. *Renewable and Sustainable Energy Reviews*, 16(4), 1958–1970. doi:10.1016/j.rser.2011.12.016
- Jalbert, J., Baker, J., Duchesney, J., Pietyka, P., Dalton, W., Blidberg, D. R., . . . Holappa, K. (2003). A solar-powered autonomous underwater vehicle. *Oceans 2003. Celebrating the Past ... Teaming Toward the Future (IEEE Cat. No. 03CH37492)*. doi:10.1109/OCEANS.2003.178503
- Crimmins, D. M., Patty, C. T., Beliard, M. A., Baker, J., Jalbert, J. C., Komerska, R. J., . . . Blidberg, D. R. (2006, October). Long-endurance test results of the solar-powered AUV system. *Oceans 2006*. doi:10.1109/OCEANS.2006.306997
- Pegau, W. S., Gray, D., & Zaneveld, J. R. V. (1997). Absorption and attenuation of visible and near-infrared light in water: Dependence on temperature and salinity. *Applied Optics*, 36(24), 6035–6046. doi:10.1364/AO.36.006035
- Kasemann, M., Rühle, K., & Reindl, L. M. (2013, September). Photovoltaic energy harvesting under low lighting conditions. Paper presented at the AMA Conferences 2013, Nürnberg, DE. doi:10.5162/sensor2013/C8.3
- Rasheduzzaman, M., Balakrishna Pillai, P., Mendoza, A. N. C., & De Souza, M. M. (2016). A study of the performance of solar cells for indoor autonomous wireless sensors. *2016 10th International Symposium on Communication Systems, Networks and Digital Signal Processing (CSNDSP)*. doi:10.1109/CSNDSP.2016.7574001
- Smardzewski, R. (2015, April). Perovskite solar cells. *Journal of the Homeland Defense & Security Information Analysis Center*, 2(1), 3–6. Retrieved from https://www.hdiac.org/wp-content/uploads/2018/04/HDIAC-Journal_Volume-2-Issue-1.pdf
- Correa-Baena, J.-P., Abate, A., Saliba, M., Tress, W., Jacobsson, T. J., Grätzel, M., & Hagfeldt, A. (2017). The rapid evolution of highly efficient perovskite solar cells. *Energy & Environmental Science*, 10(3), 710–727. doi:10.1039/C6EE03397K
- Green, M. A., Hishikawa, Y., Dunlop, E. D., Levi, D. H., Hohl-Ebinger, J., & Ho-Baillie, A. W. Y. (2018, June). Solar cell efficiency tables (version 52). *Progress in Photovoltaics: Research and Applications*, 26, 427–436. doi:10.1002/ppa.3040
- Osborne, M. (2018, June 25). Oxford PV takes record perovskite tandem solar cell to 27.3% conversion efficiency. PV-Tech. Retrieved from <https://www.pv-tech.org/news/oxford-pv-takes-record-perovskite-tandem-solar-cell-to-27.3-conversion-efficiency>
- Falmouth Scientific, Inc. (2009, August). FSI SAUV II Specifications: Solar powered autonomous underwater vehicle, long-endurance AUV. Retrieved from <http://www.falmouth.com/images/SAUVRev1.pdf>



Colin Bailie, Ph.D.
CEO, Tandem PV

Colin Bailie holds a Ph.D. in Materials Science and Engineering from Stanford University and a B.S. in Mechanical Engineering from Texas A&M University. During his time at Stanford, he performed seminal research on a new class of solar panel technology – perovskite-based tandems, which have the ability to substantially improve the power output of current solar panels being manufactured. He since started the company Tandem PV with his co-founder Chris Eberspacher to turn this academic breakthrough into commercial reality. Tandem PV was born out of Cyclotron Road, an entrepreneurial fellowship program based at Lawrence Berkeley National Laboratory.



John Love, Ph.D.
Materials Scientist, Tandem PV

John Love holds a Ph.D. in Materials Science and Engineering from University of California, Santa Barbara and a B.S. in Chemistry from Trinity College. As part of his Ph.D. research and as a postdoc, John focused on expertise in fabrication and characterization techniques for solution processed thin film photovoltaic devices based on organic semiconductors and lead halide perovskites. Since joining Tandem PV, he has focused on device optimization with an aim toward low-light applications.

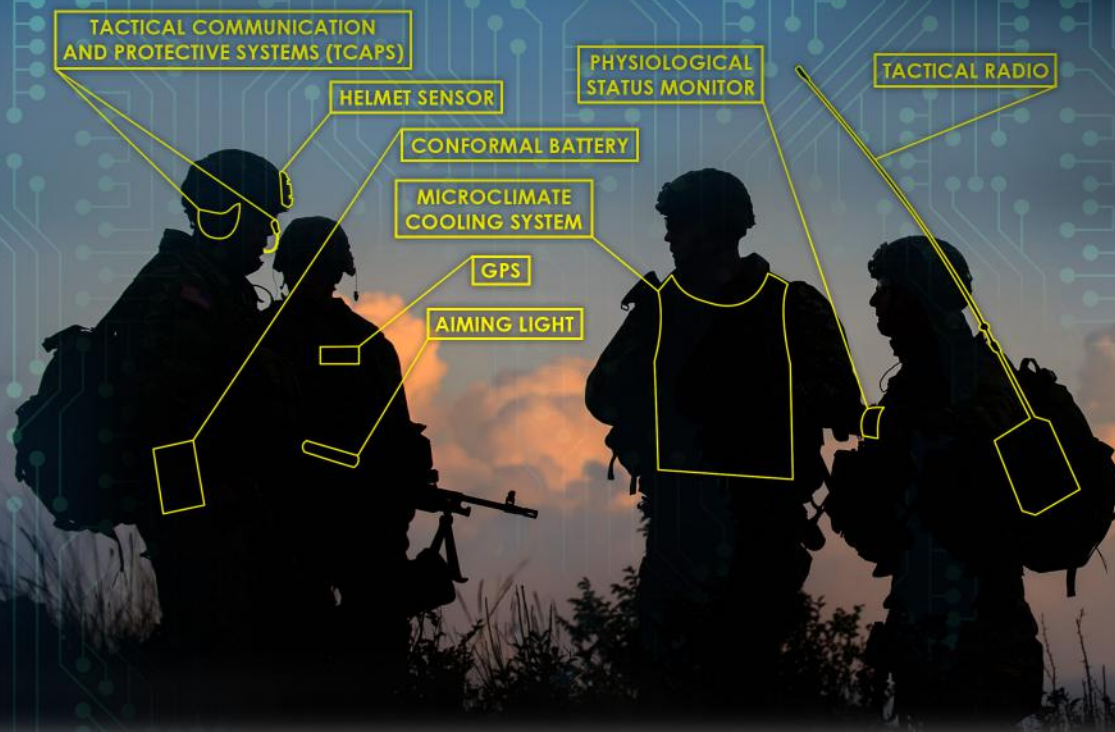
CORE ANALYSIS TASK

Visit hdiac.org or contact info@hdiac.org for more information

- Pre-competited, pre-awarded, contract vehicle
- Cap of \$500,000
- Work can begin approx. 6 weeks after approval
- Must be completed in less than 1 year

3D-PRINTED LATTICE BATTERIES

ULTRALIGHT ENERGY STORAGE FOR POWERING THE WARFIGHTER



**Rahul Panat, Jonghyun Park,
M. Sadeq Saleh, & Jie Li**

Lightweight batteries are highly consequential to a wide range of Department of Defense (DoD) applications, including the use of unmanned aerial systems (UAS), wearable devices, and light combat vehicles. Additionally, the use of increasingly sophisticated equipment has caused DoD power requirements on the battlefield to rise substantially in re-

cent years (see Figure 1). For example, a typical Army platoon in Afghanistan in 2001 required just 2.07 kilowatts per hour to power their devices. That requirement now stands at 31.35 kilowatts per hour [1–3]. Technologies that enable the production of higher-capacity batteries at the same weight (or lower) will bolster warfighter mobility and readiness.

Although several high-energy materials have been discovered in recent years, the batteries used today in everyday applications are

made of materials mastered several decades ago [4]. This is due to the fact that most novel battery materials suffer from serious reliability issues: namely, the large volume change that occurs during battery charge/discharge cycles [5].

Additional efforts have concentrated on improving the electrolytes, the electrolyte-electrode interface [6], and advancing the technologies behind Li-metal batteries and Li-air batteries [7]. However, none of these

improvements are currently available for practical application.

New Electrode Structures for Next-Generation Batteries

One of the most promising routes for increasing battery capacity is the geometric optimization of internal electrode structures. In conventional modern battery technology, electrode particles are mixed with binders and pressed into laminated structures. Such simple electrodes typically leave about 30–50 percent of the volume unutilized due to limitations in the diffusive process.

A 3D electrode, on the other hand, can permit the facile transport of ions via short diffusion path and enhanced interfacial area. Furthermore, creating a controlled porosity inside the 3D electrodes allows the electrolyte to deeply penetrate the electrode volume, leading to a very high volume utilization. This, in turn, is expected to eliminate unutilized electrode volume and reduce battery weight. To date, the major hurdle in achieving this new concept has been the fact that current 3D printing techniques are mostly limited to extrusion-based methods, which only allow interdigitated geometries [8], sometimes referred to as 2.5D structures (multiple stacked 2D layers). Note that the interdigitated geometries cannot endure load effectively and are not useful as structural materials. Therefore, with conventional 3D extrusion-based printing technology, it is impossible to realize a truly 3D structure with controlled porosity throughout the entire electrode volume.

In this article, we introduce a new concept in 3D printing technology that allows the production of battery electrodes that are lightweight, high-capacity, and display superior mechanical properties. The electrodes have a 3D lattice architecture and a controlled hierarchical porosity distribution over their entire volume. The new printing method leads to a near-full utilization of the electrode material. The technology will lead to a 50 percent (or greater) increase in specific capacity for batteries, effecting a proportional decrease in their weight. In addition, the electrodes can support a significant amount of load while storing the electrochemical energy. This addresses another attribute of batteries with potential implications for military applications: our proposed battery can be integrated into/with structural components, such as UAS wings. These superior properties may be achieved by leveraging the expertise from

two complementary areas of advanced manufacturing research and development (Carnegie Mellon University) and battery design and analysis (Missouri University of Science and Technology).

3D Electrode Fabrication via Novel 3D Printing Technology

The 3D electrodes were fabricated using an aerosol jet-based (AJ) 3D printing method, which allows for the deposition of nanoparticles dispersed in a solvent (i.e., the nanoparticle ink) onto a substrate by creating a mist of particles guided by a carrier gas. The AJ printing system includes two atomizers (ultrasonic and pneumatic), a programmable XY motion stage, and a deposition head. Figure 2(A) depicts the printing process. The platen on which the electrode was built was heated to 110 degrees Celsius, which helped dry the mass of nanoparticles (diameter of about 20 μm in the present case) by removing the solvents. The next set of droplets was then dispensed at an offset, as shown in Figure 2(A).

In order for these to adhere to the previously formed pillar, we rely on the fact that the surface forces of the droplets scale as r^2 , while the inertia forces scale as r^3 , where r is the radius of the droplet. This allows for strong adhesion forces for the droplet as compared to its inertia forces (i.e., weight) at length scales of 100 μm or less. As a result of this scaling, the printed droplet adhered to the pil-

lar rather than falling off of it. The platen heat then removed the solvent, so that the pillar is ready to receive the next droplet containing silver nanoparticles.

This process was continued until a full lattice was formed. Figure 2(B) presents a schematic of the lithiation for a $5 \times 5 \times 5$ lattice and a dense block of equivalent overall size. The charge carrying capacity of the lattice electrodes is significantly higher than that for the block electrode for the same amount of charging time. Figure 2(C) presents representative scanning electron microscope (SEM) images of printed 3D electrodes showing complex lattice geometries and porosities at different length scales. The printing produced controlled porosity at an approximately 100–300 μm length scale, while a smaller porosity at a 1 μm length scale was obtained from sintering of the nanoparticles [9]. The percentage of smaller porosity can be controlled from 1 percent to 20 percent by varying the sintering temperature [10]. The hierarchical porous electrode structures shown in Figure 2(C) are, to the best of our knowledge, the first such reported.

3D Electrode Battery Performance

The 3D electrode demonstrates an unprecedented improvement in battery performance, including a 400 percent increase in specific capacity and a 100 percent increase in areal capacity. It also demonstrates a high elec-

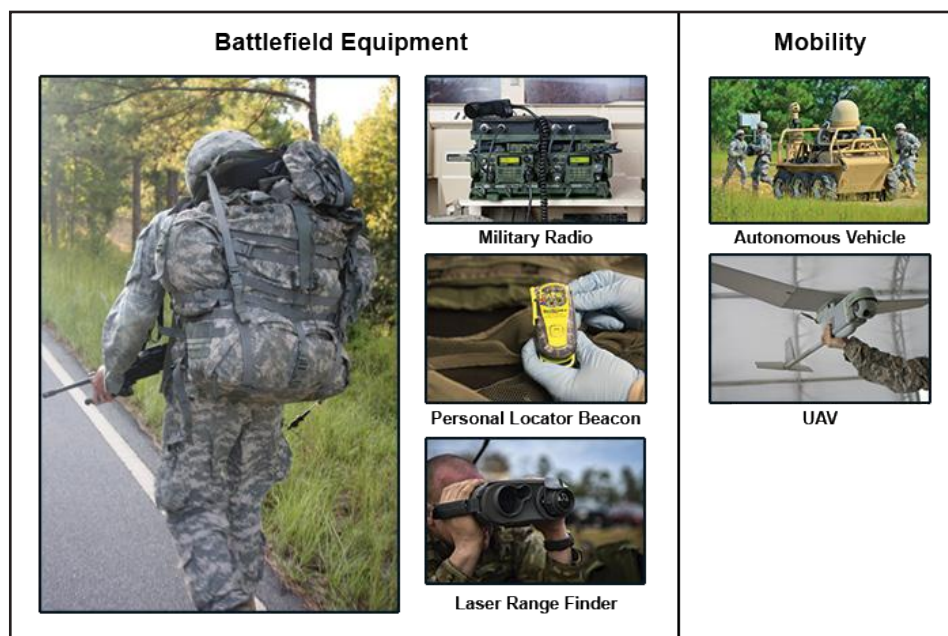


Figure 1. Examples of defense applications [3] where lightweight energy storage systems can greatly increase competitive advantage of American forces over adversaries. Images from [13-17].

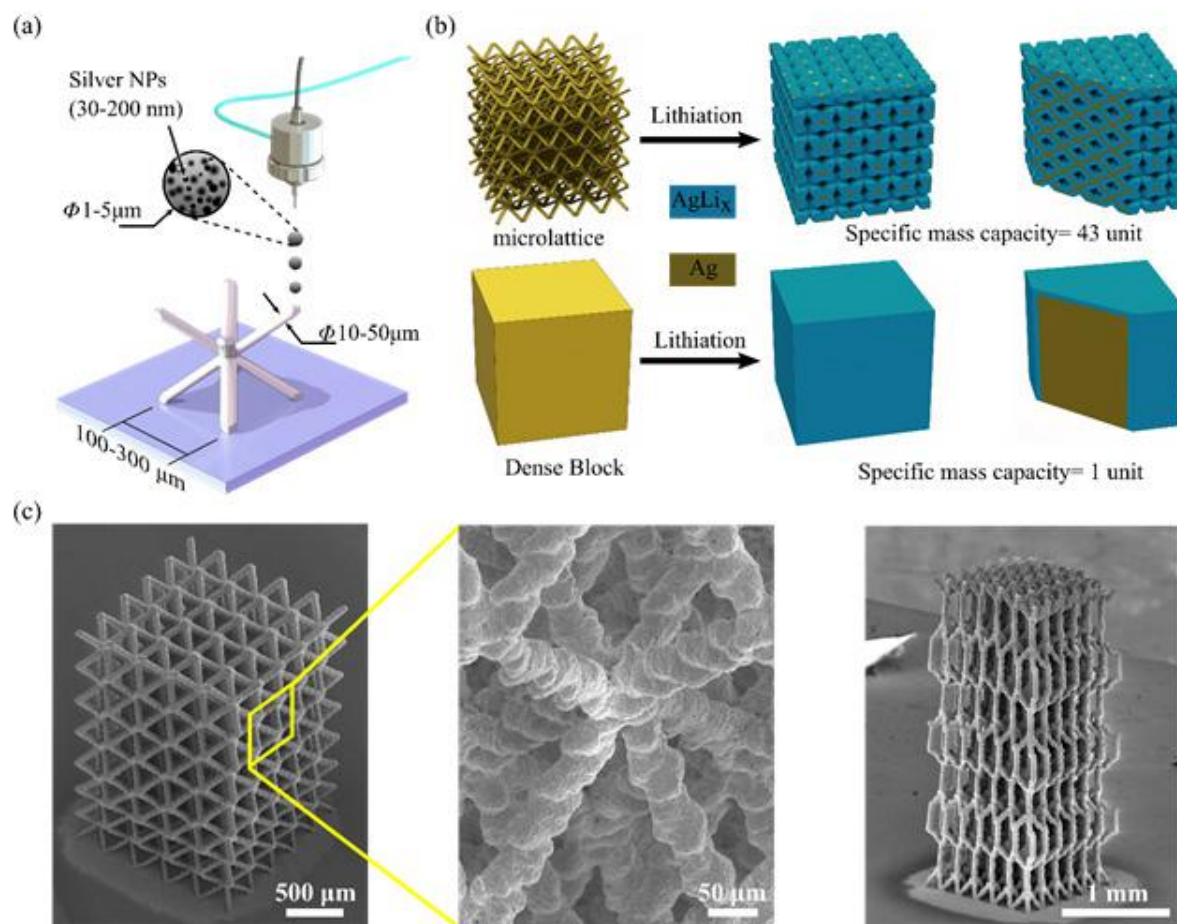


Figure 2. (A) Schematic of the 3D nanoparticle printing method, (B) Schematic of lattice electrode that provides channels for effective electrolyte transport inside its volume, and (C) Representative SEM images of the 3D porous micro-lattice electrodes.

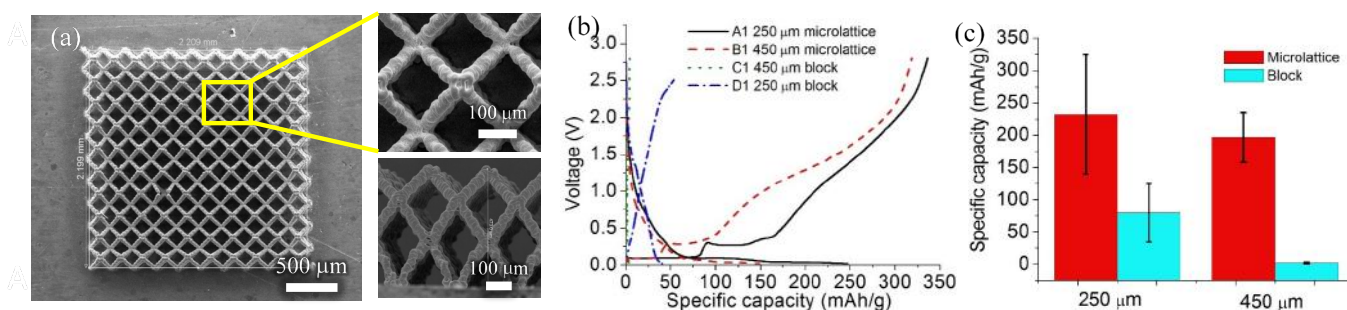


Figure 3. (A) SEM Images of 3D printed electrodes for Li-ion batteries used for electrochemical cycling in this study. (B) Specific capacity for the microlattice and block Ag structure for 250 and 450 μm thickness (C) Comparison of the average specific capacity of microlattice and block structure thicknesses of 250 μm and 450 μm .

trode volume utilization when compared to a thin, solid, Ag block electrode for the Ag-Li battery system evaluated in this work.

Figure 3(A) shows a 450 μm thick lattice electrode fabricated by 3D printing. Figure 3(B) shows the comparison of the electrochemi-

cal performance of the lattice samples (chart lines A1 and B1) and block samples of similar overall dimensions (C1 and D1) in terms of specific capacity. The lattice samples have a significantly improved specific capacity—up to four times that of the block samples—and nearly the highest reported value in the

literature for Ag (290 mAh/g) [11]. Note that our samples are much thicker than those discussed in Jung and Lee [11]. We also measured the areal capacity, which showed that the lattice sample (A1) has achieved an areal capacity of 5 mAh/cm² in the first cycle, which is twice that of the block sample.

Figure 3(C) compares the average specific capacity for both lattice and block electrodes. Despite some variation among the samples (which might be caused by different material batches), it can be confirmed that the lattice electrode structures significantly enhance the battery performance when compared to the block electrode structures. Further, after 40 electrochemical cycles, the electrode lattice shape was intact upon disassembly of the coin-cell battery during our tests, which implies a robust electrochemical-mechanical property [9].

The mechanical properties of the proposed electrode are also very promising. In order to examine any possibility that the porous electrode structures fabricated using 3D printing could act as structural materials [12], we conducted a mechanical test. The 3D lattice electrodes shown in Figure 2(C) were subjected to compressive loads in an Instron machine with an appropriate load cell, and simulations were carried out to capture their behavior. Figure 4 shows the results of the structure under compression and the corresponding stress-strain diagrams for lattices.

At first, the material acted as a cellular structure (similar to honeycombs), absorbing a large amount of deformation without failure. Strains in excess of 50 percent could be tolerated by the structure. The plateau stress could be increased by 400 percent by coating the electrode structures with a nanometer scale metallic layer. This demonstrates that the 3D printed battery electrodes can be used as structural materials.

Scalability and Future Work

The 3D nanoparticle printing process is extremely rapid. For example, a droplet of electrode material (20 μm diameter) can be printed in 4–10 milliseconds. Commercially available aerosol jet machines allow up to four printheads to operate in tandem, which further increases printing speed. And heating the platen can quicken the evaporation rate, allowing the structure to form rapidly with optimized printing programs in commercially available software (such as AutoCAD/AutoLISP). It is possible that the printing could be extended to the inkjet process, existing systems of which have thousands of printheads working in tandem. With this rapid printing process, it is possible to manufacture electrodes in high enough quantities to serve DoD power requirements.

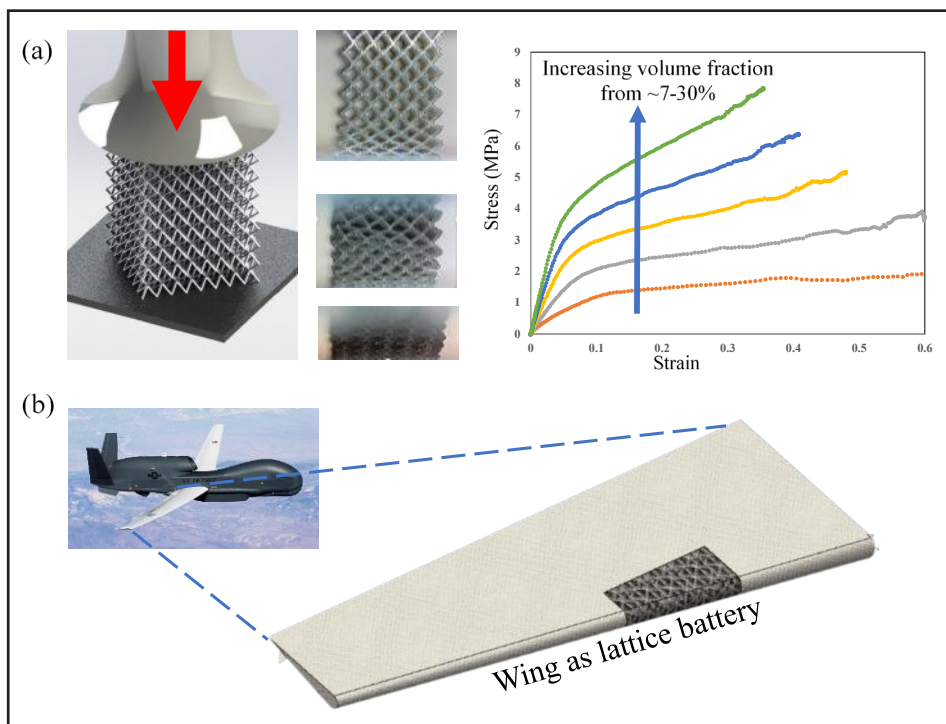


Figure 4. 3D printed electrode acting as a structural material. (A) Results showing the stress-strain response of the lattice electrodes under compressive load. The plateau stress reached about 5 MPa (stress calculated using area of a solid block of equivalent dimensions). The strength could be further increased by 4x by a nanolamination process in our lab. (B) Schematic of a drone wing having lattice batteries forming its wing.

We have established that our 3D printing method leads to the production of lattice electrodes with controlled hierarchical porosity present in three dimensions. Such electrodes enhance electrolyte transport through the electrode volume, increase the available surface area for electrochemical reaction, and relieve the intercalation-induced stress. Combined, these advances lead to an extremely potent high-capacity battery system. Future work will involve building 3D-architected electrodes from various anode and cathode materials by considering unique material properties of individual materials. Furthermore, the developed 3D-structured electrode can be integrated with structural components. We will explore building a prototype that demonstrates a hybrid structure (such as UAS wings) that also acts as a battery device—leading to versatile transport technologies that allow the structural parts to act as batteries themselves.

Conclusions and Implications for DoD

In this study, we demonstrate a 3D printing method that can create lattice electrode architectures for robust Li-ion batteries with high capacity. The specific charge capacity and areal capacity of the 3D electrodes are

shown to be several times that for comparable solid block electrodes, indicating the effectiveness of electrolyte penetration in the porous structure and improved utilization of electrode active material during the lithiation/de-lithiation cycles.

These improvements could have significant implications for DoD's provision of mobile, battery-based power to the dismantled warfighter. Using the electrode system discussed in this article could potentially result in a battery weight reduction of up to 50 percent (for the same energy density). The load of a battery pack on a warfighter in combat is considerable, and any weight reduction that doesn't compromise functionality will provide significant benefits. The improved power characteristics of our battery design could also extend to small- to medium-sized UAS and other vehicles that could store charge within structural components, thus increasing their operational range. The 3D printed lattice technology presented above may lead to an important battery solution for multiple DoD missions and needs.

Acknowledgements

The authors would like to thank Chunshan Hu and Rit Bezbaruah for several images.

References

- Magnuson, S. (2017, June 1). Power-hungry devices challenge Army researchers. National Defense Magazine. Retrieved from <http://www.nationaldefensemagazine.org/articles/2017/6/1/power-hungry-devices-challenge-army-researchers>
- Howard, C. (2015, November 18). Feeding the power-hungry beast. Military and Aerospace Electronics. Retrieved from <https://www.militaryaerospace.com/articles/print/volume-26/issue-11/technology-focus/feeding-the-power-hungry-beast.html>
- U.S. Army. (2014, August 21). International scientists discuss Soldier physical performance. Retrieved from https://www.army.mil/article/132134/International_scientists_discuss_Soldier_physical_performance/
- Mizushima, K., Jones, P., Wiseman, P., & Goodenough, J. B. (1980). Li_xCoO_2 ($0 < x < 1$): A new cathode material for batteries of high energy density. *Materials Research Bulletin*, 15(6), 783–789. doi:10.1016/0025-5408(80)90012-4
- Sethuraman, V. A., Chon, M. J., Shimshak, M., Srinivasan, V., & Guduru, P. R. (2010). In situ measurements of stress evolution in silicon thin films during electrochemical lithiation and delithiation. *Journal of Power Sources*, 195(15), 5062–5066. doi:10.1016/j.jpowsour.2010.02.013
- Armand, M., & Tarascon, J.-M. (2008, February 7). Building better batteries. *Nature*, 451(7179), 652. doi:10.1038/451652a
- Lee, J. S., Tai Kim, S., Cao, R., Choi, N. S., Liu, M., Lee, K. T., & Cho, J. (2011). Metal–air batteries with high energy density: Li–air versus Zn–air. *Advanced Energy Materials*, 1(1), 34–50. doi:10.1002/aenm.201000010
- Sun, K., Wei, T. S., Ahn, B. Y., Seo, J. Y., Dillon, S. J., & Lewis, J. A. (2013). 3D printing of interdigitated Li-Ion microbattery architectures. *Advanced Materials*, 25(33), 4539–4543. doi:10.1002/adma.201301036
- Saleh, M. S., Li, J., Park, J., & Panat, R. (2018). 3D printed hierarchically-porous microlattice electrode materials for exceptionally high specific capacity and areal capacity lithium ion batteries. *Additive Manufacturing*, 23, 70–78. doi:10.1016/j.addma.2018.07.006
- Sadeq Saleh, M., Hamidvishkasougheh, M., Zbib, H., & Panat, R. (2018). Polycrystalline micropillars by a novel 3-D printing method and their behavior under compressive loads. *Scripta Materialia*, 149, 144–149. doi:10.1016/j.scriptamat.2018.02.027
- Jung, H.-R., & Lee, W.-J. (2011). Ag/poly (3, 4-ethylenedioxythiophene) nanocomposites as anode materials for lithium ion battery. *Solid State Ionics*, 187(1), 50–57. doi:10.1016/j.ssi.2010.12.019
- Saleh, M. S., Hu, C., & Panat, R. (2017). Three-dimensional microarchitected materials and devices using nanoparticle assembly by pointwise spatial printing. *Science Advances*, 3(3), e1601986. doi:10.1126/sciadv.1601986
- U.S. Army. (2014, August 13). Army's key mid-tier radio moves forward with tests. Retrieved from <https://www.army.mil/e2/c/images/2014/08/13/358488/original.jpg>
- U.S. Air Force. (2018, January 9). AFE Airmen maintain pilot safety. Retrieved from <http://www.jber.jb.mil/News/News-Articles/NewsDisplay/Article/1411978/afe-airmen-maintain-pilot-safety/>
- U.S. Air Force. (2017). 1st SOSS HAVE ACE hosts Army Special Forces. Retrieved from <https://www.hurlburt.af.mil/News/Art/igphoto/2001719219/>
- U.S. Army RDECOM. (2016, March 30). Autonomy researchers discuss future recommendations. Retrieved from <https://www.army.mil/e2/c/images/2014/12/12/375567/original.jpg>
- U.S. Army (2015, August 21) Troopers receive new Raven UAS camer upgrade. Retrieved from <https://www.army.mil/e2/c/images/2015/08/21/406877/original.jpg>



Rahul Panat, Ph.D.
Associate Professor, Department of Mechanical Engineering, Carnegie Mellon University

Rahul Panat is an associate professor in the Department of Mechanical Engineering at Carnegie Mellon University, Pittsburgh PA. He received his Ph.D. in Theoretical and Applied Mechanics from the University of Illinois at Urbana Champaign in 2004. He spent a decade at Intel Corporation working on microelectronics manufacturing research before joining academia in 2014. His research interests are in the areas of 3D nanoparticle printing, energy storage, sensors, and bioelectronic devices. He has five patents and over 30 journal publications.



Jonghyun Park, Ph.D.
Assistant Professor, Department of Mechanical and Aerospace Engineering, Missouri University of Science and Technology

Jonghyun Park is an assistant professor in the Department of Mechanical and Aerospace Engineering at the Missouri University of Science and Technology (formerly University of Missouri Rolla). He received his Ph.D. in Mechanical Engineering from the University of Michigan in 2009. His research interests are in the areas of energy materials and systems, multiscale/multiphysics modeling, advanced manufacturing, self-assembly, and nano devices. He has over 100 journal and conference publications.



M. Sadeq Saleh
Ph.D. Candidate, Carnegie Mellon University

M. Sadeq Saleh is pursuing a Ph.D. in mechanical engineering at Carnegie Mellon University (M.S., University of Tehran). His research centers on 3D micro-device fabrication with applications in neural engineering, energy storage, and ultralight metamaterials. Saleh is a member of materials research society. His research on micro lattice batteries has received significant publicity in the academic community and the media.



Jie Li, Ph.D.
Post-doctoral Fellow, Missouri University of Science and Technology

Jie Li is a post-doc follow with the Missouri University of Science and Technology (Ph.D, Missouri University of Science and Technology). His research interests include Li-ion battery, multiscale/multiphysics modeling, and advanced manufacturing.

From yesterday's research to today's emerging technologies...



DTIC continues to pave the way for tomorrow's innovations.



With over 4 million technical reports and documents, discover the value of sharing your research on the **R&E Gateway** powered by the Defense Technical Information Center (DTIC)

For DoD CAC / ECA / PIV holders
<https://go.usa.gov/xPn8D>
Limited public collection is available at:
<https://discover.dtic.mil>

COGNITIVE PROTECTION SYSTEMS FOR THE INTERNET OF THINGS

Josh Siegel

The Internet of Things (IoT) is a family of technologies enabling connectivity, sensing, inference, and action [1, 2] that is expected to comprise 30 billion devices by 2020 [3]. IoT's meteoric growth presents opportunities for large-scale data collection and actuation. However, this growth also amplifies vulnerabilities in critical infrastructure networks and systems [4]. Civilian and military leadership remain insufficiently informed of information security risks and threats, degrading security through network effects [5, 6]. This article considers the vulnerability trajectory of internet-enabled IoT devices and presents the concept of an artificially intelligent

Cognitive Protection System (CPS) as a solution capable of securing critical infrastructure against emerging threats.

Challenges Posed by the Internet of Things

Scaling Problems

The recent proliferation of IoT devices and services has heightened the risk of unauthorized system control and data leakage [7]. Commensurate improvements in system dependability and resilience have not materialized alongside this growth [6, 8]. The defensible perimeters of a given system grow with increases in its interactivity, with a single unprotected element constituting a launchpad for attacks on connected devices [4, 9]. These vulnerabilities exist

at the intersections of cyber, physical, and human elements—areas critical to the value that IoT offers, and easily probed through standard network interfaces [10]. For example, in 2014, the non-profit Open Web Application Security Project surveyed IoT perimeters at large and identified 19 IoT attack surfaces and 130 vulnerability types [8]. Modes of attack such as the use of rogue applications, unauthorized communications, improper patching, and poor encryption [2] mirror the challenges of information technology (IT) more generally, while others specifically leverage IoT's physicality. Device transference in IoT systems poses new attack vectors [11], and actuators may cause physical damage [7, 9]. These problems are only worsened by the rapid design and commercial manufactur-

ing cycle, and the presence of enduring, hard-coded vulnerabilities that may outlast the lifespan of a device's original manufacturer or vendor [7, 9].

IoT attacks seek to cause information leakage, denial of service, or physical harm [2]. Exploits of IoT vulnerabilities address hardware, software, people, or processes, and their severity can be amplified by configuration problems or Trojan horses [1]. In some cases, analytics comprise an attack [12] and in all cases, the characteristics of an attack evolve over time [13]. The financial cost of information insecurity is significant, with the average corporate data breach in 2017 costing \$3.62 million [5], and taking a median of 200 days to detect in 2014 [10]. In a military context, system complexity is higher (e.g., Department of Defense [DoD] "green" buildings have tens of thousands of potentially vulnerable sensors [12]), techniques are more sophisticated, and potential consequences are more severe.

Hyperconnectivity has also eroded the security provided by airgaps. Remote management unlocks opportunities for unauthorized users to jump across networks and commandeer programmable logic controllers, placing infrastructure at risk due to weak supervisory control and data acquisition (SCADA) systems [5, 14].

The Unintended Consequences of Connectivity

Because the IoT provides such a large attack surface, it can serve as a force multiplier for malicious actors. Commodity devices have already disrupted critical infrastructure (i.e., the DynDNS distributed denial-of-service [DDoS] attack, in which "Mirai" malware exploited under-protected consumer webcams) [7, 15–17] and silently collected unauthorized information (via VPNFilter router malware) [18]. Hospitals and cities have been locked down by ransomware [18–20]. And cyberattacks are increasing in frequency and complexity [10], posing a growing threat to mission readiness [13].

Just as a personal fitness application inadvertently shared the locations of warfighters in 2018 [7, 21] decision-makers invite unanticipated consequences in the interest of short-term goals—for example, placing hackable voice service microphones in

cars or cameras at road intersections [22]. The same "digital breadcrumbs" that make IoT useful for intelligence data collection and analysis [23, 24] can also leak intelligence-related data; one potentially common example of this is the risk of smart televisions serving as a conduit for intercepting two-factor authentication audio [2]. A warfighter using a WiFi-controlled power outlet may leak network credentials, allowing the plain-text interception of encrypted data. Or, multiple outlets could be cycled to trigger a harmonic, causing an electrical power substation to enter a safety shutoff [25]. The true cost of inexpensive commodity IoT devices is high, and the risks are difficult to anticipate. For example, IT personnel may not consider a scenario in which routers are corrupted to track the location of a deployed unit; and thus may not defend against such a potentiality [26]. Defense contractors may not know (or forget) that an attacker could lower their smart thermostat's temperature, causing internal water lines to burst in the winter. Installing a smart lock not only means that a key can be copied, but also that digital access can be subverted [7].

Proposed Solutions

Conventional cyber-physical security systems rarely consider other devices as potential indirect entry points [6]. A critical first step is to be aware of all the capabilities of a new technology—whether or not their use is envisioned—and to explain them to those potentially impacted. In the context of IoT and critical infrastructure, better education, thoughtful design, and vigilance will improve outcomes [16]. The National Institute of Standards and Technology, the Center for Internet Security, and IEEE have all issued IoT security guidelines, while the Federal Trade Commission encourages engineered-in protection. However, these guidelines lack the means for effective enforcement [7]. The DoD suggests conducting a risk analysis and implementing IoT only where necessary, while ensuring that devices use end-to-end encryption, monitoring network traffic, and using equipment from trusted vendors with managed supply chains [12]. This goal is complicated by the fact that risk assessment is convoluted with the cascading effects of connectivity [13].

Although DoD guidance documents further suggest how to purchase, set up, use, and decommission devices [2], civilian IoT net-

works are capable of undermining internal security efforts (e.g., consumer routers denying service to DoD critical network infrastructure, or vice-versa [12]). The Department of Homeland Security and the White House have suggested that government and industry must collaborate to ensure that security advances leave the internet open, interoperable, secure, and reliable, while protecting critical networks and computing infrastructure [18, 27]. Outside these frameworks, questions remain. How can we be trusted to get IoT security right, when individual users struggle to keep passwords safe and software patched? If information security education does not seem effective, how can practitioners mitigate misconfiguration risks? And, what if computation within durable infrastructure is incapable of running next-generation algorithms?

These questions highlight a problem central to IoT security: the need to confront resource constraints. For example, sensor redundancy improves data trustworthiness—but only at the expense of increased energy, computation, and financial costs [11]. Context-aware systems, discussed below, provide one approach to implementing resource-conscious, adaptive IoT security.

Cognitive Protection Systems

An emerging connectivity architecture implements "Data Proxies" to digitally duplicate the physical world on remote endpoints, using sensor data to build state-space system representations. Unlike digital twins, which typically use the richest-available information to mirror an object, Data Proxies intelligently schedule sensor sampling to meet application demands while minimizing cost. Physical and statistical models rooted in control theory expand these sparse data. Proxies may therefore indirectly measure the state of unobservable variables, and do so using a fraction of the resources required for traditional twinning [28–30]. For example, in developing a usage-based insurance application, the Proxy reduced mobile device power and bandwidth consumption by a factor of 20. This architecture is illustrated in Figure 1.

In this architecture, devices only interact directly with their own digital avatar residing in the Cloud, Fog, or another uncon-

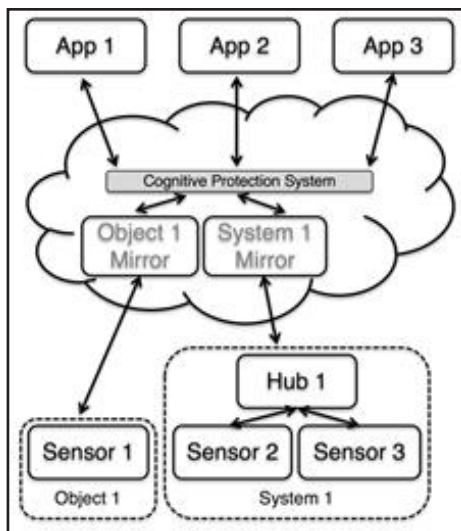


Figure 1. Objects and systems are mirrored in remote computation, where scalable resources allow the CPS to simulate commands and identify anomalies.

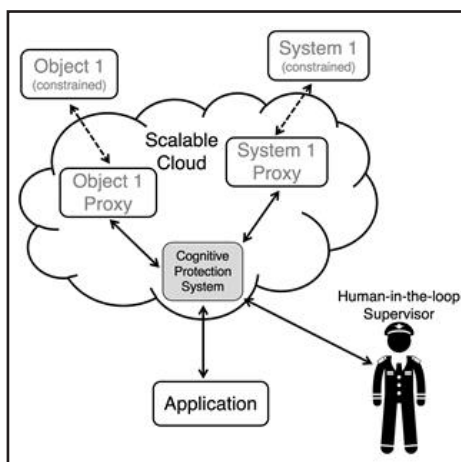


Figure 2. Object avatars and applications interact with one another through the CPS. There are no device-to-device connections, reducing exposed communications. In the event the CPS has low confidence in a critical decision, external verification may be requested.

strained computing node. Avatars then interact within the unconstrained computing environment, enabling a system of digital guardians using scalable computation to monitor and moderate interactions [17].

By limiting direct device communications to a single endpoint, the number of exposed channels in need of protection is reduced, while mirroring devices on unconstrained hardware creates a pathway to support computationally-intensive improvements. Another advantage of device mirrors interacting with one another (rather than the devices themselves) is that data can be uploaded once and multiply used. This reduces redundant sampling to conserve

resources such as battery life and network bandwidth [28–30].

This device-to-device airgap is similar to the way a young child interacts with the world: delegating uncertain actions through their guardian. With Data Proxies, one or more “precocious” devices communicate through a secure channel with a digital guardian possessing broader world-views, richer perception, and enhanced cognitive powers ideally suited to protecting dependents. This direct-to-Cloud approach has a further advantage in the context of IoT: device replacement is simplified, as only a single interaction must be assumed (the new device assumes the old device’s mirror, rather than requiring each device and service interaction to be separately configured). This improves system flexibility and adaptability, creating an interoperable and dynamic glue layer resistant to fragmentation.

It is this resource-conserving, guardian-mirrored architecture that forms the basis for an IoT-centric security architecture known as a cyber-physical system (CPS). CPSs address three types of targeted and unintentional threats:

- *data threats*, in which information (flow) compromises a protected system
- *control threats*, wherein malicious or invalid commands result in a dangerous outcome
- *system threats*, such as mechanical faults

Their performance requires trustworthy IoT hardware and proper installation, configuration, and maintenance procedures. This is a challenge, as devices can be subverted in the supply chain, in manufacturing, at time of installation, and during use [12].

CPSs are built upon the Data Proxy architecture’s underlying system models, and the knowledge that the flow of information is restricted to between avatars. The interaction of device mirrors using the CPS as an intermediate gateway is depicted in Figure 2. Data Proxies work in conjunction with known and learned rule definitions, artificial intelligence, and simulation, to enable the CPSs constituent elements of “Cognitive Firewalls” (CF) and “Cognitive Supervisors” (CS).

Traditional firewalls monitor network traffic to identify possible information leakage, which is necessary but not sufficient to protect against the physical attacks possible with the IoT, such as maliciously issuing commands that cause equipment to exceed safe control limits. Part of a CPS, a CF is a self-learning system capable of evaluating commands for safety in context, allowing only safe commands to pass from the Cloud to the end device.

CFs use scalable computation, context information, system models, and observations to test commands before execution. When commands are sent to connected devices, they are simulated in digital environments run within the Cloud or Fog. If the results are undesirable, the command is blocked; if the results are questionable, the command is sent up a hierarchical chain to seek authorization [28–30]. Safe commands pass to the end device unaltered, with delay dependent upon network conditions and available computational power (for instance, a model robotic arm within a factory tested and relayed or rejected commands within 20 milliseconds). The use of artificial intelligence (AI) allows the system’s policies to adapt to unpredictable attacks, acting autonomously rather than upon rigid rules. Applying context brings reasoning to the system to help address unexpected scenarios. For example, a CF might learn the safe temperature range for the occupants within an environment and reject commands that cause an HVAC system to exceed these limits.

One variation on the CF protects against localized attacks. The CF may be run partially offline; for example, within a powerful gateway device connected to sensing and actuation modules within an aircraft, or operated within a processor’s secure enclave to monitor dependent virtual machines. These implementations display lower latency, at the cost of less-scalable computation, but they serve a valuable purpose in responding to threats or connectivity lapses in real time. An offline CF could have prevented the physical effects of the Stuxnet worm by identifying the impact of malicious commands targeted at SCADA systems by testing commands associated with the worm’s rootkit, and blocking commands intended to cause catastrophic damage to centrifuges.

Local CFs can also respond to mission-crit-

ical faults before sensor data arrives at a remote server for analytics and decision making. A hybrid local/remote approach can mirror the human body's unconscious impulse response. For example, when touching a hot stove, the body retracts the arm autonomously, before the pain signal reaches the brainstem. Afterwards, the brain processes the injury and devises rules to avoid a repeat.

Note that a CF can monitor states that are not obviously physical in nature. For example, a command requesting a high frequency temperature reading (when the measured environment has a long time constant) could be identified as a problematic request. Over-sampling might result in poor quality data, or the saturation of on-board computation, or the depletion of a device's battery—an extreme form of a denial-of-service attack. A CF could simulate the impact of data requests on resource consumption, compute the likelihood of a locked-up processor or a dead battery, and reject the request or automatically reduce temperature measurement to a safe rate.

The same models behind resource-efficient mirroring and the CF enable the creation of CSs, artificially intelligent systems capable of identifying and responding to anomalies directly, or notifying a human when things start to feel wrong [28–30]. CSs apply context information and rules, learning the relationship between system inputs and outputs to raise alerts when performance does not match expectations. For example, a CS could learn the relationship among on-base water flow meters and autonomously identify a water leak or siphoning event. The approach also works in a digital context, and typical network traffic patterns can be learned—so that a base's targeting by a DDoS attack can be detected and mitigated.

Consider a real-world military example for the CPS: for over a decade, the DoD has increased its use of high-tech power distribution solutions to improve delivery efficiency. A remote installation might have its own microgrid, with programmable logic controllers managing diesel generators, transformers, or battery banks. Electronic infrastructure can be allowed online [31] to provide for remote monitoring in order for officers to estimate resource demands and schedule appropriate resupply, or else to disconnect non-critical circuits, prolonging

operation when resupply is not imminent.

Putting the grid online offers insight and controllability benefits, but exposes critical infrastructure to exploitation. By implementing semi-local computation (an on-site Fog) to run a CPS, and learning context through physics-based models augmented with additional data (e.g., daily schedules, planned operations, number of individuals on-site, weather forecast), a microgrid could monitor itself and the CS could identify anomalies that suggest that energy is being consumed unexpectedly, or that a connected device poses a fire hazard [31].

The CF could possibly identify a malicious actor's attempt to run the generator over-speed to cause an equipment-damaging power surge or early fuel depletion. In both cases, the CF could reject commands that would otherwise interrupt attached critical services and notify personnel of the attempted attack. The CPS is capable of serving as a critical tool in enabling secure and efficient connectivity for DoD operations, and improving system resilience in the face of emerging threats to the IoT.

Security-forward Thinking

Not all attacks are avoidable. The ability to recover from or regenerate performance after an unexpected event is important for securing IoT's place in the management of critical infrastructure. Cyber-resilience constitutes a bridge between sustaining operations of a system, while ensuring mission execution and retaining critical function throughout an attack [13].

Specifically, resilient systems must plan for, absorb, recover from, and adapt to known and unknown threats through hardening, diversification, adaptability, and thoughtful degradation. Systems can propagate control in order to minimize cascading domino effects [13]. Resilience is developed and engineered at the micro-, meso-, or macro-scale, assuring the performance of individual components or interfaces, architectural or system properties, or entire missions, respectively [32].

Linkov & Kott [13] suggest the use of active agents—both human and artificial—to absorb, recover, and adapt to attacks. The proposed CPS system discussed above, implemented properly, embodies this approach to self-healing systems.

The most resilient systems both prevent attacks and prepare for unavoidable attacks. They continue operating while defending themselves; constrain or minimize an attack's reach; and adapt to avoid future occurrences [32]. The DoD has identified smart, self-healing systems as an area for future development [33]. Here, too, adaptive AI could be applied to detect, respond to, and operate in the face of an ongoing attack. Using a CPS for heightened situational awareness will enable rapid response and attack mitigation, thereby improving outcomes. With broader connectivity, the models learned at one military installation can be readily deployed to others, developing digital herd immunity.

Conclusion

We have seen that pervasive connectivity and the expansion of the IoT pose opportunities and challenges in developing and sustaining the operation of critical infrastructure. DoD has the potential to take a leadership position in the IoT, working toward common goals of protecting, defending, and securing information infrastructure, digital networks, and remote actuators [5]. To build a safer future, education and awareness are critical; IoT practitioners must regularly conduct security surveys to identify all possible risks and approaches to remediation [2]. This includes the easily-foreseeable entry points as well as the evolving frontier of connectivity.

Finally, we explored the use of AI to develop a context-aware CPS making use of learned system models to test commands for safety in a simulated environment to execution. These same enabling technologies can build increased system resilience in the face of internal and external threats. Developers must make efforts to develop “smart, smart things” with embedded security [24], long lifecycles with computational headroom and provisions for upgradability, and support products for their entire lifecycles.

Practitioners and users need to carefully consider the unintended consequences of using a connected system. They should also remain cognizant of the fact that while it is necessary to follow best available security practices, those, too, can be undermined by a complex web of interactions.

References

1. Tedeschi, S., Mehnen, J., Tapolou, N., & Roy, R. (2017). Secure IoT devices for the maintenance of machine tools. *Procedia CIRP*, 59, 150–155. doi:10.1016/j.procir.2016.10.002
2. U.S. Government Accountability Office. (2017, July 27). Internet of Things: Enhanced assessments and guidance are needed to address security risks in DOD (GAO-17-668). Retrieved from <https://www.gao.gov/assets/690/686203.pdf>
3. Nordrum, A. (2016, August 18). Popular Internet of Things forecast of 50 billion devices by 2020 is outdated. *IEEE Spectrum*. Retrieved from <https://spectrum.ieee.org/tech-talk/telecom/internet/popular-internet-of-things-forecast-of-50-billion-devices-by-2020-is-outdated>
4. Klinedinst, D. J., Land, J., & O'Meara, K. (2017, October). *2017 merging Technology Domains Risk Survey*. Pittsburgh, PA: Carnegie Mellon University Software Engineering Institute. Retrieved from <https://resources.sei.cmu.edu/library/asset-view.cfm?asset-id=505311>
5. Bardwell, A., Buggy, S., & Walls, R. (2017, December). *Cybersecurity Education for Military Officers* (MBA Professional Report). Monterey, CA: Naval Postgraduate School. Retrieved from https://calhoun.nps.edu/bitstream/handle/10945/56856/17Dec_Bardwell_Buggy_Walls.pdf?sequence=1&isAllowed=y
6. McDermott, T., Horowitz, B., Nadolski, M., Meierhofer, P., Bezzo, N., Davidson, J., & Williams, R. (2017, September 29). *Human Capital Development – Resilient Cyber Physical Systems* (SERC-2017-TR-113). Hoboken, NJ: Stevens Institute of Technology Systems Engineering Research Center. Retrieved from <http://www.dtic.mil/dtic/tr/fulltext/u2/1040186.pdf>
7. U.S. Government Accountability Office. (2017, May). Technology assessment: Internet of Things: Status and implications of an increasingly connected world (GAO-17-75). Retrieved from <https://www.gao.gov/assets/690/684590.pdf>
8. Morin, M. E. (2016, September). *Protecting Networks Via Automated Defense Of Cyber Systems* (Master's thesis). Monterey, CA: Naval Postgraduate School. Retrieved from <https://www.hsdl.org/?view&did=796527>
9. Higgenbotham, S. (2018, June 20). Six ways IoT security is terrible. *IEEE Spectrum*. Retrieved from <https://spectrum.ieee.org/telecom/security/6-reasons-why-iot-security-is-terrible>
10. Zach, D., Elhabashy, A. E., Wells, L. J., & Camelio, J. A. (2016). Cyber-physical vulnerability assessment in manufacturing systems. *Procedia Manufacturing*, 5, 1060–1074. doi:10.1016/j.promfg.2016.08.075
11. Cañedo, J., Hancock, A., & Skjellum, A. (2017, Fall). Trust management for cyber-physical systems. *Homeland Defense & Security Information Analysis Center Journal*, 4(3), 15–18. Retrieved from https://www.hdiac.org/wp-content/uploads/2018/04/Trust_Management_for_Cyber_Physical_Systems_Volume_4_Issue_3-1.pdf
12. U. S. Department of Defense. (2016, December), DoD policy recommendations for the Internet of Things (IoT). DoD Chief Information Officer. Retrieved from <https://www.hsdl.org/?abstract&did=799676>
13. Linkov, I., & Kott, A. (2019). Fundamental concepts of cyber resilience: Introduction and overview. In Kott & Linkov (Eds.), *Cyber Resilience of Systems and Networks* (pp. 1–25). Basel, CHE: Springer International Publishing AG.
14. Glenn, C., Sterbenz, D., & Wright, A. (2016, December 20). *Cyber Threat and Vulnerability Analysis of the U.S. Electric Sector*. Idaho Falls, ID: Idaho National Laboratory. doi:10.2172/1337873
15. Perloth, N. (2016, October 21). Hackers used new weapons to disrupt major websites across U.S. *The New York Times*, A1. Retrieved from <https://www.nytimes.com/2016/10/22/business/internet-problems-attack.html>
16. Sarma, S., & Siegel, J. (2016, November 30). Bad (Internet of) Things. *ComputerWorld*. Retrieved from <https://www.computerworld.com/article/3146128/internet-of-things/bad-internet-of-things.html>
17. Lucero II, L. (2018, May 27). F.B.I.'s urgent request: Reboot your router to stop rusia-linked malware. *The New York Times*, B4. Retrieved from <https://www.nytimes.com/2018/05/27/technology/router-fbi-reboot-malware.html>
18. U.S. Department of Homeland Security. (2018, May 15). U.S. Department of Homeland Security Cybersecurity Strategy. Retrieved from https://www.dhs.gov/sites/default/files/publications/DHS-Cybersecurity-Strategy_1.pdf
19. Osborne, C. (2018, January 17). US hospital pays \$55,000 to hackers after ransomware attack. *ZDNet*. Retrieved from <https://www.zdnet.com/article/us-hospital-pays-55000-to-ransomware-operators/>
20. Newman, L. H. (2018, April 23). Atlanta spent \$2.6M to recover from a \$52,000 ransomware scare. *Wired*. Retrieved from <https://www.wired.com/story/atlanta-spent-26m-recover-from-ransomware-scare/>
21. Chappell, B. (2018, January 29). Pentagon reviews GPS policies after soldiers' Strava tracks are seemingly exposed NPR. Retrieved from <https://www.npr.org/sections/thetwo-way/2018/01/29/581597949/pentagon-reviews-gps-data-after-soldiers-strava-tracks-are-seemingly-exposed>
22. U. S. Government Accountability Office. (2016, September). Data and analytics innovation: Emerging opportunities and challenges (GAO-16-659SP). Retrieved from <https://www.gao.gov/assets/680/679903.pdf>
23. Montalbano, E. (2018, January 30). The US Military's IoT problem is much bigger than fitness trackers. *The Security Ledger*. Retrieved from <https://securityledger.com/2018/01/security-personnel-challenges-stymie-dods-adoption-iot/>
24. Johnson, B. D., Vanatta, N., Draudt, A., & West, J. R. (2017, September 13). *The New Dogs of War: The Future of Weaponized Artificial Intelligence*. U.S. Army Cyber Institute at West Point and Arizona State University's Threatcasting Lab. Retrieved from <http://www.dtic.mil/docs/citations/AD1040008>
25. Greenberg, A. (2017, September 6). Hackers gain direct access to US power grid controls. *Wired*. Retrieved from <https://www.wired.com/story/hackers-gain-switch-flipping-access-to-us-power-systems/>
26. Adib, F., & Katabi, D. (2013, August). See through walls with Wi-Fi! Paper presented at the SIGCOMM'13 conference, Hong Kong, China. Retrieved from <https://people.csail.mit.edu/fadel/papers/wivi-paper.pdf>
27. The White House. (2018, September). *National Cyber Strategy of the United States of America*. Retrieved from <https://www.whitehouse.gov/wp-content/uploads/2018/09/National-Cyber-Strategy.pdf>
28. Siegel, J. E., Kumar, S., & Sarma, S. E. (2018, August). The future Internet of Things: secure, efficient, and model-based. *IEEE Internet of Things Journal*, 5(4), 2386–2398. doi:10.1109/JIOT.2017.2755620
29. Siegel, J. E., & Kumar, S. (Forthcoming). Cloud, context, and cognition: Paving the way for efficient and secure IoT implementations. In Ranjan, R. (Ed.), *Integration of Cloud Computing, Cyber Physical Systems and Internet of Things*. Berlin, DE: Springer-Verlag.
30. Siegel, J. E. (2016, June). Data proxies, the cognitive layer, and application locality: Enablers of cloud-connected vehicles and next-generation Internet of Things (Doctoral dissertation). Cambridge, MA: Massachusetts Institute of Technology. Retrieved from <https://dspace.mit.edu/handle/1721.1/104456>
31. Siegel, J.E. (2018, September). Real-time Deep Neural Networks for internet-enabled arc-fault detection. *Engineering Applications of Artificial Intelligence*, 74, 35–42. doi:10.1016/j.engappai.2018.05.009
32. Kott, A., Blakely, B., Henshel, D., Wehner, G., Rowell, J., Evans, N., . . . Møller, A. (2018, April). *Approaches to Enhancing Cyber Resilience: Report of the North Atlantic Treaty Organization (NATO) Workshop IST-153* (ARL-SR-0396). Adelphi, MD: U.S. Army Research Laboratory. Retrieved from <https://arxiv.org/ftp/arxiv/papers/1804/1804.07651.pdf>
33. Grain, D. (2014, November 14). *Critical Infrastructure Security and Resilience National Research and Development Plan: Final Report and Recommendations*. National Infrastructure Security Council. Retrieved from <https://www.dhs.gov/sites/default/files/publications/NIAC-CISR-RD-Plan-Report-508.pdf>



Josh Siegel, Ph.D.
Assistant Professor, Michigan State University

Josh Siegel is an assistant professor at Michigan State University and the lead instructor for the Massachusetts Institute of Technology's (MIT) Internet of Things Bootcamp. Siegel was previously a research scientist at MIT and the founder of automotive companies. He received his Ph.D. (2015), S.M. (2013) and S.B. (2011) in mechanical engineering from MIT. Siegel and his companies have been recognized with accolades, including the Lemelson-MIT Student Prize and the MassIT Government Innovation Prize. He has multiple issued patents, published in top scholarly venues, and been featured in popular media. Siegel's ongoing research develops architectures for secure and efficient connectivity, applications for pervasively sensed data, and intelligent vehicle diagnostics.



ADVANCING SPACE SITUATIONAL AWARENESS FOR NATIONAL SECURITY

Chad Pyle

Space Situational Awareness (SSA) is the predictive knowledge and characterization of natural and/or synthetic resident space objects (RSOs) and the broader operational environment upon which space operations depend [1]. Space surveillance systems contribute to SSA by employing multiple sensor networks to detect, characterize, and track RSOs. Many of these resident space objects represent a significant threat to U.S. communication and surveillance systems, in part because an estimated majority of these objects remain undetected.

As space systems use continues to increase, navigation and operation are likely to grow more difficult as additional traffic and debris contribute to congestion. Government organizations, non-governmental organizations, and private firms alike are seeking to gain and advance space capabilities, making SSA increasingly critical as space steadily becomes more crowded and contested.

Overview

An RSO can be a fabricated object, such as a satellite, spacecraft, or debris, or a natural object, like an asteroid or meteoroid. There are currently more than 23,000 confirmed trackable objects present in low Earth orbit (LEO) and geosynchronous Earth orbit (GEO), according to the U.S. Space Surveil-

lance Network (part of the Joint Space Operations Center, U.S. Strategic Command) [2]. These objects weigh an estimated total of 7,500 tons [3]. Most of these RSOs were cataloged by tracking them throughout operation, or from observed fragmentation events. According to the Joint Space Operations Center, of those 23,000 objects, roughly 4,800 are satellites, with slightly more than a quarter of those being operational [2].

With only approximately 1,700 operational satellites in orbit [4], the vast majority (by count) of RSOs orbiting our planet are types of debris. Based on statistical modelling and estimation derived from observations and analysis, there are more than 29,000 RSOs that measure greater than 10 centimeters (cm) in length; more than 750,000 objects measuring between 1 and 10 cm, and more than 166 million objects smaller than 1 cm [5]. This debris can originate from space missions that intentionally discard certain objects or parts during delivery and operations [6]. This type of RSO includes objects such as empty fuel/propellant tanks, separation and packaging equipment, payload shrouds, and even lens caps [6]. Other debris can be attributed to failure and fragmentation events that occur in orbit.

Fragmentation consists of in-orbit object breakups—more than 200 objects have experienced a fragmentation event since the first recognized orbital fragmentation event occurred in June 1961 [6]. Spacecraft also

typically deteriorate over time, leading to gradual breakup of the craft, which is referred to as “anomalous debris [6].”

In addition to debris tracking and monitoring, SSA also involves the detection, characterization, and tracking of all orbital launches and the subsequent tracking of their payloads once in orbit. Synthetic RSOs can pose both intentional and unintentional threats, and being able to distinguish between the two is imperative for homeland defense [1]. Adversarial entities continually seek to develop capabilities aimed at hampering U.S. space operations [1], making the ability to monitor and track all payloads vital to national security by assuring the Department of Defense’s (DoD) continued operational security in space.

The sheer number of objects orbiting our planet is considerably large, and these objects have the potential to cause significant damage to spacecraft and space operations. According to the National Aeronautics and Space Administration (NASA), the International Space Station has been forced to conduct 25 avoidance maneuvers in its 20 years of operation [4]. Additionally, NASA reported 21 avoidance maneuvers by unmanned spacecraft in 2017 alone [4]. These avoidance maneuvers can only be initiated for known objects, which are typically larger objects. No reliable capabilities currently exist for detecting objects smaller than 10 cm, which, according to NASA, pose the highest

Image Credit

Photo illustration created by HDIAC and adapted from a photo by NASA’s Goddard Space Flight Center/JSC (Available for viewing at: https://svs.gsfc.nasa.gov/vis/a010000/a011200/a011229/Earth_Debris_Large.jpg) and Adobe Stock.

penetration risk to the majority of operational spacecraft [4].

Highlighting that threat, current collision avoidance detection and maneuver activities are at present conducted only for *tracked* objects, which constitute less than 1 percent of all potentially mission-ending orbital debris threats [4]. This leaves a number of critical commercial and government systems at a high level of risk for impact or attack. This includes nearly all commercial communications systems, such as radio and television assets, as well as several mission-critical military and government systems including the Military Global Positioning System Augmentation System [7] and Wide Area Augmentation System (WAAS) [8]. The WAAS is a satellite navigation system operated by the Federal Aviation Administration that provides service to all classes of aircraft, including vertically-guided landing approaches, meteorological conditions, route navigation, and airport departures and arrivals [8].

Perhaps the most critical system at risk is the network of missile defense satellites located in GEO. One such system is the Space-Based Infrared System operated by Air Force Space Command (AFSPC), which is designed to “meet jointly defined requirements of the defense and intelligence communities in support of the missile early warning, missile defense, battlespace awareness, and technical intelligence mission areas [9].” The Geosynchronous Space Situational Awareness Program satellites, tasked with supporting U.S. Strategic Command (USSTRATCOM) space surveillance operations, are also at risk from RSO impacts [10].

RSO Detection

Detection of any object in space can be a difficult task, given the scope and nature of the problem. Nevertheless, space- and ground-based optical and radar measurements have proven to be viable detection methods [11]. However, these methods are mostly limited to the detection of objects larger than 10 cm [11]. In GEO, specifically, these methods are exceptionally poor at detecting objects that are small in size or present only faint electromagnetic signals [11]. This is due to the inverse square law, which holds that signal source intensity is inversely proportional to the square of the distance. This means that by the time a radar signal has travelled to an object and reflected back to the detector, the

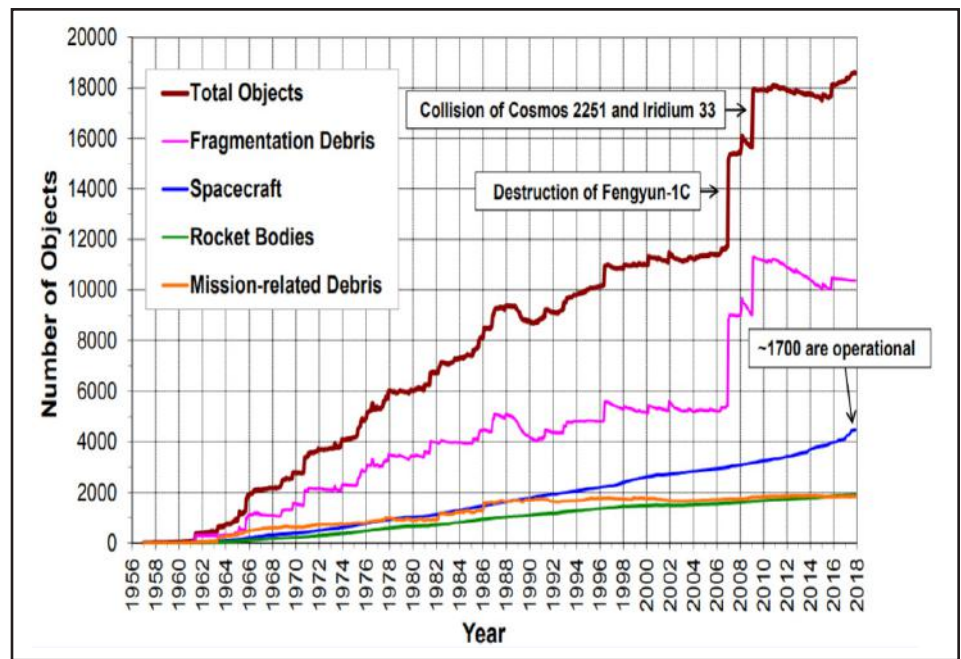


Figure 1. Rough approximation of all known objects in Earth orbit 10cm or larger [25].

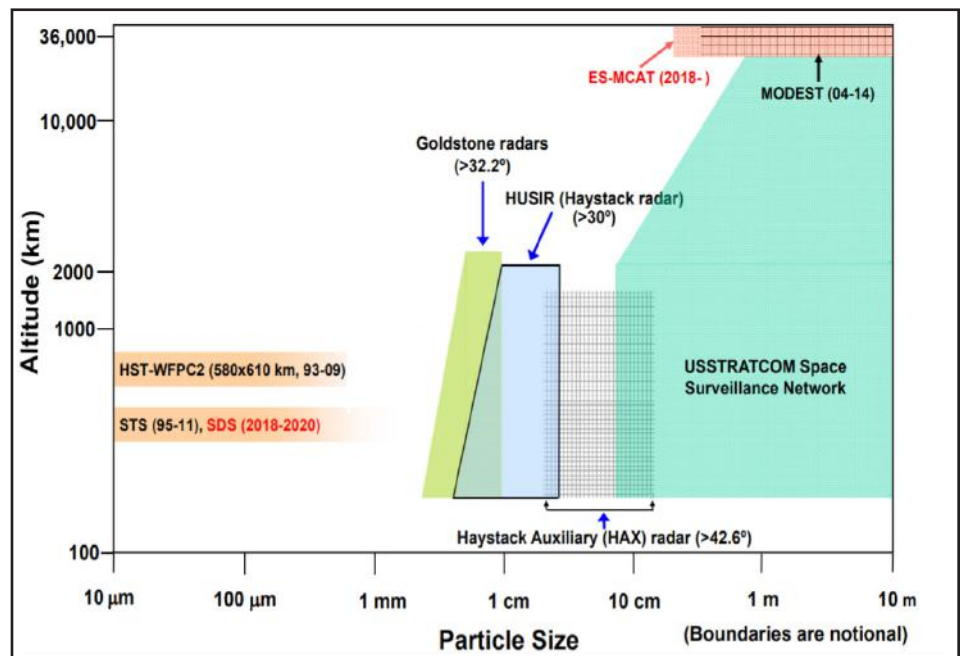


Figure 2. SSA Coverage for the United States. Shows coverage areas of space debris observation capabilities and large gaps in coverage area [25].

signal intensity will be inversely proportional to the fourth power for the range to target. At GEO altitudes—approximately 22,000 miles up—RSO detection capabilities are largely nonexistent [11]. In fact, above LEO altitudes of roughly 1,240 miles, any object smaller than 10 cm is essentially undetectable [4]. For objects around 1 millimeter in size, there is currently no technology capable of detection at any altitude [4].

While USSTRATCOM, AFSPC, and NASA consistently operate and update space surveillance systems for RSO activity [2], the

detection and identification capabilities of these systems need to keep pace with the increasing threat presented by the growing orbital landscape. According to researchers at the Guggenheim School of Aerospace Engineering at the Georgia Institute of Technology, approximately 8 percent of cataloged RSOs reside in GEO-like orbits [11]. Fundamentally, the quantities, types, sizes, and orbits of the vast majority of these objects are relatively unknown, excluding consistently bright and relatively stable-orbit objects [11]. This is in part due to their size, reflectivity, or high area-to-mass ratio that makes them

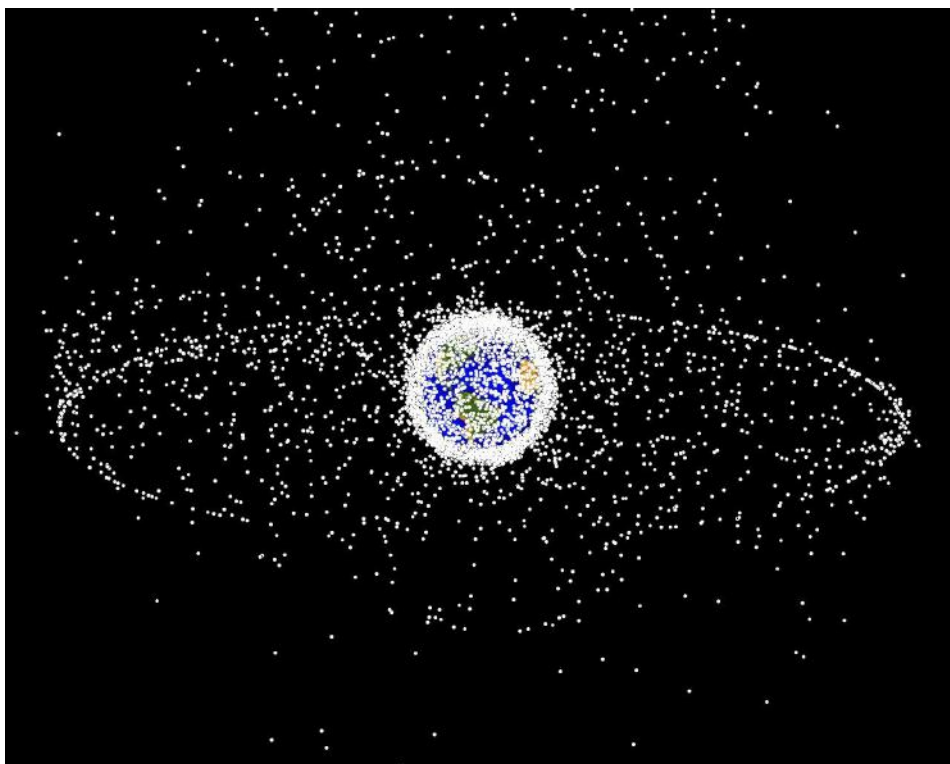


Figure 3. "The GEO images are images generated from a distant oblique vantage point to provide a good view of the object population in the geosynchronous region (around 35,785 km altitude) [26]."

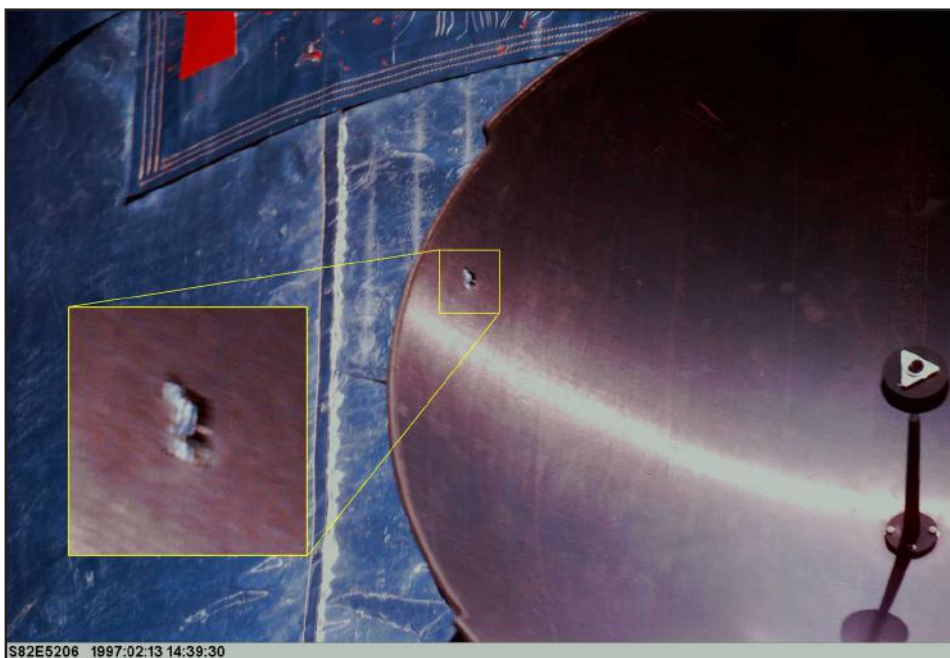


Figure 4. An impact that completely penetrated the antenna dish of the Hubble Space Telescope [26].

particularly susceptible to orbital perturbation [11].

To help combat this gap in SSA, in early 2018 these Georgia Tech researchers put forth a novel method for identifying previously undetectable objects using archival fluxgate magnetometer data generated by the NASA

Time History of Events and Macroscale Interactions during Substorms [11]. The idea is to measure the strength of induced magnetic fields generated by charged space objects as they pass near a magnetometer [11]. Thanks to the presence of charged particles in the atmosphere and solar wind, many RSOs develop a Coulomb charge [11]. Since any

moving charged object generates an electric and magnetic field, it becomes possible to detect the object by detecting its magnetic field—hence the usefulness of the magnetometer in detecting moving, charged, RSOs.

As reported by a research team from the Air Force Institute of Technology, many of the algorithms currently employed to detect RSOs use a "matched-filter or spatial correlator on long-exposure data to make a detection decision at a single pixel point of a spatial image based on the assumption that the data follow a Gaussian distribution [12]." Long-exposure imaging in daylight conditions requires stacking numerous short-exposure images in order to avoid overexposure, which provides an opportunity to increase detection capabilities [12]. Their idea involves developing an algorithm that drastically improves the traditional set of images by "selectively removing short-exposure frames of data that do not positively contribute to the overall signal-to-noise ratio of the averaged image [12]." Cleaning the image stack in this fashion has the potential to extend RSO detection capabilities for smaller and dimmer objects.

Other promising avenues for increased RSO detection include using streak observations with advanced image processing techniques and computational abilities to increase optical detection of RSOs from a space-based platform [13]. Additional efforts involve using networked image sensors to determine angular velocity associated with an object and identifying a direction of motion to initiate a search for the possibly identified object [14].

RSO Characterization

In addition to *detecting* RSOs, it is equally important to be able to *characterize* detected objects. Characterization of RSOs is what separates our awareness of a satellite RSO from space debris RSO, and it is what determines which RSOs may pose a threat. Determination of shape, size, makeup, and orbital dynamics are also crucial in classifying satellite types. Within the context of space arms control, treaties currently in force prevent the placement of weapons of mass destruction in orbit, but do very little to restrict other types of platforms or satellites [15]. Some national security analysts estimate that space could be weaponized by early 2020 [15], meaning that technology and techniques to accurately characterize and classify newly detected objects will need to be established now to maintain an appropriate level of intelligence

and security in the future.

One novel solution put forward by researchers at the Air Force Office of Scientific Research (AFOSR) suggests an integrated approach involving continuous variables to characterize space objects through joint search, detection, and classification, along with tracking problems previously deemed too computationally intense [16]. This approach to overcoming computational hurdles involves using artificial intelligence and machine learning techniques that follow automatic approaches [16].

One such technique includes the use of methods based on dynamic data-driven application systems for the approximation of solutions to the Finite Set Statistics (FISST) recursion equations using randomized Markov chain Monte Carlo algorithms and Gaussian Mixture models [16]. The goal of this AFOSR project is to maximize characteristic information regarding space objects, which will in turn lead to a higher level of SSA.

Fellow researchers at AFOSR are taking a different approach by studying advancements in image analysis and applications involving 3D imaging and characterization [17]. The project's objectives include the enhancement of the computational speed of Bayesian error estimations; the development of spectropolarimetric modeling of RSOs to extract dimensional and material characteristics; the enhancement of highly turbulent atmospheric modeling; and the production of phase-masks to allow 3D imaging of RSOs [17]. These would provide a full characterization of any detected RSO, allowing for object classification. Beyond classifying an object as a satellite (versus debris, etc.), it would also provide critical details to the intent or mission objective of any payload delivered by another nation. Using an object's detailed 3D image along with its material characteristics, differentiating a surveillance satellite from a possible weapons platform or navigation satellite is likely to become decidedly easier.

RSO Tracking

Tracking RSOs can be difficult due to multiple sources of uncertainty, which include but are not limited to varied data sources, orbital mechanics, and object kinematics. The high cost and amount of resources required to achieve the direct, active monitoring of all



Figure 5. After in space repairs to the Hubble Space Telescope, the returned parts show many orbital debris impacts [26].

RSOs with current technology makes it an impractical task. Because the bulk of RSO tracking is currently conducted by calculating orbital paths (not via direct monitoring), effective tracking of the majority of RSOs requires precise prediction of orbital characteristics and identification of alterations to orbital parameters. Improving prediction capabilities will allow for a higher level of safety and security for both spaceflights and satellite operations while navigating through orbit.

Researchers at AFOSR are creating tracking abilities by developing advanced orbital prediction capabilities through the application of physics-based machine learning, which allows them to be able to account for the unevenly distributed and heterogeneous measurements of RSOs by exploiting discrete orthogonal polynomials [18]. A separate effort at AFOSR is pursuing the ability to dynamically calibrate sensor measurements for the near-real-time tracking and characterization of RSOs [19]. The objective is to quantify the source of errors in object tracking results from dynamic mismodeling of ground-based observations, as compared to measurement-related inconsistencies [19].

There are numerous other projects underway at AFOSR that aim to solve the RSO problem. For example, one effort is deploying FISST methodology on non-Euclidean manifolds with the goal of detecting, tracking, identifying, and characterizing multiple RSOs simultaneously [20]. Alternatively, another project is developing analytical and compu-

tational tools to improve tracking via the “optimal planning and scheduling of disparate sources of information, integrating sensing with stochastic models, uncertainty characterization and forecasting, and integration of sensor data with model predictions [21].”

Tracking RSOs becomes especially complicated when the object possesses active maneuvering capabilities. Detecting and sustaining the continual tracking of an actively maneuvering object presents immense chal-

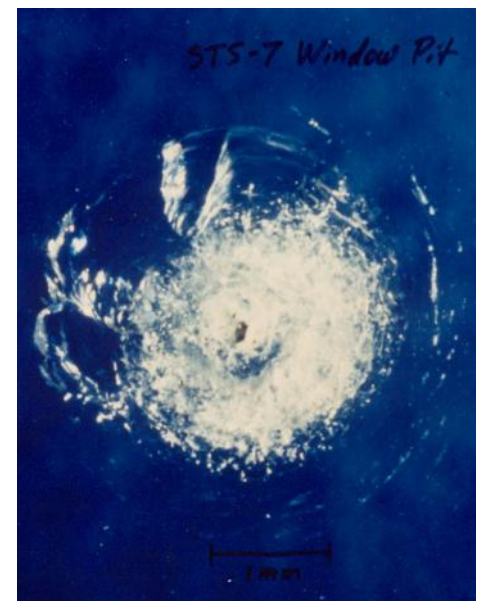


Figure 6. Window pit from orbital debris on STS-007. Upon examination of the impact, it was determined that the impacting object was approximately 0.01cm in diameter and travelling roughly 5km/s [26].

allenges, due to the issues presented by modelling orbital parameters that can continually change. Given the sheer number of operational satellites currently present in LEO and GEO (and projected rates of increase), the need for additional surveillance capabilities and systems is clear. Having the ability to discern operational intent of a maneuvering object is even more critical. This is illustrated by DoD's desire to develop capabilities to rapidly detect evasive intent and behavioral identification in uncertain space environments [22]. Solicitations like the "Rapid Discovery of Evasive Satellite Behaviors" [22] point to the need for increased surveillance capabilities to support SSA. However, as improvements in monitoring capabilities lead to increased data processing needs, a logical solution is an autonomous method for tracking RSOs. Researchers at the Virginia Polytechnic Institute and State University

have taken the novel approach of creating an autonomous sensor network for tracking multiple maneuvering and non-maneuvering satellites using data from the Space Object Surveillance and Identification network [23].

Other solutions involve a significant boost to data processing capabilities in addition to increased monitoring capabilities. With an increase in optical data there follows the need for faster optical data processing. The use of directional statistics could provide that increase. By using Fisher-Bingham-Key distribution for "observation-to-track association of angles-only optical data [24]," researchers at Applied Defense Solutions have shown a better data association than standard approaches that are more prone to Type II errors [24]. As described, this is "desirable in SSA scenarios when the modeled dynamics deviate from the true dynamics or in scenar-

ios with unknown optical measurement biases [24]."

Conclusion

Significant research and technical development, including increased pattern recognition, real-time optical abilities, and computational algorithms for real-time classification, goes into the detection, tracking, and characterization of RSOs. These capabilities play a critical role in the accurate accounting of derelict spacecraft and space debris, and in the tracking of active, operational spacecraft that could pose a risk to national interests. As countries continue to develop spacecraft designed for close-proximity and on-orbit servicing operations, advancing space situational awareness provides an important way to mitigate any potential threats.

References

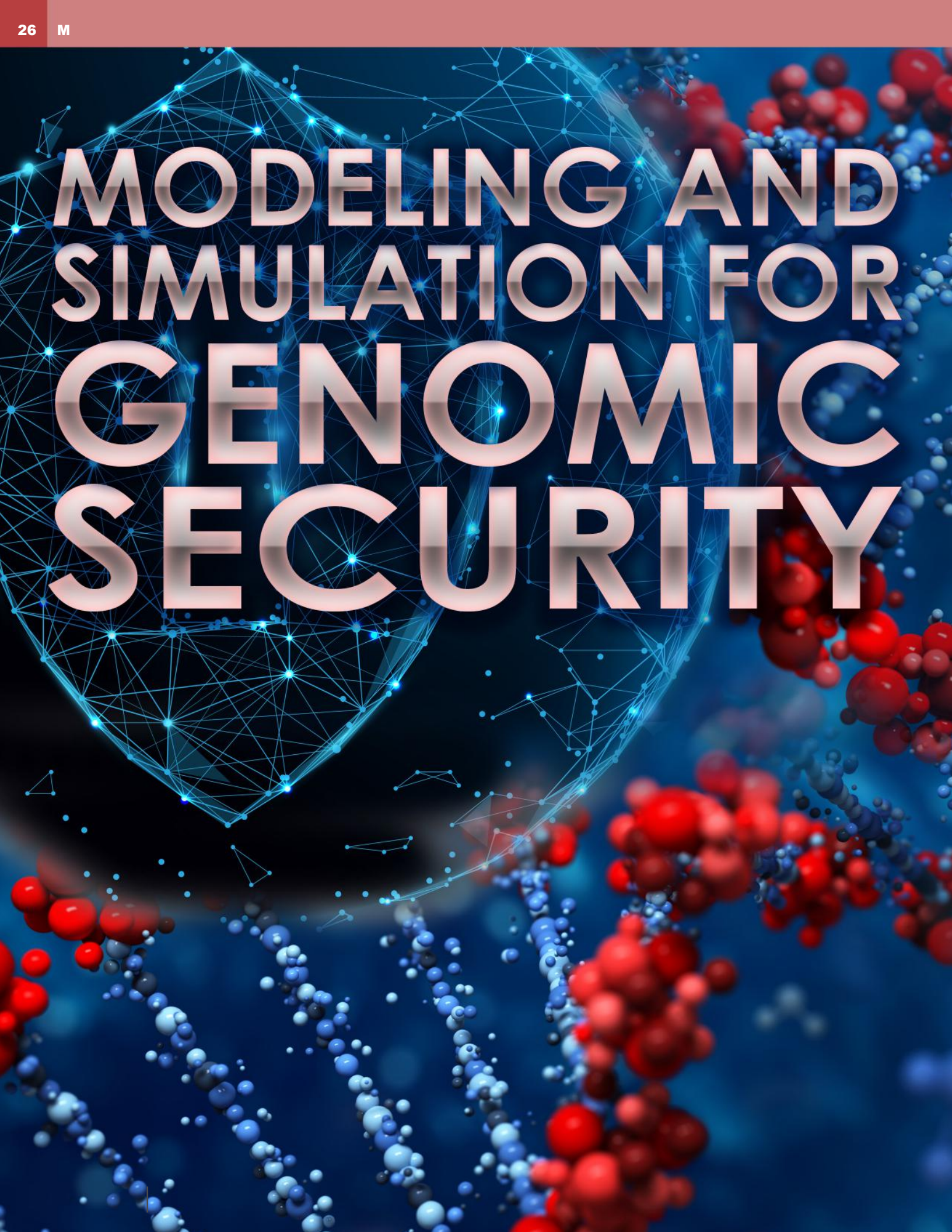
1. Joint Chiefs of Staff. Space Operations (Joint Publication No. 3-14). (2018, April). U.S. Department of Defense. Retrieved from http://www.jcs.mil/Portals/36/Documents/Doctrine/pubs/jp3_14.pdf
2. Space-Track. (n. d.). SAIC. Retrieved from <https://www.space-track.org/>
3. European Space Agency. (2018, February). Space debris. Retrieved from https://www.esa.int/Our_Activities/Operations/Space_Debris/About_space_debris
4. Liou, J.-C. (2018, February). USA Space debris environment, operations, and research updates. Paper presented at the 55th Session of the Scientific and Technical Subcommittee Committee on the Peaceful Uses of Outer Space, United Nations, Vienna, AUT. Retrieved from <https://ntrs.nasa.gov/archive/nasa/casi.ntrs.nasa.gov/20180001749.pdf>
5. European Space Agency. (2018, January). Space debris by the numbers. Retrieved from https://www.esa.int/Our_Activities/Operations/Space_Debris/Space_debris_by_the_numbers
6. NASA. (2018, April). *Handbook for Limiting Orbital Debris* (NASA-HANDBOOK 8719.14). Washington, D.C. Retrieved from <https://standards.nasa.gov/standard/nasa/nasa-hdbk-871914>
7. Regeon, P. A. (2002, September 30). Military Global Positioning System (GPS) Augmentation System (MGAS). Arlington, VA: Office of Naval Research. Retrieved from <http://www.dtic.mil/dtic/tr/fulltext/u2/a630533.pdf>
8. Federal Aviation Administration. (2018, June 26). Satellite Navigation - Wide Area Augmentation System (WAAS). Retrieved from https://www.faa.gov/about/office/org/headquarters_offices/ato/service_units/techops/navservices/gnss/waas/
9. Air Force Space Command. (2016, December). Space based infrared system. Retrieved from <http://www.afspc.af.mil/About-Us/Fact-Sheets/Display/Article/1012596/space-based-infrared-system/>
10. Air Force Space Command. (2017, March 22). Geosynchronous space situational awareness program. Retrieved from <http://www.afspc.af.mil/About-Us/Fact-Sheets/Article/730802/geosynchronous-space-situational-awareness-program-gssap/>
11. Brew, J., & Holzinger, M. (2018). Probabilistic resident space object detection using archival THEMIS fluxgate magnetometer data. *Advances in Space Research*, 61(9), 2301–2319. doi:10.1016/j.asr.2018.01.045
12. Becker, D., & Cain, S. (2018). Improved space object detection using short-exposure image data with daylight background. *Applied Optics*, 57(14), 3968–3975. doi:10.1364/AO.57.003968
13. Vallduriola, G., Scharf, A., Pittet, J., Utzmann, J., Trujillo, D., Vananti, A., . . . Daens, D. (2018, June). The use of different architectures and streak observations algorithms to detect space debris. *ARCS Workshop 2018: 31th International Conference on Architecture of Computing Systems*. Retrieved from <https://ieeexplore.ieee.org/document/8385435/>
14. Freedman, J., & Halvorson, E. (2018). *U.S. Patent No. 9916507*. Washington, DC: U.S. Patent and Trademark Office.
15. Chow, B. G. (2018, Summer). Space arms control: A hybrid approach. *Strategic Studies Quarterly*. Retrieved from http://www.airuniversity.af.mil/Portals/10/SSQ/documents/Volume-12_Issue-2/Chow.pdf
16. Air Force Office of Scientific Research. (2018/12/15-2020/12/14). URED Project Abstract: C1160 An Integrated Approach to Space Situational Awareness. EF128595.
17. Air Force Office of Scientific Research. (2015/08/15-2019/02/14). URED Project Abstract: Innovations in Statistical Image Analysis and Applications to 3D Imaging for Improved SSA. EF126284.
18. Air Force Office of Scientific Research. (2016/04/15-2019/04/14). URED Project Abstract: Advanced Orbit Prediction for Resident Space Objects through Physics-based Learning. EF127426.
19. Air Force Office of Scientific Research. (2017/12/05-2018/12/14). URED Project Abstract: STARBROOK EXPRESS Dynamic Calibration of Sensor Measurements for Near Real-time Space Object Tracking and Characterization. EF130266.
20. Air Force Office of Scientific Research. (2015/12/01-2017/11/30). URED Project Abstract: Finite Set Statistics on Manifolds for Space Object. EF127106.
21. Air Force Office of Scientific Research. (2015/07/15-2018/07/14). URED Project Abstract: Optimal Sensor Tasking for Space Situational Awareness. EF126320.
22. Small Business Innovation Research (SBIR) Program. (2017). Rapid Discovery of Evasive Satellite Behaviors. Topic Number AF17-CT02. Retrieved from <https://www.sbir.gov/sbirsearch/detail/1319195>
23. Nastasi, K. M., & Black, J. (2018). An autonomous sensor management strategy for monitoring a dynamic space domain with diverse sensors. *2018 AIAA Information Systems-AIAA Infotech @ Aerospace* (AIAA 2018-0890). doi:10.2514/6.2018-0890
24. Faber, W. R., Hussein, I. I., Kent, J. T., Bhattacharjee, S., & Jah, M. (2018). Optical data processing using directional statistics in a multiple hypothesis framework with maneuvering objects. *2018 AIAA Information Systems-AIAA Infotech @ Aerospace* (AIAA 2018-1971). doi:10.2514/6.2018-1971
25. Liou, J.-C. (2018). *USA space debris environment, operations, and research updates*. Presented at the 55th Session of the Scientific and Technical Subcommittee Committee on the Peaceful Uses of Outer Space, United Nations, Vienna. Retrieved from <https://ntrs.nasa.gov/archive/nasa/casi.ntrs.nasa.gov/20180001749.pdf>
26. NASA. (n. d.). Astromaterials Research & Exploration Science. Retrieved from <https://orbitaldebris.jsc.nasa.gov/photo-gallery.html>



Chad Pyle
Technical Research Specialist and Software Developer, HDIAC

Chad Pyle is a technical research specialist and software developer for HDIAC. He holds a B.S. in physics from the University of Tennessee where he worked with the Astrophysics Group at Oak Ridge National Laboratory creating and studying computational models of the stellar remnants of core-collapse supernova. Pyle also has background in physics-based combat solutions in video games and web development.

MODELING AND SIMULATION FOR GENOMIC SECURITY



Corey Hudson & Glory Aviña

In 2011, the National Academies of Sciences, Engineering, and Medicine released a major report titled, *Toward Precision Medicine: Building a Knowledge Network for Biomedical Research and a New Taxonomy of Disease* [1]. Looking to develop a framework for classifying human disease based on molecular biology and epidemiology, the report laid out a roadmap for what would become known as precision medicine. The National Academies proposed that the U.S. government sequence the genomes of a million participants in order to begin developing ways of linking individual medical histories with broader insights drawn from genomic data. In 2015, the Departments of Defense, Health and Human Services, and Veterans Affairs acted upon this recommendation, initiating the “All of Us” million-genome sequencing effort.

Genomic data can aid the Department of Defense (DoD) and the warfighter in a multitude of ways. For example, genetic testing could allow military health personnel to precisely tailor dosages to the rate at which individual warfighters metabolize certain medications, allowing for precise pain management that reduces the potential for dependencies. Genomic data can also provide medical staff with key insights into mental health treatment. A 2018 study of the pharmacogenomics of 1,871 moderately to severely depressed patients found that genetic testing, when combined with targeted prescription, led to substantial improvements in depression outcomes [2]. As both of these examples illustrate, genomic data has the potential to significantly improve warfighter medical treatments and health across a range of medical needs.

Since the start of the All of Us project, hundreds of thousands of human genomes have been fully sequenced. Since the start of the All of Us project, hundreds of thousands of human genomes have been fully sequenced. In January 2017, Illumina—the largest sequencing firm—reported that 500,000 human genomes have been sequenced worldwide, up from just 65,000 two years before [3, 4]. Other groups, including the Eli & Edyth Broad Institute of the Massachusetts Institute of Technology

and Harvard, and BGI (formerly the Beijing Genomics Institute), are also engaged in large-scale sequencing [5–7]. However, reductions in sequencing costs have presented new challenges related to high-volume data storage, distribution, and analysis [8]. Conservative estimates predict that 1 zettabyte of genomic sequencing data will be generated annually by 2025, requiring future data storage capabilities on the exabyte scale [8].

This volume of data may soon overload the ability of conventional on-site storage to hold and process genomic data. Because of this, a large amount of the current and future stored and processed genomic data is being handled by cloud service providers [9]. Genomic data at all levels of processing are potentially sensitive—capable of revealing characteristics of an individual’s identity, including information about sex, disease risk factors, race, and ethnic background. Tools and methods for improving the protection of genomic data are an important consideration for DoD and a requirement for secure operations.

Key Considerations

DoD is the first and most critical layer of homeland defense and security. As such, DoD must protect its warfighters and their associated data, as this work is directly related to national security. Therefore, DoD should be on the cutting edge of cybersecurity research and innovation, ensuring the protection of all systems on which warfighter data is transferred and located.

One major issue with securing genomic data is that its underlying digital infrastructure was built in an academic and generally open-access environment. This means that many of the standard protocols, software, and best practices need to account for risk and misuse. Protecting genomic data requires attention to several key issues:

- (a) Securing the equipment: Including the sequencers, validation equipment, storage devices, etc.
- (b) Assuming that all data providing genomic information (no matter how fragmented) contains information that can be used to target individuals.

(c) Maintaining data integrity over the life-cycle of the data—from creation, processing, analysis, and long-term storage.

(d) Assuming that software pipelines (which may contain a couple or dozens of individual programs) have not had a formal security audit, and that commercial solution packages use open source software.

(e) Understanding that data created or processed for other purposes (e.g., previous medical treatment) may have been handled on cloud servers (including foreign servers).

(f) Appreciating the dual-nature of precision treatment. (Precision treatment is a way of targeting interventions to an individual's personal biochemistry, but this level of data should be protected to avoid data misuse.)

Any full-scale application of genomics in a security setting requires attention to these six issues. There is a clear need to protect genomic data through robust systems and measures. The rapid development of genomic data technology and the lack of full-scale security assessment in genomics has meant that many systems that handle critically important data possess under-studied risks. Furthermore, the piecemeal auditing of systemic parts may lead to gaps in security or reduced capabilities. Modeling and simulating the ways in which genomic data are stored, accessed, and retrieved for analysis is a useful method for testing genomic data systems.

Modeling and Assessment of Genomic Data

One approach to modeling and assessment is to develop a full-scale realistic model, sometimes called “genomics-in-a-box.” These models combine a realistic data source (i.e., human genomic analysis run through an analogous sequencing source), realistic throughput (hundreds to thousands of individuals at a time), and use of the same software and hardware components employed by genomic data systems. Human operators can function *in the loop* during these assessments, making decisions based on realistic scenarios. Researchers at Sandia National Laboratories have termed this modeling strategy Emulytics™.

Emulytics™ comes from the combination of “emulative network computing” and “analytics.” Emulytics™ provides the capability to combine real, emulated, and simulated devices into a single system-level experiment to answer a va-

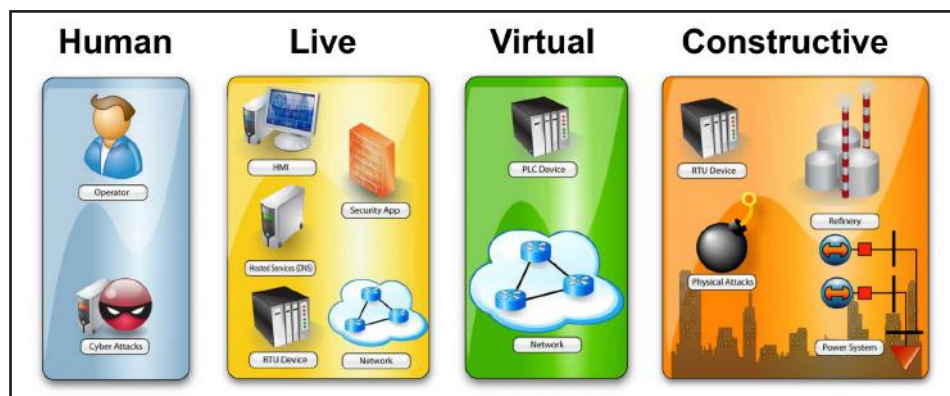


Figure 1. What is Emulytics™? Courtesy of Sandia National Laboratories.

riety of cyber-related questions. Using Emulytics™, one can employ mechanisms to rapidly specify and deploy complex networked information systems of routers, switches, hosts, services, and applications, and integrate systems that can be configured and used for controlled experimentation as well as interactive exploration of system behavior [10].

The Emulytics™ testing approach has several notable features. First, it allows thorough red-teaming without the risk of damage to the primary systems. Second, Emulytics™ allows probing of software and hardware components as well as their interfaces (i.e., the critical and often fragile points where various components must interact). The Emulytics™ testing approach also provides for the assessment and wargaming of data exfiltration and manipulation. This process allows red-teams to “think like the enemy” and determine where the risks lay in infrastructure. The real challenge in this analysis is scaling to the immense amount of genomic data.

Emulytics™ and Genomic Testing

One application of Emulytics™ in genomic security is through the modeling and assessment of large-scale genomic systems. These systems frequently require large suites of software and the interaction of multiple hardware components, handling terabytes of data per day. Incremental assessment may give a sense of which software are vulnerable, but not how these vulnerabilities affect the larger system.

Data Production and Hardware Modeling

A central aspect of Emulytics™ is data production and transfer. There are two main strategies for this production: (a) generation of realistic random data, and (b) the cloning of

real data. There are a variety of methods for randomly generating realistic genomic data. Most of these rely on the random production of non-proprietary data formats (e.g., FASTQ, FASTA, SAM, VCF). The production of this data typically takes an initial data source (e.g., the reference human genome) and splits and randomizes the data, rearranging it into the desired format. The second approach involves mirroring traffic between hardware and software. This requires direct access to the raw data. This may be harder to collect in many instances, but has the distinct advantage of directly modeling the raw data producing equipment (e.g., an Illumina sequencer).

Software Library

A secondary aspect of designing and applying security tests, experiments, and audits is having a library of genomic software. There are no canonical genomic software workflows. Typically, workflows are built based on install suitability, experience with the software, available technical support, speed, performance, and accuracy. There are regularly hundreds of distinct software options strung across each of dozens of steps. Determining the risks posed by a particular software choice oftentimes means having not only the software, but also the version in place. Emulytics™ allows efficient pipeline creation, which can then allow plug-and-play pull and switch for different software alternatives. This is primarily done because there is an existing genomic software library.

External Resources

Oftentimes external resources are included in various aspects of a genomics pipeline. From the systems perspective, a cloud server is simply a storage and processing resource that communicates across particular protocols and limits certain aspects of resource function. Emulytics™ allows quick creation of external

resources. These can be partitioned to investigate different security scenarios. For instance, many of the reference genomes are stored on FTP servers, without encryption. This may create security problems that can be investigated during assessment. Analysts can also, for example, investigate the security vs. performance trade-offs that occur when offboarding fundamental operations to cloud service providers.

Vulnerability Replay

One means of experimental assessment of vulnerabilities is to follow a hypothesis-guided approach. This is the model that Emulytics™ employs. To determine the impact of a known vulnerability, it is important to know what can be held constant, and which vulnerabilities change under evolving conditions. There are issues of scale that create new vulnerabilities, usually owing to automation and decreased visibility. There are also vulnerabilities that may affect entire classes of operations—for example, a flawed data format that can be identified from testing and assessing a variety of software op-

tions. Directing testable security hypotheses requires an ability to make assumptions about which part of the system can be held constant and to create and test alternative scenarios by varying other parts of the system.

Conclusion

The DoD can utilize genomic testing for personalized health management, particularly for military forces. For example, there is great potential in using genomic data to manage pain and mental health. However, keeping access to genomic data secure and safe requires DoD-led research and development.

Protocols, processes, and security plans must be established in order to provide access to genomic data by authorized parties and limiting access only to those individuals. Emulytics™ is one methodology that can be leveraged to expand genomic security research and development by understanding where the vulnerabilities are at different levels of scale, and building solutions and mitigation plans to address them.

The overall goal for genomic security is for warfighters to keep their data secure but accessible to those who are assisting the mission. Cybersecurity experimentation through Emulytics™ could help to continuously move us in that direction.

Disclaimer

Supported by the Laboratory Directed Research and Development program at Sandia National Laboratories, a multi-mission laboratory managed and operated by National Technology and Engineering Solutions of Sandia, LLC, a wholly owned subsidiary of Honeywell International, Inc., for the U.S. Department of Energy's National Nuclear Security Administration under contract DE-NA0003525. This paper describes objective technical results and analysis. Any subjective views or opinions that might be expressed in the paper do not necessarily represent the views of the U.S. Department of Energy or the United States Government. SAND2018-13633 J.

References

1. National Research Council (2011). *Toward Precision Medicine: Building a Knowledge Network for Biomedical Research and a New Taxonomy of Disease*. Washington, D.C., *The National Academies Press*. doi: 10.17226/13284
2. Tanner, J.-A., et al. (2018). Combinatorial pharmacogenomics and improved patient outcomes in depression: Treatment by primary care physicians or psychiatrists. *Journal of psychiatric research* 104: 157-162. doi: 10.1016/j.jpsychires.2018.07.012
3. Herper, M. (2017). Illumina Promises to Sequence Human Genome for \$100 - But Not Quite Yet. *Forbes*. Retrieved from <https://www.forbes.com/sites/matthewherper/2017/01/09/illumina-promises-to-sequence-human-genome-for-100-but-not-quite-yet/#6971dac8386d>
4. Gebelhoff, R. (2015). Sequencing the genome creates so much data we don't know what to do with it. *The Washington Post*. Retrieved from https://www.washingtonpost.com/news/speaking-of-science/wp/2015/07/07/sequencing-the-genome-creates-so-much-data-we-dont-know-what-to-do-with-it/?utm_term=.494c19cdf76d
5. Broad Communications (2018). Broad Institute Sequences its 100,000th whole human genome on National DNA Day. *Broad Communications*. Retrieved from <https://www.broadinstitute.org/news/broad-institute-sequences-its-100000th-whole-human-genome-national-dna-day>
6. BGI (2018). "Genome DECODE Program." *Genome DECODE Program*. Retrieved 20 August 2018, from <https://gdp.bgi.com/page/index/en/>.
7. Helmy, M., et al. (2016). Limited resources of genome sequencing in developing countries: Challenges and solutions. *Applied and Translational Genomics* 9: 15-19. doi: 10.1016/j.atg.2016.03.003
8. Stephens, Z. D., et al. (2015). Big data: astronomical or genetical? *PLoS biology* 13(7): e1002195. doi: 10.1371/journal.pbio.1002195
9. Langmead, B. and A. Nellore (2018). Cloud computing for genomic data analysis and collaboration. *Nature Review Genetics* 19: 208-219.
10. Urias, V., et al. (2015). Emulytics™ at Sandia National Laboratories. *MODSIM World*, Virginia Beach, VA.



Corey M. Hudson, Ph.D.
Computational Biologist, Sandia National Laboratories – Livermore

Corey Hudson is a computational biologist at Sandia National Laboratories located in Livermore, California. He has a Ph.D. in Informatics from the University of Missouri. Corey has been at Sandia since 2013 and leads teams in cybersecurity, machine learning, synthetic biology and genomics. His principal work is modeling and simulating cybersecurity risks in realistic and large-scale genomic systems and highly automated synthetic biology facilities.



Glory Aviña, Ph.D.
Quantitative Psychologist, Sandia National Laboratories – Livermore

Glory Aviña is a quantitative psychologist at Sandia National Laboratories, located in Livermore, California. She has a Ph.D. in experimental psychology and an MBA in international management from the University of New Mexico. Aviña has been at Sandia since 2006 and formerly managed the Wearables at The Canyon for Health project, funded by the Defense Threat Reduction Agency's Chemical and Biological Technologies department. She now serves as manager of the Cyber Security Assessment department which helps steward Emulytics™. Her expertise is in human-subjects studies, quantifying the human dimension through experimental design and novel analytics, and managing cognitive load through intelligent web crawling and text analytics.



Homeland Defense & Security
Information Analysis Center

Technical Inquiry Services

Four **Free Hours** of Research within our eight focus areas Available to **academia, industry, and other government agencies**



Focus Areas

Alternative Energy
Biometrics
CBRN Defense
Critical Infrastructure
Cultural Studies
Homeland Defense
Medical
WMD

Log on to hdiac.org to submit a
technical inquiry form
or contact inquiries@hdiac.org

ELECTRONIC STICKERS

FOR WIRELESS PHYSIOLOGICAL MONITORING IN A TACTICAL ENVIRONMENT



Carmel Majidi

Wireless physiological sensing in tactical environments has the potential to greatly enhance health outcomes in combat casualty care. Not only does it provide actionable data for field care; it can also supply personal health metrics and environmental data for use in downrange care, medical research, and strategic planning [1].

Such wireless sensing systems can also be used to detect warfighter fatigue, “thermal work strain [2],” chemical or biological exposure [3], and dynamic physical information that could be useful to a team operating in the field (e.g., activity classification, gesture monitoring) [4]. More broadly, wearable physiological status monitoring (PSM) devices represent a new class of military technologies that has the potential to improve readiness and “support decisions and actions in response to operating in a threat environment [5, 6].”

To meet this potential, such systems should (a) operate in real time, (b) function wirelessly, (c) be capable of multi-modal sensing, and (d) be compatible with existing situational awareness systems like Nett Warrior.

The development of wireless PSM technologies for tactical combat casualty care (TCCC) and warfighter readiness has involved the adaptation of commercial wearables [3, 1] as well as the pursuit of new research into novel material architectures and sensor technologies. The former includes commercial off-the-shelf devices like smartwatches, activity/fitness trackers, and augmented reality headsets (including “smart glasses”). While these devices are readily available and offer plug-and-play functionality, they have limited sensing modalities and satisfy only a few of the requirements for tactical PSMs. Instead, progress in this space depends on achieving fundamental research and development (R&D) advancements in wearables technology. As described below, these efforts fall within the following categories: (a) novel biological and chemical sensors, (b) material

architectures for stretchable, skin-mountable circuitry, and (c) methods for the integration of microelectronics for sensing, signal processing, and wireless data transmission.

Biological and Chemical Sensors

In recent years, researchers have achieved remarkable progress developing sensors that use lab-on-a-chip microfluidics, genetic engineering, and/or synthetic biology to detect biomarkers, toxins, and other biological or chemical analytes. These sensors typically measure analytes via electrochemical or optical/visual cues based on photonics or fluorescence [7]. The sweat-sensing patch discussed in Rose et al. [8] is illustrative of the state of advanced wearable biosensing technology.

The patch is a bandage-like electronic sticker that contains functionalized electrodes for measuring Na^+ concentrations in sweat; a microfluidic paper pad for fluid and vapor transport; and radio-frequency identification (RFID) circuitry for the near field communication (NFC)

Image Credit

Photo illustration created by HDIAC and adapted from a photo by CMU Morphing Matter Lab (PI: Lining Yao), CMU Soft Machines Lab (PI: Carmel Majidi), a U.S. Army photo (Available for viewing at: <https://asc.army.mil/web/news-female-specific-body-armor-earns-high-praise/>), and Adobe Stock.

of sensor readings to a nearby smartphone. Although this particular model only measures concentrations of sodium, its electrodes could be functionalized with an ion-selective polymer ionophore membrane to measure K^+ , Cl^- , Mg^{2+} , and other ions that can be used to establish baseline physiological states and monitor changes in the balance of electrolytes within sweat. Such multiplexed perspiration analysis was subsequently demonstrated in a multi-electrode patch capable of measuring glucose and lactate concentrations (see Figure 1A) [9]. In lieu of RFID-based communications, the patch interfaces with a smartphone via Bluetooth radio transceiver. While this allows for higher bandwidths in data transmission, it does require an on-board battery and electronics for power regulation. In both implementations, wearable electronic functionality is accomplished using a flexible printed circuit board (fPCB). Although not *stretchable*, fPCBs display adequate compliance for conformable contact with select parts of the body, including the wrist, forehead, or chest.

Another example of advanced biosensing is the hybrid sensor shown in Figure 1B, which combines electrophysiological and chemical biosensing modalities [10]. This sensor is composed of a thin, flexible polyester sheet connected to a Bluetooth transceiver, a printed circuit board for signal processing, and a series of screen-printed electrodes capable of both sweat lactate sensing and electrocardiography (ECG). Because of its mechanical compliance, the sensor can conform to the body, and is capable of simultaneously monitoring cardiac activity (e.g., heart rate) and lactate levels during perspiration. As with the other implementations discussed above, the sensors reported by Imani et al. [10] are flexible but not stretchable.

In general, mechanical flexibility is essential for ensuring close contact and acquiring accurate physiological status measurements. For some applications, however, flexibility is not enough—the sensor should also be stretchable and able to support high elastic strains. This allows the sensor to be placed on joints or rounded (i.e., non-developable) parts of the body without running the risk of impairing natural motion or delaminating. Stretchable functionality in a biosensor

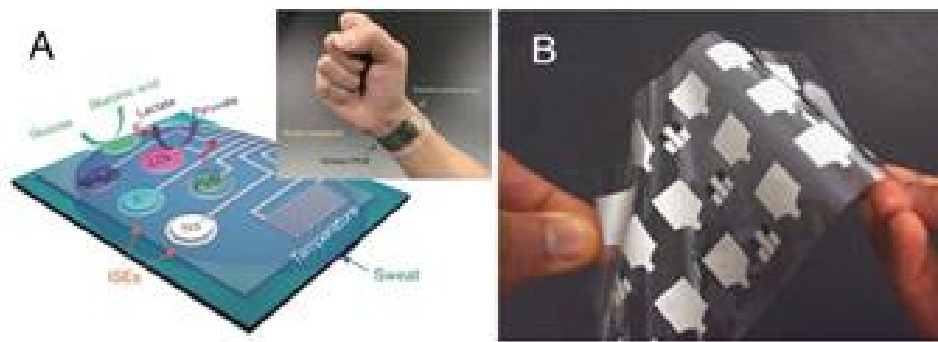


Figure 1. (A) Multi-electrode sweat-sensing patch for more complete perspiration analysis [9]. (B) Flexible biosensor capable of ECG and sweat sensing [10].

would also enable its incorporation into stretchable fabrics that can be pulled over the skin.

Therefore, R&D efforts in wearable PSM technology are increasingly focused on ways to combine biosensors with skin-like electronics that are soft and elastic, as well as thin and flexible.

Epidermal Electronics

One approach for achieving stretchable functionality is to create wearable circuits using wavy or serpentine wiring. This so-called *deterministic* approach to stretchable circuits is commonly used in epidermal electronics like the multi-modal wireless sensor shown in Figure 2A [11]. Such a circuit measures a variety of biosignals, including ECG, temperature, and strain, and transmits its data via NFC. As with the sweat sensing patch reported in Rose et al. [8], this circuit does not require an on-board battery, instead harvesting power through electromagnetic induction. Such multi-modal sensing allows for a wide range of PSM functionalities, such as tracking muscle contractions, cardiac monitoring, and electroencephalography for monitoring alpha wave oscillations associated with neural activity.

The serpentine shape of the traces allows the circuit to stretch or wrinkle while preserving the natural mechanics of the skin. Such patterning is accomplished using lithographic techniques that combine conventional clean-room microfabrication tools with unconventional materials and novel processing steps.

More recent efforts in epidermal electronics have focused on techniques that

eliminate clean-room lithography in order to enable rapid, inexpensive fabrication. The human-computer interaction R&D community has adopted the popular approach of printing conductive inks on transferrable “temporary tattoo” film using standard commercial inkjet printers. Examples of this approach include the *Skintillates* and *SkinMarks* architectures reported in Lo et al. [12] and Weigel et al. [13], respectively. While these circuits are ultra-thin and allow for very close contact with the body, the circuit traces have limited conductivity and stretchability, and are less reliable than wiring for digital electronics.

Recently, our research group, the Soft Machines Lab at Carnegie Mellon University, partnered with the Soft and Printed Microelectronics Laboratory at the University of Coimbra (Portugal) to develop methods for the rapid and inexpensive fabrication of epidermal electronics that overcome some of the limitations of prior techniques [14]. In this materials architecture, the circuit is composed of thin films of liquid metal (LM) alloy coated on silver-based conductive ink traces printed on a temporary tattoo transfer film. The LM alloy is a non-toxic blend of gallium and indium, fully sealed by the tattoo film and thin coating of silicone elastomer. As shown in Figure 2B, the circuit adheres to skin and can be populated with micro-electronic components.

The LM coating has two functional roles. First, it binds to the conductive ink and prevents the traces from cracking when stretched. Second, it acts as a room-temperature solder for connecting the pins of the surface-mounted microelectronics to the terminals of the thin-film circuit. This novel approach to epidermal electronics

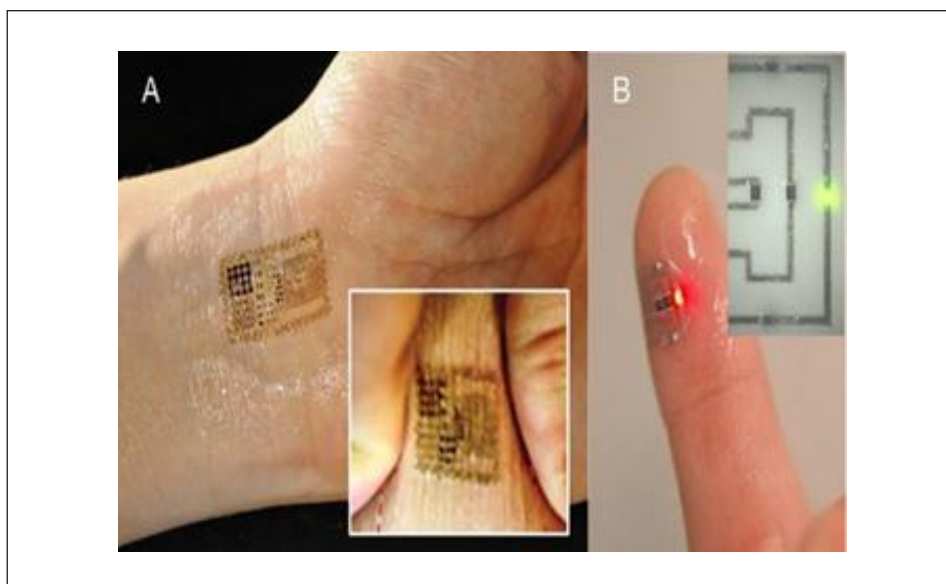


Figure 2. (A) Epidermal electronic circuit for multi-modal physiological sensing [11]. (B) Electronic tattoo with LM-coated conductive ink circuitry [14].



Figure 3. (A) Skin-mounted wireless circuit for pulse oximetry [16]. (B) Flexible glove biosensor with a portable potentiostat mounted to the back of the hand [17].

allows for the seamless integration of integrated-circuit microchips and other packaged microelectronics that could be used for sensing, signal processing, power regulation, and data transmission. As the materials and fabrication methods for stretchable circuits and epidermal electronics grow more sophisticated, R&D efforts must pursue techniques to integrate these circuits with rigid microelectronics for signal processing, wireless communication, and power regulation.

Robust electrical and mechanical interfacing between soft, thin-film circuits and rigid, packaged electronics is challenging because stress concentrations and the potential for material failure are greatest

near regions where there is a mechanical impedance mismatch. Overcoming this challenge is essential for creating soft, sticker-like wireless PSM technologies that maintain digital circuit functionality under bending, stretching, contact pressure, abrasion/rubbing, impact, and other conditions that can arise during TCCC.

Microelectronics Integration

Materials architectures and manufacturing methods for integrating biosensors, thin-film stretchable circuits, and packaged microelectronics stand as an open challenge for the next generation of wearable PSM devices. The complete integration of functional components for wireless biosensors that adhere to the skin (and

operate outside of laboratory conditions) has already met with some success. One example is the Bluetooth-enabled PSM system presented in Figure 3A [15]. Here, serpentine copper wiring and an fPCB are used to create a photonic pulse oximetry circuit that conforms to the tip of a finger. The circuit is able to measure the heart rate and blood oxygenation level of a human subject pedaling on a stationary bike.

The circuit is produced using a laser-based rapid prototyping approach in which copper film is patterned with a 355 nm Nd:YAG UV laser micromachining (UVLM) system, and then transferred to a medical-grade adhesive using a selective bonding technique. The circuit is then sealed with a z-axis tape that is conductive through its thickness and allows for via connections between the circuit terminals and surface-mounted electronics. The latter includes a pulseox chip and fPCB with components for battery power and Bluetooth. More recently, a z-axis conductor has been incorporated into a soft and wearable pulseox circuit in which the serpentine copper traces were replaced with gallium-based LM wiring that was also patterned using UVLM [15].

The integration of a wearable sensor and body-mounted electronics is also presented in Mishra et al. [16], which combines flexible and textile-based sensors for vapor-phase detection of organophosphorus agents. In this implementation, the biosensing circuit is connected to a portable potentiostat attached to the back of the hand (Figure 3B). The potentiostat performs electrochemical characterization and wirelessly transmits the readings to a smartphone. Whereas the integrated system reported by Bartlett et al. [17] functions like a data skin or electronic sticker, the device in Mishra et al. [16] is described as a "lab-on-a-glove" that combines wireless electronics and wearable biosensing with electrochemical analysis.

Conclusions

Compared to the ruggedized portable medical devices currently used in TCCC applications, the wireless PSM sticker technologies presented above are in a nascent stage of development. Nevertheless, recent years have witnessed

promising advancements in the merging of soft materials engineering with micro-fabrication and microelectronics. This has enabled the creation of integrated, wireless, and skin-adhesive biosensing PSM technologies. Further progress may require more robust methods for interfacing stretchable circuitry with rigid microelectronic components. Another challenge for next-generation wearables is the provision of electrical power.

This is especially true in prolonged field care scenarios, in which a sensor must remain operational for up to 72 hours. One promising approach is to use alternative energy sources, like the biofuel cell introduced in Garcia et al. [18] to

power a sensor for sweat lactate monitoring. Innovations like these represent an exciting step toward next-generation PSM technologies capable of supporting prolonged operation with limited maintenance or user intervention.

As the material architectures for wireless PSM stickers mature, future efforts should seek to improve the algorithms that translate biosensor readings into actionable data. Such algorithms must account for variations in sensor placement on the body, physical activity, and individual physiology. Compared to conventional medical equipment, wireless electronic stickers enabled with continuous real-time monitoring introduce chal-

lenges related to perspiration, changes in physical activity and environment, and motion artifacts.

Addressing these challenges will require extensive clinical and field studies in order to source data, perform expert-supervised classification, and create training sets that can be incorporated into learning-based algorithms for diagnostics and decision-making. Integrating PSM technologies into TCCC practice may also require the eventual replacement of civilian wireless standards and data management tools with Department of Defense-approved systems.

References

- Montgomery, R. R., & Anderson, Y. L. (2016, March). *Battlefield medical network: Biosensors in a tactical environment* (Master's thesis). Monterey, CA: Naval Postgraduate School. Retrieved from <http://www.dtic.mil/dtic/tr/fulltext/u2/1027506.pdf>
- Looney, D. P., Buller, M. J., Welles, A. P., Leger, J. L., Stevens, M., Gribok, A. V., Hoyt, R. W., & Rimpler, W. V. (2017, May). Accuracy of ECTemp models in predicting core temperature and circadian rhythm indicators from heart rate: 1600 Board #275 June 1 900 AM – 1030 AM. *Medicine & Science in Sports & Exercise*, 49(5S), 454. doi:10.1249/01.mss.0000518130.78412.af
- Aviña, G., & Nichols, G. (2018, March 22). Wearables for physiological monitoring and the DoD [Webinar]. Homeland Defense & Security Information Analysis Center. Retrieved from <https://www.hdiac.org/webinar/hdiac-webinar-wearables-for-physiological-monitoring-and-the-dod/>
- Metu, S., Sadler, L., & Winkler, R. (2015). Wearable notification via dissemination service in a pervasive computing environment (Rep. No. ARL-TR-7449). Adelphi, MD: Army Research Laboratory, Computational an Information Sciences Directorate. Retrieved from <https://www.arl.army.mil/arl-reports/2015/ARL-TR-7449.pdf>
- Hirschberg, D. L., Samuels, A. C., Rosenzweig, C. N., Lux, M. W., Emanuel, P. A., Miklos, A. E., . . . Brooks, J. R. (2016, May). Assessment of wearable technology for integrated decision support (Rep. No. ECBC-TR-1377). Fort Belvoir, VA: Defense Threat Reduction Agency. Retrieved from <http://www.dtic.mil/dtic/tr/fulltext/u2/1009537.pdf>
- Friedl, K. E., Buller, M. J., Tharion, W. J., Potter, A. W., Manglapus, G. L., & Hoyt, R. W. (2016, March). Real time physiological status monitoring (RT-PSM): Accomplishments, requirements, and research roadmap (Rep. No. TN16-2). Natick, MA: U.S. Army Research Institute of Environmental Medicine. Retrieved from <http://www.dtic.mil/dtic/tr/fulltext/u2/a630142.pdf>
- Vigneshvar, S., Sudhakumari, C. C., Senthilkumaran, B., & Prakash, H. (2016, February 16). Recent advances in biosensor technology for potential applications – An overview. *Frontiers in Bioengineering and Biotechnology*, 4(11), 1–9. doi:10.3389/fbioe.2016.00011
- Rose, D. P., Ratterman, M. E., Griffin, D. K., Hou, L., Kelley-Loughnane, N., Naik, R. R., . . . Heikenfeld, J. C. (2015, June). Adhesive RFID sensor patch for monitoring of sweat electrolytes. *IEEE Transactions on Biomedical Engineering*, 62(6), 1457–1465. doi:10.1109/TBME.2014.2369991
- Gao, W., Emaminejad, S., Nyein, H. Y. Y., Challa, S., Chen, K., Peck, A., . . . Lien, D. H. (2016, January 28). Fully integrated wearable sensor arrays for multiplexed in situ perspiration analysis. *Nature*, 529(7587), 509–514. doi:10.1038/nature16521
- Imani, S., Bandodkar, A. J., Mohan, A. V., Kumar, R., Yu, S., Wang, J., & Mercier, P.P. (2016, May 23). A wearable chemical–electrophysiological hybrid biosensing system for real-time health and fitness monitoring. *Nature Communications*, 7(11650), 1–7. doi:10.1038/ncomms11650
- Kim, D-H., Lu, N., Ma, R., Kim, Y. S., Kim, R. H., Wang, S., . . . Yu, K.J. (2011, August 12). Epidermal electronics. *Science*, 333(6044), 838–843. doi:10.1126/science.1206157
- Lo, J., Lee, D. J. L., Wong, N., Bui, D., & Paulos, E. (2016, June). Skintillates: Designing and creating epidermal interactions. *Proceedings of the 2016 ACM Conference on Designing Interactive Systems*, 853–864. doi:10.1145/2901790.2901885
- Weigel, M., Nittala, A. S., Olwal, A., & Steimle, J. (2017, May). SkinMarks: Enabling interactions on body landmarks using conformal skin electronics. *Proceedings of CHI 2017 (SIGCHI Conference on Human Factors in Computing Systems)*, 3095–3105. doi:10.1145/3025453.3025704
- Tavakoli, M., Malakooti, M. H., Paisana, H., Ohm, Y., Marques, D. G., Alhais Lopes, P., . . . Majidi, C. (2018, July). EGain-assisted room-temperature sintering of silver nanoparticles for stretchable, inkjet-printed, thin-film electronics. *Advanced Materials*, 30(29), 1801852. doi:10.1002/adma.201801852
- Lu, T., Markvicka, E. J., Jin, Y., & Majidi, C. (2017, June). Soft-matter printed circuit board with UV laser micropatterning. *ACS Applied Materials & Interfaces*, 9(26), 22055–22062. doi:10.1021/acsami.7b05522
- Mishra, R. K., Hubble, L. J., Martin, A., Kumar, R., Barfidokht, A., Kim, J., . . . Wang, J. (2017, March). Wearable flexible and stretchable glove biosensor for on-site detection of organophosphorus chemical threats. *ACS Sensors*, 2(4), 553–561. doi:10.1021/acssensors.7b00051
- Bartlett, M. D., Markvicka, E. J., & Majidi, C. (2016, September). Rapid fabrication of soft, multilayered electronics for wearable biomonitoring. *Advanced Functional Materials*, 26(46), 8496–8504. doi:10.1002/adfm.201602733
- Garcia, S. O., Ulyanova, Y. V., Figueroa-Teran, R., Bhatt, K. H., Singhal, S. and Atanassov, P. (2016). Wearable sensor system powered by a biofuel cell for detection of lactate levels in sweat. *ECS Journal of Solid State Science and Technology* 5(8), M3075–M3081. doi:10.1149/2.0131608jss



Carmel Majidi, Ph.D.
Associate Professor, Mechanical Engineering, Carnegie Mellon University

Carmel Majidi, Ph.D., is an associate professor of Mechanical Engineering at Carnegie Mellon University, where he leads the Soft Machines Lab. His research group leverages insights and practices from solid mechanics, microfabrication, and bio-inspired robotics to create machines and electronics that are primarily composed of soft and mechanically deformable materials. Majidi is particularly interested in approaches that are practical from a rapid prototyping, wearable computing, or robotics implementation perspective. This includes efforts to enable robust mechanical and electrical interfacing between soft-matter systems and conventional microelectronics. He has received Young Investigator Awards from DARPA, ONR, AFOSR, and NASA.

REVIVING DORMANT NERVES

AFTER SPINAL CORD INJURY



Bo Chen & Zhigang He

Spinal cord injuries (SCI) occur frequently in combat. One study, completed in 2015, indicated that the incidence of combat spinal trauma during the conflicts in Iraq and Afghanistan may range from 7.4 percent to 12 percent of all warfighter injuries [1, 2]. In both military and civilian-related cases of SCI, most patients do not end up with a completely transected spinal cord. However, more than 50 percent of these patients completely lose muscle control and sensation below the injury level [3, 1]. This suggests that spared connections in incompletely transected spinal cords are functionally dormant.

As we researched strategies to turn on these spared circuits, we discovered that enhancing functions of the potassium chloride (K⁺/Cl⁻) co-transporter 2 (KCC2) protein—by either pharmacological or gene therapy approaches—is able to activate intraspinal relay

pathways and lead to functional recovery in a mouse model of SCI [1]. These findings suggest a new strategy for improving recovery after SCI in humans.

Challenges

Functional deficits associated with SCI result from damaged anatomical connections and failed information exchange between the brain and the portion of the spinal cord below the lesion [4]. Therefore, a large focus of research and development in the field has been to develop strategies that promote nerve regeneration to rebuild the lost connections [5, 6].

However, it is known that in many patients with full functional deficits, not all connections are severed—raising the question of why such spared connections are non-functional. Interestingly, clinical studies have shown that when combined with rehabilitative training, electrical spinal stimulation applied to the spinal cord can result in a certain degree of voluntary functional recovery in chronically-paralyzed patients, likely by activating the dormant spared connec-

tions [7, 8]. However, once the stimulation is removed, the recovered function immediately disappeared. Thus, it is crucial to understand why the spared spinal circuitry is dysfunctional after a spinal cord injury and how it can be more persistently reactivated.

Non-biased Screening for Function-Enhancing Small Molecule Compounds

SCI triggers numerous alterations in the neuronal circuits in and out of the spinal cord. In light of the success of electrical stimulation, we reasoned that altering neuronal excitability might be a way to activate the dormant connections. Thus, we conducted a small-scale compounds screening in staggered lesioned mice with two hemisections at thoracic level T10 and, contralaterally, at T7. This model spares axons crossing the midline between T7 and T10, but still results in hindlimb paralysis [9, 10]. Among all compounds tested, we found that treatment of CLP290, a KCC2 agonist [11], for 6–8 weeks best restored weight-bearing stepping ability in paralyzed mice (see Figure 1). Such treat-

ment failed to improve functions in mice with total transection at T8, suggesting that it likely targets the dormant intraspinal relay pathways.

KCC2-based Gene Therapy Promotes Functional Recovery

Previous studies conducted by other research groups have observed KCC2 down-regulation in injured spinal cords [12, 13], but KCC2's relevance to functional deficits and recovery has not been formally tested. To fill this gap, we used viral vector-based strategies to over-express KCC2 in different groups of neurons and assessed the functional outcomes. We found that non-selective expression of KCC2 in all neurons of the brain and spinal cord mimics the effects of CLP290.

Strikingly, selective expression of KCC2 in inhibitory interneurons between and around the staggered spinal lesions was sufficient to achieve improved functional recovery in injured mice with double hemisection at T7 and T10. These data suggest that the downregulation of KCC2 in inhibitory interneurons, which are part of the spared intraspinal relays, renders the circuit dysfunctional and prevents functional recovery in incomplete SCI. Consistent with these results, our mechanistic studies further showed that KCC2-related treatments transformed the injured spinal circuit from a

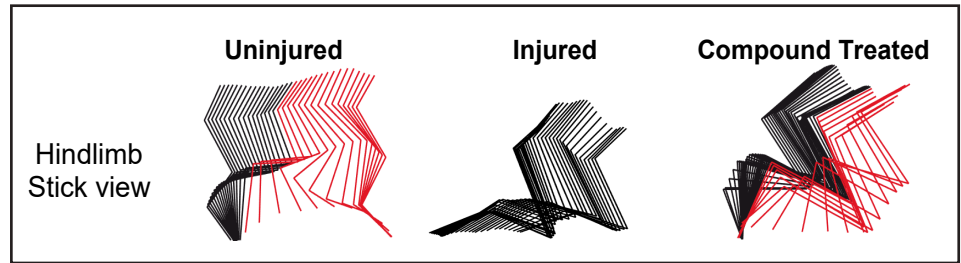


Figure 1. Color-coded stick view decomposition of mouse hindlimb movements during walking (uninjured), dragging (injured) and stepping (compound treated injured group) [4].

mal-functional to a functional state, which in turn facilitated the transmission of brain-derived signals to the lumbar spinal cord below the lesion.

Conclusions

Our results indicate that injury-induced KCC2 down-regulation is a critical mechanism that contributes to the dysfunction of spared neuronal connections after SCI. Importantly, restoring KCC2 function could reinstate the ability of spared neuronal connections to participate in the spinal relays involved in hindlimb function.

Because KCC2 agonists could be administered systematically without detectable side effects [4, 11], this approach may have direct implications in clinical treatments of SCI. Further development of this approach may ac-

celerate the rate at which injured warfighters recover from the debilitating effects of SCI.

Towards this goal, further studies should assess the functional outcomes of such manipulations in other injury models and seek to optimize a therapeutic regimen for possible clinical studies. As electrical stimulation may modulate neuronal excitability, it would be informative to assess (a) whether shared or distinct mechanisms underlie the action of electrical stimulation and KCC2 manipulations, and (b) whether these methods could be used in combination to further enhance the extents and/or duration of functional recovery after SCI. Finally, major advances have been made elsewhere in developing strategies to promote axon regeneration, which could be combined with KCC2-mediated modulations to maximize functional restoration after SCI.

References

- Bernstock, J. D., Caples, C. M., Wagner, S. C., Kang, D. G., & Lehman, R. A. Jr. (2015). Characteristics of combat-related spine injuries: A review of recent literature. *Military Medicine*, 180(5), 503–512. doi:10.7205/MILMED-D-14-00215
- Schoenfeld, A. J., Newcomb, R. L., Pallis, M. P., Cleveland, A. W. 3rd, Serrano, J. A., Bader, J. O., . . . Belmont, P. J. Jr. (2013). Characterization of spinal injuries sustained by American service members killed in Iraq and Afghanistan: A study of 2,089 instances of spine trauma. *Journal of Trauma and Acute Care Surgery*, 74(4), 1112–1118. doi:10.1097/TA.0b013e31828273be
- Kakulas, B. A. (1999). A review of the neuropathology of human spinal cord injury with emphasis on special features. *Journal of Spinal Cord Medicine*, 22, 119–124. doi:10.1080/10790268.1999.11719557
- Chen, B., Li, Y., Yu, B., Zhang, Z., Brommer, B., Williams, P. R., . . . He, Z. (2018). Reactivation of dormant relay pathways in injured spinal cord by KCC2 manipulations. *Cell*, 174(3), 521–535. doi:10.1016/j.cell.2018.06.005
- Sofroniew, M. V. (2018, May). Dissecting spinal cord regeneration. *Nature*, 557(7705), 343–350. doi:10.1038/s41586-018-0068-4
- He, Z., & Jin, Y. (2016, May 4). Intrinsic control of axon regeneration. *Neuron*, 90(3), 437–451. doi:10.1016/j.neuron.2016.04.022
- Angeli, C. A., Edgerton, V. R., Gerasimenko, Y. P., & Harkema, S. J. (2014, May). Altering spinal cord excitability enables voluntary movements after chronic complete paralysis in humans. *Brain*, 137(Pt 5), 1394–1409. doi:10.1093/brain/awu038
- Harkema, S., Gerasimenko, Y., Hodes, J., Burdick, J., Angeli, C., Chen, Y., . . . Edgerton, V. R. (2011, June 4). Effect of epidural stimulation of the lumbosacral spinal cord on voluntary movement, standing, and assisted stepping after motor complete paraplegia: A case study. *Lancet*, 377(9781), 1938–1947. doi:10.1016/S0140-6736(11)60547-3
- Courtine, G., Song, B., Roy, R. R., Zhong, H., Herrmann, J. E., Ao, Y., . . . Sofroniew, M. V. (2008, January). Recovery of supraspinal control of stepping via indirect propriospinal relay connections after spinal cord injury. *Nature Medicine*, 14(1), 69–74. doi:10.1038/nm1682
- an den Brand, R., Heutschi, J., Barraud, Q., DiGiovanna, J., Bartholdi, K., Huerli-mann, M., . . . Courtine, G. (2012, June 1). Restoring voluntary control of locomotion after paralyzing spinal cord injury. *Science*, 336(6085), 1182–1185. doi:10.1126/science.1217416
- Gagnon, M., Bergeron, M. J., Lavertu, G., Castonguay, A., Tripathy, S., Bonin, R. P., . . . De Koninck, Y. (2013, November). Chloride extrusion enhancers as novel therapeutics for neurological diseases. *Nature Medicine*, 19(11), 1524–1528. doi:10.1038/nm.3356
- Boulenguez, P., Liabeuf, S., Bos, R., Bras, H., Jean-Xavier, C., Brocard, C., . . . Vinay, L. (2010, March). Down-regulation of the potassium-chloride cotransporter KCC2 contributes to spasticity after spinal cord injury. *Nature Medicine*, 16(3), 302–307. doi:10.1038/nm.2107
- Cote, M. P., Gandhi, S., Zambrotta, M., & Houle, J. D. (2014, July 2). Exercise modulates chloride homeostasis after spinal cord injury. *Journal of Neuroscience*, 34(27), 8976–8987. doi:10.1523/JNEUROSCI.0678-14.2014



Bo Chen, Ph.D. (Left) and Zhigang He, Ph.D. (Right)
F.M. Kirby Neurobiology Center of Boston Children's Hospital, Harvard Medical School

Bo Chen, Ph.D., is a research fellow and Zhigang He, Ph.D., is professor of neurology and ophthalmology at F.M. Kirby Neurobiology Center of Boston Children's Hospital, Harvard Medical School. Their main research interests are axon regeneration and functional recovery after spinal cord injury and other forms of CNS injuries.

PRESERVING WARFIGHTER HEARING

OPTICAL COHERENCE TOMOGRAPHY LEADS TO NOVEL AND IMPROVED THERAPIES



**Patricia M. Quiñones,
Brian E. Applegate,
& John S. Oghalai**

The exposure of military personnel to blast trauma—such as that from improvised explosive devices—can lead to ear injury and hearing deficits like sensorineural hearing loss (SNHL) and tinnitus [1]. A study conducted in 2003 found that 69 percent of returning warfighters demonstrated some level of noise-induced hearing loss (NIHL), with a majority suffering from either SNHL (29 percent) or tinnitus (30 percent) [2]. Furthermore, a 2007 study concluded that 58 percent of military personnel who suffered blast-related injuries also presented some type of hearing loss, with SNHL affecting 47 percent of those subjects [3].

Besides affecting a warfighter's ability to function, SNHL produces long-term disabilities that require long-term management and treatment. Hearing loss (due to all causes) affects over 30 million Americans [4]. Currently, further research is necessary to define the optimum acute management and to increase the num-

ber of treatments available for hearing deficits that may occur as a result of conditions on the battlefield [5]. While hearing aids can help to some degree, they are expensive, can be uncomfortable, and do not improve speech clarity. Patients with SNHL have reduced quality of life [6], often because it causes debilitating tinnitus. Therefore, it is imperative to understand the mechanism of injury and to develop therapies based on a molecular understanding of the changes that happen as a result of blast or noise trauma.

A direct means of assessing both inner ear morphology and function is critical for developing treatments for extremely common, yet currently untreatable, battlefield injuries such as blast- and noise-induced sensorineural hearing loss. We are focused on developing optical coherence tomography (OCT) for diagnosing inner ear disease. Using this technique, we show that osmotic disruption of the ear is visible with OCT imaging and the damage can be partially prevented by reversing the imbalance. We find OCT to be an invaluable research tool to understand and develop treatments for blast trauma to the inner ear in animal models. It can

also potentially be further developed to help diagnose and treat human hearing loss.

Optical Coherence Tomography for Live Cochlea Visualization

Our ability to design better interventions for patients is frustrated by the inability to visualize the pathologic tissue damage responsible for the problem within the inner ear. It follows that an optical technique that allows non-invasive visualization of cochlear structures is necessary. OCT is a non-invasive method of visualizing soft-tissue structures on a microscale that is conceptually similar to ultrasound, but uses light rather than ultrasonic waves. OCT is a real-time imaging modality that produces high-resolution 3D images [7, 8]. By directing a light beam onto tissue and measuring back-scattered light as a function of depth, OCT provides non-invasive subsurface imaging with no contact needed between the probe and tissue. OCT is FDA-approved for clinical use in imaging the eye and the coronary arteries. The inner ear is another obvious use for this optical imaging technique because the volume of tissue responsible for hearing loss and bal-

Image Credit

Photo illustration created by HDIAC and adapted from U.S. Marines photo by Cpl. Gabino Perez (Available for viewing at: <https://www.marines.mil/Photos/igphoto/2002059237/>), U.S. Army photo by Sgt. Justin Geiger (Available for viewing at <http://www.eucom.mil/media-library/Article/35827/us-soldiers-hone-explosive-capabilities-at-saber-strike-17>), and Adobe Stock.

ance disorders is very small, it is surrounded by clear fluid, and it is easily damaged by invasive methodologies.

We have adapted this modern optical technique not only to visualize inner ear structures like the auditory portion, the cochlea, but also to measure vibrations of the inner ear structures using a technique called vibrometry that determines how well the cochlea is functioning (see Figure 1). Images taken with OCT clearly show the three compartments of the cochlea (scala vestibuli [SV], scala media [SM] and scala tympani [ST]), Reissner's membrane (RM) that separates SV from SM, along with the gross anatomical structure of the Organ of Corti (tectorial membrane [TM], reticular lamina and basilar membrane [BM]), where the primary receptors for sound—the hair cells—reside (see Figure 1B). Additionally, vibrometry of different Organ of Corti structures (e.g., BM and TM) show the sharp tuning and large gains of cochlear amplification (see Figure 1C and D; BM: 62.3 ± 0.6 dB, TM: 65.3 ± 0.5 dB, $n=3$, 11 kHz). Using OCT, we can now diagnose changes that happen in the cochlea in response to blast injury or noise-exposure.

Blast- and Noise-induced Models of Hearing Loss

The cochlea is the body's most sensitive pressure transducer because it houses the hair cells, which use their receptor organelle, the hair bundle, to transduce mechanical energy from pressure waves into electrochemical signals. There are two types of hair cells: inner hair cells (IHCs) and outer hair cells (OHCs). IHCs send sensory information to the brain, while OHCs amplify and tune the response of the ear. OHCs are highly mechanosensitive and easily damaged by loud sounds that result in strong pressure waves in the ear. Therefore, the classical explanation for hearing loss due to blast or noise exposure is trauma to the hair cells. Hair cell death occurs through a variety of pathways [9, 10] that result in permanent hearing loss, which can be measured as elevated auditory thresholds.

However, an additional mechanism of noise-induced hearing loss, known as cochlear synaptopathy, also occurs. Synaptopathy results in reduced communication between the hair cell and its afferent nerve fiber either via a decrease in the number of communication sites, known as synapses, or a degeneration of the postsynaptic auditory nerve fiber. The mechanism of synaptopathy is thought to be primarily due to an excess release of the hair

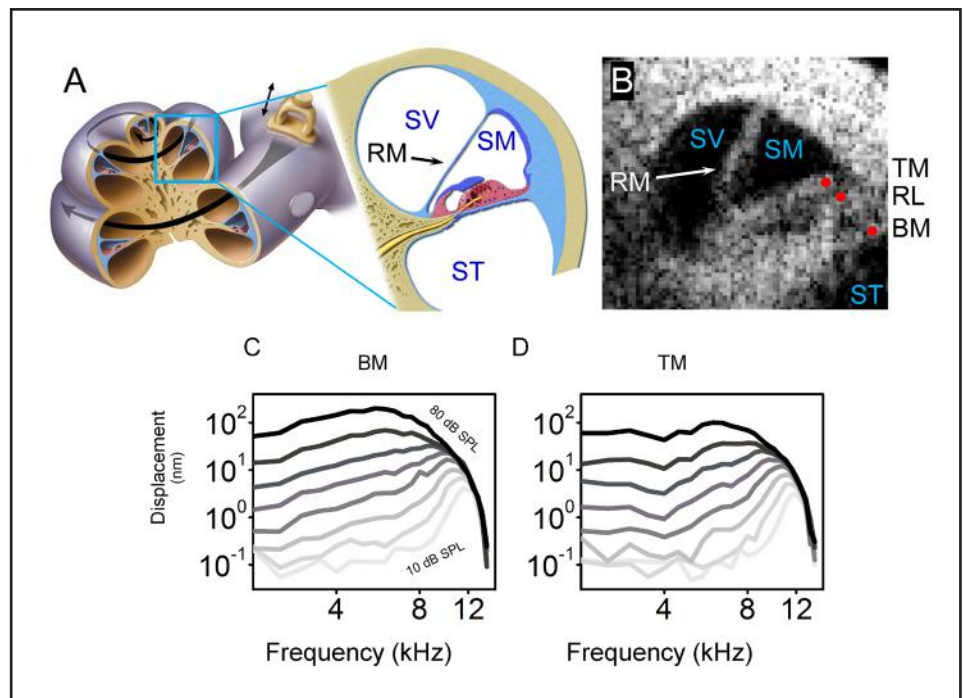


Figure 1. Optical coherence tomography and vibrometry in the mouse cochlea. (A) Illustration of a cross-sectional view of the cochlea, with expanded view of the apical turn where this data was collected. SV, scala vestibuli; SM, scala media; ST, scala tympani; RM, Reissner's membrane. (B) Cross-sectional OCT image of the mouse cochlea. Red dots highlight common locations for vibrometry measurements. TM, tectorial membrane; RL, reticular lamina; BM, basilar membrane. Vibratory responses from (C) BM and (D) TM in the live mouse cochlea shown in (B) display tuned responses centered near the BF (best frequency ~12 kHz). Adapted from [22].

cell afferent neurotransmitter, glutamate, after hair cell overstimulation, or secondarily to extracellular adenosine 5'-triphosphate (ATP) release from other traumatized cells, which leads to Ca^{2+} channel activation [11, 12]. This results in the toxic entry of ions and water into synaptic boutons [13–15], which damages the dendrite and produces loss of synaptic ribbons, the presynaptic components of hair cells [16–18]. Loss of synapses and auditory neurons does not necessarily elevate the threshold of hearing, but instead affects neural encoding at higher sound intensities, so it has been called "hidden" hearing loss [19]. There are no effective medical treatments to prevent hearing loss via either mechanism after traumatic noise exposure.

As with noise, inner ear damage from improvised explosive devices, which causes a primary blast injury, results from the direct effect of the high pressure wave upon the tissue [20]. To determine if the etiology of blast-wave exposure matched that of noise exposure, we custom-built a blast chamber to deliver blast waves to mice (see Figure 2A–D). This system is pressurized with compressed air, which when released, produces a single compression wave that travels down a metal tube and develops a shock front that creates

a blast wave by the time it reaches the mouse. Our chamber could generate peak pressures of up to 186 kPa, corresponding to a sound intensity of 199 dB SPL (sound pressure level) at the position of the mouse [21].

OCT Can Diagnose Dynamic Changes in the Inner Ear

Equipped with OCT as a diagnostic tool, a 2018 study showed that dynamic inner ear changes due to blast trauma could be elucidated [22]. Serially imaging the cochlea of anesthetized mice exposed to a single blast wave approximating that of a roadside bomb (peak pressures 130 ± 9 kPa [~ 196 dB SPL], see Figure 2E) showed that during the first three hours after the blast, there was progressive bulging of Reissner's membrane—consistent with an increase in endolymph volume, or endolymphatic hydrops [23] (see Figure 3A). By one day after the blast, Reissner's membrane returned to a normal position where it remained for at least one week (see Figure 3B–D). In contrast, unexposed control mice demonstrated no change in Reissner's membrane (see Figure 3E), indicating that OCT imaging does not cause endolymphatic hydrops. Following euthanasia, Reissner's membrane progressively shifted inward (see Figure 3F), consistent with

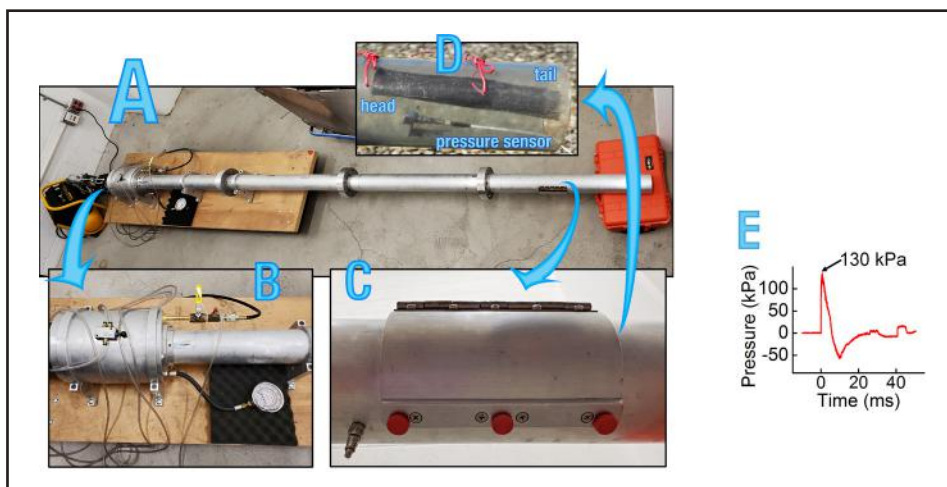


Figure 2. The blast chamber. (A) A picture of the blast chamber. (B) A zoom in of the blast chamber and pressure gauge. (C) A close up of the end of the blast tube, which houses the mouse and (D) the protective sheath and the pressure sensor. (E) The blast wave pressure monitored by a sensor positioned just below the mouse.

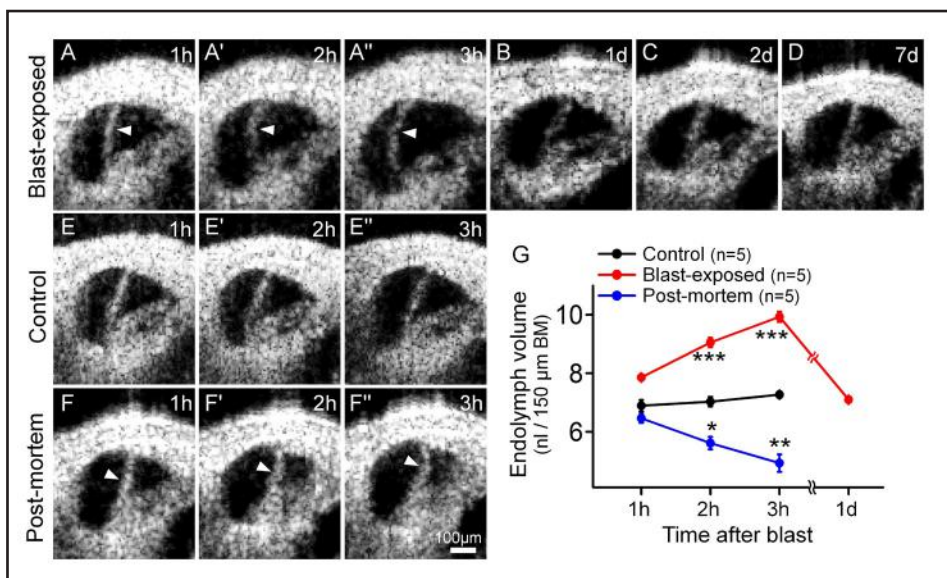


Figure 3. Blast exposure produces transient endolymphatic hydrops. (A) Endolymphatic hydrops progressively developed within the first three hours after blast exposure. Images are from one representative mouse. (B–D) OCT images from different representative mice showed normal endolymph volume one, two and seven days after blast exposure. (E) OCT images from a representative live control mouse over three hours demonstrated normal endolymph volume. (F) OCT images from an unexposed control mouse followed for three hours after euthanasia demonstrated progressive reductions of endolymph volume. (G) Scala media volume over time in blast-exposed mice, living control mice, and unexposed control mice post-mortem. * $P < 0.05$, ** $P < 0.01$, *** $P < 0.001$. Adapted from [22].

reduced endolymph secretion by the stria vascularis post-mortem [24, 25]. Quantifying endolymph volume within scala media confirmed OCT is able to assess dynamic endolymphatic fluid volume changes (see Figure 3G). Furthermore, because the presence of endolymphatic hydrops is indicative of a change in osmotic balance of the cochlea, we looked for further damage in the ear that might cause, or result from, this imbalance.

After visualizing gross morphological changes in live mice after blast trauma, Kim et al. [22]

used *in vitro* microscopy techniques with finer resolution to visualize cells and their different structures. High-resolution, scanning electron microscopy revealed immediate hair bundle damage in the cochlear base (see Figure 4A–B) that was not present in unexposed control animals. Labeling hair cells in the cochlea with fluorescent markers showed bundle damage was followed by outer hair cell loss one week post blast exposure (see Figure 4C–D). In contrast to the localized loss of outer hair cells, ribbon synapses were lost throughout the cochlea seven days after the blast (see Figure

4E–H). These two different patterns of damage highlight the distinct mechanisms underlying hair cell death and neuronal trauma [21, 22]. The pattern of basal hair cell loss is well-established and is due to the large forces applied to the stereociliary bundles [10, 26]. Because there is no obvious explanation for why the pattern of neuronal damage did not match that of the hair cells, Kim et al. [22] hypothesized that the former was due to the endolymphatic hydrops that developed.

Osmotic Imbalance Leads to Cochlear Synaptopathy

To test if endolymphatic hydrops caused synaptopathy throughout the cochlea, Kim et al. [22] applied the simple chemical principles of osmosis and diffusion. Application of varying tonicity solutions to the middle ear draws fluids into or out of the perilymphatic and endolymphatic spaces within the fluid-filled cochlea (see Figure 5A). Such fluid application is a safe clinical technique [27–29]. A solution with fewer solutes than that found in perilymph and endolymph (hypotonic) would force water into the cochlea, which should result in endolymphatic hydrops. In contrast, a hypertonic solution, i.e., a solution that has a higher solute concentration than perilymph and endolymph, should drain fluids from the inner ear via osmosis. This is what is needed to reverse endolymphatic hydrops. Solutions with a similar salt concentration as body fluids, normotonic solutions, should not change the endolymph volume.

Applying a hypotonic solution for 5.5 hours did indeed induce endolymphatic hydrops in mice (see Figure 5B). Furthermore, measuring cochlear function using the vibrometry aspect of OCT showed that these mice had normal vibratory responses (see Figure 5C–D). Therefore, isolated endolymphatic hydrops (i.e., not associated with mechanical trauma of stereociliary bundles) does not alter the OHC-based mechanical response. However, synaptic ribbon counts were reduced after the hypotonic challenge to a level similar to that found after blast exposure even though there was no loss of OHCs ($n=4$) (see Figure 5E–G). Thus, endolymphatic hydrops in isolation causes cochlear synaptopathy.

The Mechanism of Synaptopathy After Trauma is Similar in the Ear and Brain

Excitotoxicity—the toxic effects of too much neurotransmitter release due to overstimulation—is a known mechanism for synaptopathy,

not only in the cochlea [13–16], but also in the central nervous system after traumatic brain injury (TBI) [30] and likely blast-induced neurotrauma seen in military personnel [31]. Kim et al. [22] tested if this was the mechanism underlying hydrops-induced synaptopathy in the cochlea. For these studies, a more direct method (perilymphatic perfusion of either normotonic or hypotonic artificial perilymph over one hour) was used to cause endolymphatic hydrops and study both the pre- (using CtBP2 immunolabeling) and post-synaptic (using Homer immunolabeling [32]) sides of the IHC synapse (see Figure 6). Mice perfused with hypotonic perilymph again developed hydrops and had reduced CtBP2 and Homer puncta counts that were less well co-localized. In these mice, the CtBP2 and Homer puncta counts and co-localization could be preserved by mitigating the effects of the released neurotransmitters by blocking the postsynaptic AMPA glutamate receptor with the drug, CNQX (see Figure 6E). Thus, blocking hydrops-induced excitotoxicity is a viable means of protecting synapses. However, because blocking synaptic transmission can have deleterious side effects [33], we searched for a simpler therapeutic.

Osmotic Stabilization as a Treatment for Blast Injury

By causing endolymphatic hydrops with a hypotonic solution, Kim et al. [22] hypothesized that endolymphatic hydrops could be reversed using a hypertonic solution applied to the middle ear. Furthermore, because synaptopathy resulted from hydrops, neutralizing the osmotic imbalance should prevent it. To test if endolymphatic hydrops could be reversed, OCT images were taken three hours after blast-exposure when endolymphatic hydrops had developed. Addition of hypertonic, artificial perilymph to the middle ear did reverse endolymphatic hydrops, but normotonic saline did not (see Figure 7A–C). Next, OHCs and synapses were assessed to see if hypertonic saline could protect from outer hair cell loss and synaptopathy. After blast exposure, the hypertonic solution was applied to the round window, and two months later, hair cells and synapses were counted throughout the cochlea (see Figure 7D–F).

While unexposed control mice had no OHC loss, blast-exposed mice that were not treated with the hypertonic solution had substantial OHC loss in the cochlear base, scattered loss in the middle, and no loss in the apex. Hair cell counts were the same in these untreated ears and those treated with normotonic or hypertonic saline (see Figure 7G). There were sub-

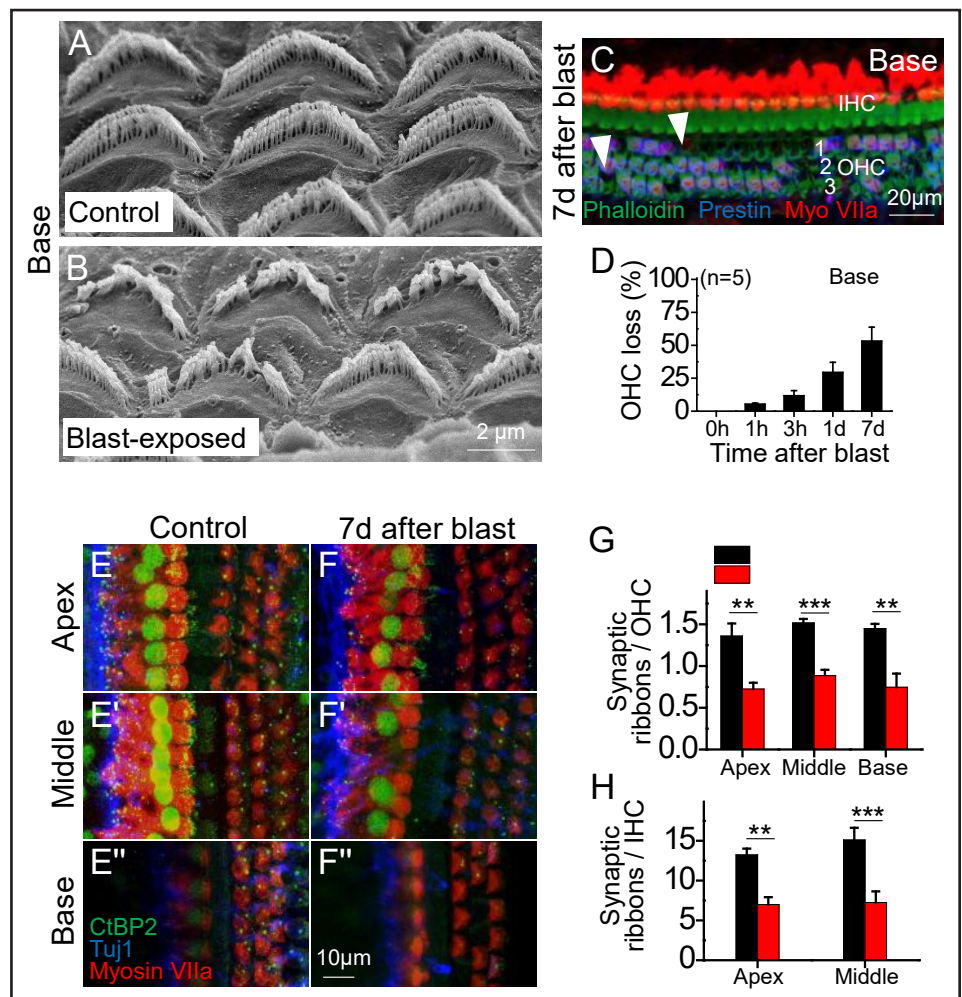


Figure 4. Blast exposure causes stereociliary trauma, hair cell loss, and cochlear synaptopathy. (A, B) Scanning electron microscopic images of OHC stereociliary bundles in representative control and blast-exposed mice. (C) The cochlear epithelium seven days after blast exposure. Immunolabeling was done to visualize all hair cells (Myosin VIIa) and outer hair cells (OHCs) (Prestin). Representative locations of missing hair cells are shown (arrowheads). (D) Quantification of OHC loss seven days after blast exposure in the basal regions. (E, F) The cochlear epithelium seven days after blast exposure. Immunolabeling was done to visualize synaptic ribbons in hair cells (CtBP2), hair cells (Myosin VIIa), and auditory neurons (Tuj1). (G, H) Quantification of synaptic ribbons per OHC and IHC in control and blast-exposed mice. $**P < 0.01$, $***P < 0.001$. Adapted from [22].

stantial reductions in the number of synaptic ribbons per OHC and IHC in untreated ears and in ears treated with normotonic artificial perilymph (see Figure 7H–I). However, treatment with the hypertonic solution prevented most of this synaptic loss. Thus, hypertonic treatment of post-traumatic endolymphatic hydrops preserved roughly half the synaptic ribbons that would have been lost without treatment, but had no impact on OHC loss.

Discussion

The data presented in Kim et al. [22] reveal several fundamental mechanisms that underlie blast-induced sensorineural hearing loss (see Figure 8). The most significant finding of Kim et al. [22] is that osmotically stabilizing the cochlear fluids after the blast exposure

prevents cochlear synaptopathy, even though hair cell fate remains unchanged [22, 34]. The initiating step of the problem is the mechanically induced trauma to the OHC stereociliary bundle. The fate of these traumatized OHCs is set immediately and is not changed by any of the tested interventions. Clearly, there is a need for further research to understand how to preserve hair cells after traumatic events. As it is now feasible to integrate high-throughput expression analysis data from independent experiments [35], perhaps studying expression differences when comparing hair cells that survive after bundle damage [36] against those hair cells that succumb to bundle damage [22] could elucidate the molecular causes of hair cell degeneration.

In contrast to the fate of the hair cells, cochlear

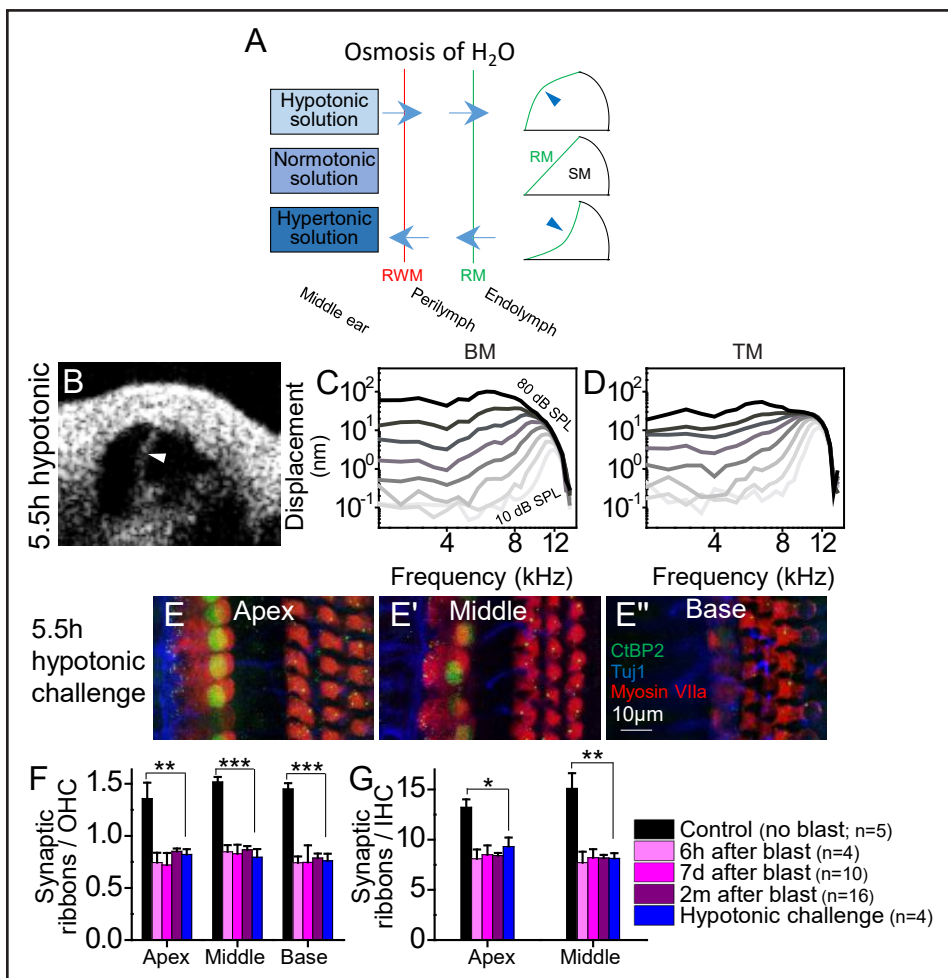
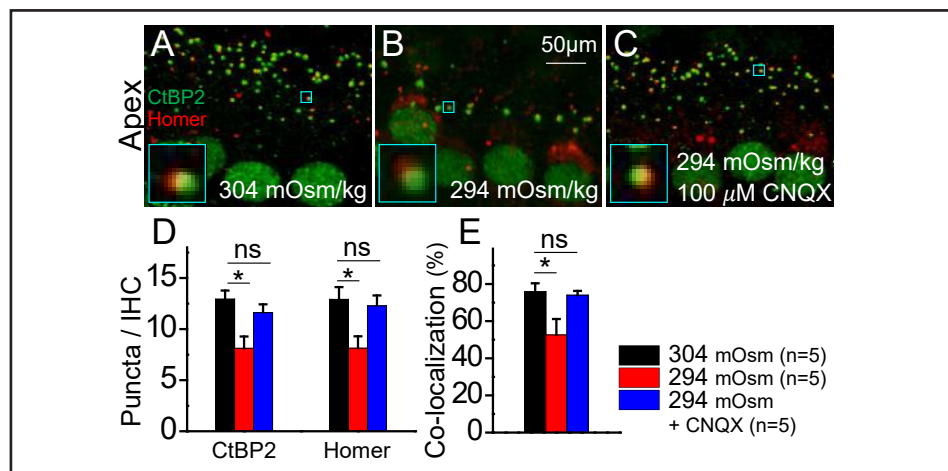


Figure 5. Osmotic insult can lead to endolymphatic hydrops and cochlear synaptopathy. (A) A simple model of non-invasive osmotic challenge via the round window membrane (RWM) to alter the volume of endolymph and shift Reissner's membrane (RM). Hypotonic solution applied to the middle ear causes endolymphatic hydrops whereas hypertonic solution reduces endolymphatic volume. Normotonic solution has no effect. **(B–D)** A representative mouse cochlea with endolymphatic hydrops induced by the application of hypotonic challenge to the middle ear. Vibratory responses for both the BM and TM were normal. **(E)** The cochlear epithelium harvested from a mouse with endolymphatic hydrops induced by hypotonic challenge to the middle ear. **(F, G)** Endolymphatic hydrops caused a loss of synaptic ribbons similar to that found after blast exposure. * $P < 0.05$, ** $P < 0.01$, *** $P < 0.001$. Adapted from [22].

the post-traumatic endolymphatic hydrops over-stimulates them or because nearby damaged cells release ATP that creates calcium waves across the epithelium [12, 38]. The excitotoxicity of excess glutamate causes ion and H₂O entry into synaptic boutons, and this swelling is associated with either temporary or permanent damage [13–15]. Finally, the loss of the bouton leads to loss of synaptic ribbons inside the hair cell [16]. Because synapse loss was reduced with a blocker of excitotoxicity, this suggests that antiexcitotoxic therapies like those used for TBI [37] may also prevent cochlear synaptopathy after blast injury.



The results of our study also suggest a novel treatment for blast-induced trauma that will protect warfighters from hidden hearing loss, for which there is currently no reliable and validated diagnostic test [39]. Osmotically stabilizing the inner ear after noise exposure may offer an important therapeutic approach to preserve hearing. We show that treatment is efficacious in mice using a middle ear injection technique that is commonly used in the clinic and could be used on the battlefield as it only requires a concentrated salt solution in an ear drop. Similarly, such injections may be an alternative treatment for vestibular diseases, like Meniere's disease, in which endolymphatic hydrops causes episodic vertigo, fluctuating hearing loss, and roaring tinnitus [23, 40–43], negatively impacting a patient's quality of life. Future work may seek to reveal the exact molecular mechanism underlying the permanent cochlear synaptopathy. To this end, noise-exposure models that we showed also develop endolymphatic hydrops can be used to understand if both modalities of inner ear trauma have similar etiologies [22] and to create more targeted interventions that allow hearing pres-

Figure 6. Excitotoxic block prevents cochlear synaptopathy induced by hydrops. (A–C) The cochlear epithelium harvested from representative mice perfused for 1 hour with 304 mOsm (A), 294 mOsm (B), or 294 mOsm + 100 μM CNQX (C) artificial perilymph. Immunolabeling was done to visualize pre-synaptic ribbons in IHCs (CtBP2) and post-synaptic auditory nerve boutons (Homer). Co-localization of the pre- and post-synaptic terminals is shown (insets). **(D)** Hypotonic challenge reduced CtBP2 and Homer counts. Blocking glutamate with CNQX preserved both the pre- and post-synaptic terminals. * $P < 0.05$; ns, not significant. **(E)** Hypotonic challenge reduced the rate of CtBP2 and Homer co-localization; this effect was also reversed with CNQX. Adapted from [22].

synaptopathy has a delayed-onset involving several steps. First, endolymphatic hydrops occurs, likely because K⁺ is not removed fast enough from the endolymph after stereociliary trauma. We showed that this, like brain ede-

ma after TBI, can be treated by osmotic stabilization—protecting from further symptoms that may occur downstream or concomitantly [22, 37]. Next, hair cells release excess neurotransmitters, which may occur because

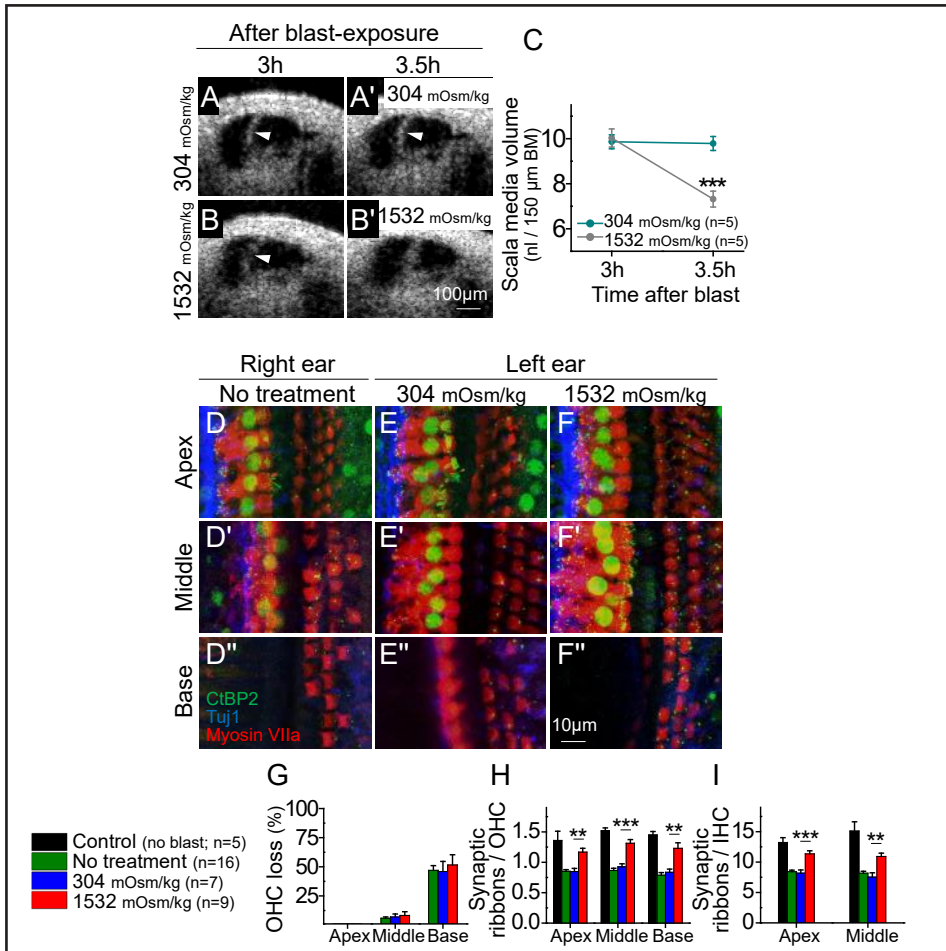


Figure 7. Osmotic treatment of endolymphatic hydrops partially rescues synaptic ribbon loss after blast exposure. (A, B) Representative mice were treated with normotonic or hypertonic challenge three hours after blast exposure. Repeat images were taken 30 minutes later. **(C)** Normotonic artificial perilymph had no impact on post-traumatic endolymphatic hydrops whereas hypertonic artificial perilymph normalized endolymphatic volume. **(D–F)** The cochlear epithelium from representative mice two months after blast exposure. Mice had either no treatment **(D)**, normotonic, artificial perilymph application to the middle ear after the blast **(E)**, or hypertonic, artificial perilymph application to the middle ear after the blast **(F)**. Immunolabeling was done to visualize synaptic ribbons in hair cells (CtBP2), hair cells (Myosin VIIa), and auditory neurons (Tuj1). **(G–I)** Quantification of OHC loss and synaptic ribbons per OHC and IHC. Hypertonic artificial perilymph reduced the loss of synaptic ribbons but did not affect the degree of OHC loss. ** $P < 0.01$, *** $P < 0.001$. Adapted from [22].

ervation in stressful environments.

While Kim et al. [22] focused on changes within the cochlea for which interventions are not currently available, blast exposure can also result in disruption of structures peripheral to the cochlea like the middle ear ossicles and the tympanic membrane. Such trauma results in conductive hearing disorders. Disruption of the ossicular chain is commonly treated with ossicular reconstructive surgery to restore hearing.

However, the outcomes vary greatly. While the variation is not entirely understood, an accepted contributing factor is the choice of the length of the prostheses [44, 45]. However, there is currently no imaging technology that can provide pre-operative or intra-operative quantitative guidance on optimal prosthetic length. Scar tissue formation around the prosthesis can also adversely affect hearing outcomes, and there is no reliable way to identify this problem. Therefore, if the outcome is poor it is often difficult to determine the cause and whether a revision surgery is indicated [46].

Because OCT has both the spatial and temporal resolution to measure the morphological features and function of the ear, it may provide this much needed diagnostic ability in humans, leading to better outcomes and lower health care costs. The challenge with utilizing OCT for interrogating the middle ear space is access, which requires adaptations in the current hardware so that entry can be gained through the ear canal or Eustachian tube. Thus, continuing technological advancements on the OCT system can lead to better diagnostics that can swiftly impact and improve clinical care of warfighters after blast injury.

References

- Dougherty, A. L., MacGregor, A. J., Han, P. P., Viirre, E., Heltemes, K. J., & Galarneau, M. R. (2013). Blast-related ear injuries among U.S. military personnel. *Journal of Rehabilitation Research & Development*, 50(6), 893–904. doi:10.1682/JRRD.2012.02.0024
- Helfer, T. M., Jordan, N. N., & Lee, R. B. (2005). Postdeployment hearing loss in U.S. Army soldiers seen at audiology clinics from April 1, 2003, through March 31, 2004. *American Journal of Audiology*, 14(2), 161–168. doi:10.1044/1059-0889(2005)018
- Cave, K. M., Cornish, E. M., & Chandler, D. W. (2007). Blast injury of the ear: clinical update from the global war on terror. *Military Medicine*, 172(7), 726–730. doi:10.7205/MILMED.172.7.726
- Pleis, J. R., & Lethbridge-Cejku, M. (2006). Summary health statistics for U.S. adults: National Health Interview Survey, 2005. *Vital Health Statistics* 10(232), 1–153.
- Muzaffar, S. J., Orr, L., Rickard, R. F., Coulson, C. J., & Irving, R. M. (2018). Mitigating noise-induced hearing loss after blast injury. *Trauma*, 1–7. doi:10.1177/146040861875519
- Yankaskas, K. (2013). Prelude: noise-induced tinnitus and hearing loss in the military. *Hearing Research*, 295, 3–8. doi:10.1016/j.heares.2012.04.016
- Huang, D., Swanson, E. A., Lin, C. P., Schuman, J. S., Stinson, W. G., Chang, W., ... Puliafito, C. A., et al (1991). Optical coherence tomography. *Science*, 254(5035), 1178–1181. doi:10.1126/science.1957169
- Izatt, J. A., Kulkarni, M. D., Wang, H. W., Kobayashi, K., & Sivak, M. V. (1996). Optical coherence tomography and microscopy in gastrointestinal tissues. *IEEE Journal of Selected Topics in Quantum Electronics*, 2(4), 1017–1028. doi:10.1109/2944.577331
- Yang, C. H., Schrepfer, T., & Schacht, J. (2015). Age-related hearing impairment and the triad of acquired hearing loss. *Frontiers in Cellular Neuroscience*, 9(276), 1–12. doi:10.3389/fncel.2015.00276
- Furness, D. N. (2015). Molecular basis of hair cell loss. *Cell and Tissue Research*, 361(1), 387–399. doi:10.1007/s00441-015-2113-z
- Mammano, F., Frolenkov, G. I., Lagostena, L., Belyantseva, I. A., Kurc, M., Dodane, V., ... Kachar, B. (1999). ATP-Induced Ca(2+) release in cochlear outer hair cells: localization of an inositol triphosphate-gated Ca(2+) store to the base of the sensory hair bundle. *Journal of Neuroscience*, 19(16), 6918–6929. doi:10.1523/JNEUROSCI.19-16-06918.1999
- Piazza, V., Ciubotaru, C. D., Gale, J. E., & Mammano, F. (2007). Purinergic signalling and intercellular Ca2+ wave propagation in the organ of Corti. *Cell Calcium*, 41(1), 77–86. doi:10.1016/j.ceca.2006.05.0011
- Pujol, R., & Puel, J. L. (1999). Excitotoxicity, synaptic repair, and functional recovery in the mammalian cochlea: a review of recent findings. *Annals of the New York Academy of Sciences*, 884, 249–254. doi:10.1111/j.1749-6632.1999.tb08646.x
- Mayer, M. L., & Westbrook, G. L. (1987).

- Cellular Mechanisms Underlying Excitotoxicity. *Trends in Neurosciences*, 10(2), 59–61. doi:10.1016/0166-2236(87)90023-3
15. Choi, D. W., & Rothman, S. M. (1990). The role of glutamate neurotoxicity in hypoxic-ischemic neuronal death. *Annual Review of Neuroscience*, 13, 171–182. doi:10.1146/annurev.ne.13.030190.001131
 16. Moser, T., & Starr, A. (2016). Auditory neuro-pathy—neural and synaptic mechanisms. *Nature Reviews Neurology*, 12(3), 135–149. doi:10.1038/nrneurol.2016.10
 17. Lin, H. W., Furman, A. C., Kujawa, S. G., & Liberman, M. C. (2011). Primary neural degeneration in the Guinea pig cochlea after reversible noise-induced threshold shift. *Journal of the Association for Research in Otolaryngology*, 12(5), 605–616. doi:10.1007/s10162-011-0277-0
 18. Kujawa, S. G., & Liberman, M. C. (2009). Adding insult to injury: cochlear nerve degeneration after "temporary" noise-induced hearing loss. *Journal of Neuroscience*, 29(45), 14077–14085. doi:10.1523/JNEUROSCI.2845-09.2009
 19. Schaeffe, R., & McAlpine, D. (2011). Tinnitus with a normal audiogram: physiological evidence for hidden hearing loss and computational model. *Journal of Neuroscience*, 31(38), 13452–13457. doi:10.1523/JNEUROSCI.2156-11.2011
 20. Garner, J., & Brett, S. J. (2007). Mechanisms of injury by explosive devices. *Anesthesiology Clinics*, 25(1), 147–160. doi:10.1016/j.anclin.2006.11.002
 21. Cho, S. I., Gao, S. S., Xia, A., Wang, R., Salles, F. T., Raphael, P. D., . . . Oghalai, J. S. (2013). Mechanisms of hearing loss after blast injury to the ear. *PLoS One*, 8(7), e67618. doi:10.1371/journal.pone.0067618
 22. Kim, J., Xia, A., Grillet, N., Applegate, B. E., & Oghalai, J. S. (2018). Osmotic stabilization prevents cochlear synaptopathy after blast trauma. *Proceedings of the National Academy of Sciences*, 115(21), E4853–E4860. doi:10.1073/pnas.1720121115
 23. Schuknecht, H. F. (1993) *Pathology of the ear*, 2nd Ed. Malvern, PA: Lea & Febiger.
 24. Zdebik, A. A., Wangemann, P., & Jentsch, T. J. (2009). Potassium ion movement in the inner ear: insights from genetic disease and mouse models. *Physiology (Bethesda)*, 24, 307–316. doi:10.1152/physiol.00018.2009
 25. Patuzzi, R. (2011). Ion flow in stria vascularis and the production and regulation of cochlear endolymph and the endolymphatic potential. *Hearing Research*, 277(1-2), 4–19. doi:10.1016/j.heares.2011.01.010
 26. Liu, C. C., Gao, S. S., Yuan, T., Steele, C., Puria, S., & Oghalai, J. S. (2011). Biophysical mechanisms underlying outer hair cell loss associated with a shortened tectorial membrane. *Journal of the Association for Research in Otolaryngology*, 12(5), 577–594. doi:10.1007/s10162-011-0269-0
 27. Oghalai, J. S., Tonini, R., Rasmus, J., Emery, C., Manolidis, S., Vrabc, J. T., & Haymond, J. (2009). Intra-operative monitoring of cochlear function during cochlear implantation. *Cochlear Implants International*, 10(1), 1–18. doi:10.1002/cii.372
 28. Cooper, N. P., & Rhode, W. S. (1996). Fast travelling waves, slow travelling waves and their interactions in experimental studies of apical cochlear mechanics. *Auditory Neuroscience*, 2(3), 207–217.
 29. Wenzel, G. I., Xia, A., Funk, E., Evans, M. B., Palmer, D. J., Ng, P., . . . Oghalai, J. S. (2007). Helper-dependent adenovirus-mediated gene transfer into the adult mouse cochlea. *Otology & Neurotology*, 28(8), 1100–1108.
 30. Margulies, S., Hicks, R., et al. (2009). Combination therapies for traumatic brain injury: prospective considerations. *Journal of Neurotrauma*, 26(6), 925–939. doi:10.1089/neu.2008-0794
 31. Cernak, I., & Noble-Haeusslein, L. J. (2010). Traumatic brain injury: an overview of pathobiology with emphasis on military populations. *Journal of Cerebral Blood Flow & Metabolism*, 30(2), 255–266. doi:10.1038/jcbfm.2009.203
 32. Martinez-Monedero, R., Liu, C., Weisz, C., Vyas, P., Fuchs, P. A., & Glowatzki, E. (2016). GluA2-containing AMPA receptors distinguish ribbon-associated from ribbonless afferent contacts on rat cochlear hair cells. *eNeuro*, 3(2). doi:10.1523/ENEURO.0078-16.2016
 33. Ikonomidou, C., & Turski, L. (2002). Why did NMDA receptor antagonists fail clinical trials for stroke and traumatic brain injury? *Lancet Neurology*, 1(6), 383–386. doi:10.1016/S1474-4422(02)00164-3
 34. Wallis, C. (2018, August 1). Ba-Boom! There goes your hearing. *Scientific American*, 319(2), 24. doi:10.1038/scientificamerican0818-24
 35. Hertzano, R., & Elkon, R. (2012). High throughput gene expression analysis of the inner ear. *Hearing Research*, 288(1-2), 77–88. doi:10.1016/j.heares.2012.01.002
 36. Jia, S., Yang, S., Guo, W., & He, D. Z. (2009). Fate of mammalian cochlear hair cells and stereocilia after loss of the stereocilia. *Journal of Neuroscience*, 29(48), 15277–15285. doi:10.1523/JNEUROSCI.3231-09.2009
 37. Kochanek, P. M., Jackson, T. C., Ferguson, N. M., Carlson, S. W., Simon, D. W., Brockman, E. C., . . . Dixon, C. E. (2015). Emerging therapies in traumatic brain injury. *Seminars in Neurology*, 35(1), 83–100. doi:10.1055/s-0035-1544237
 38. Chan, D. K., & Rouse, S. L. (2016). Sound-induced intracellular Ca²⁺ dynamics in the adult hearing cochlea. *PLoS One*, 11(12), e0167850. doi:10.1371/journal.pone.016785037
 39. Plack, C. J., Leger, A., Prendergast, G., Kluk, K., Guest, H., & Munro, K. J. (2016). Toward a Diagnostic Test for Hidden Hearing Loss. *Trends in Hearing*, 20. doi:10.1177/2331216516657466
 40. Sajjadi, H., & Paparella, M. M. (2008). Meniere's disease. *Lancet*, 372(9636), 406–414. doi:10.1016/S0140-6736(08)61161-7
 41. Schuknecht, H. F. (1976). Pathophysiology of endolymphatic hydrops. *European Archives of Otorhinolaryngology*, 212(4), 253–262.
 42. Salt, A. N., & Plontke, S. K. (2010). Endolymphatic hydrops: pathophysiology and experimental models. *Otolaryngologic Clinics of North America*, 43(5), 971–983. doi:10.1016/j.otc.2010.05.007
 43. Valk, W. L., Wit, H. P., Segenhout, J. M., Dijk, F., van der Want, J. J., & Albers, F. W. (2005). Morphology of the endolymphatic sac in the guinea pig after an acute endolymphatic hydrops. *Hearing Research*, 202(1-2), 180–187. doi:10.1016/j.heares.2004.10.010
 44. Morris, D. P., Bance, M., van Wijhe, R. G., Kieffe, M., & Smith, R. (2004). Optimum tension for partial ossicular replacement prosthesis reconstruction in the human middle ear. *Laryngoscope*, 114(2), 305–308. doi:10.1097/00005537-200402000-00024
 45. Ulku, C. H., Cheng, J. T., Guignard, J., & Rosowski, J. J. (2014). Comparisons of the mechanics of partial and total ossicular replacement prostheses with cartilage in a cadaveric temporal bone preparation. *Acta Oto-Laryngologica*, 134(8), 776–784. doi:10.3109/00016489.2014.898187
 46. Stone, J. A., Mukherji, S. K., Jewett, B. S., Carrasco, V. N., & Castillo, M. (2000). CT evaluation of prosthetic ossicular reconstruction procedures: what the otologist needs to know. *Radiographics*, 20(3), 593–605. doi:10.1148/radiographics.20.3.g00ma03593



Patricia M. Quiñones, Ph.D.
Postdoctoral Scholar, University of Southern California

Patricia M. Quiñones recently joined the laboratory of Dr. Oghalai as a postdoctoral scholar at USC. She received her Ph.D. at UCLA studying hair cell synaptic release. Her research interests include understanding the diverse mechanisms underlying signal transduction in the auditory and vestibular systems that arise from the heterogeneity found in different species. She is also interested in fostering diversity in higher education through mentorship, teaching and outreach.



Brian E. Applegate, Ph.D.
Associate Professor of Biomedical Engineering, Texas A&M University

Brian Applegate received his Ph.D. in chemistry from Ohio State University. He won a National Institutes of Health postdoctoral fellowship award to continue his training at Duke University in biomedical engineering. Upon completing his fellowship, he joined the faculty of Texas A&M University where he is currently an Associate Professor of Biomedical Engineering. He is a recipient of the NSF Career award and a fellow of the Optical Society of America. His research interests are to develop novel biophotonic technologies and apply them to the diagnosis and monitoring of human disease.



John S. Oghalai, M.D.
Chair, University of Southern California Caruso Department of Otolaryngology - Head and Neck Surgery

John Oghalai is a board certified physician in both Otolaryngology – Head and Neck Surgery and Neurotology. His clinical expertise in diseases of the ear is internationally shared through his leading clinical surgical textbook (*Atlas of Neurotologic and Lateral Skull Base Surgery*, Springer) and over 120 research papers in scholarly journals. His research lab also receives grant funding from the National Institutes of Health to study and develop new treatments for hearing loss. As department chair, he passionately leads a team of over 120 members that share his dedication to providing empathetic patient care, performing scientific research to discover better treatments for disease, and educating the next generation of clinicians and scientists. Prior to coming to USC in 2017, he held faculty positions at Baylor College of Medicine and Stanford University.

Calendar of Events

January 2019

01/23 - 01/24 • San Diego, CA

M [Military Operational Medicine Symposium](#)

February 2019

02/05 - 02/07 • Redstone Arsenal, AL

HDS [Modern Threats: Surface-to-Air Missile Systems Conference](#)

02/13 - 02/15 • San Diego, CA

HDS [WEST 2019](#)

02/06 - 02/07 • Tampa, FL

HDS [Military Additive Manufacturing Summit & Tech Showcase](#)

March 2019

03/03 - 03/08 • Ventura, CA

CBRN [ChemBio Terrorism Defense: Detection, Countermeasures and Prevention of Chemical and Biological Threats](#)

03/26 • Alexandria, VA

B [Biometrics Institute U.S. Conference 2019](#)

03/26 - 03/28 • Scottsdale, AZ

B [Wearable Robotics](#)



Call for Papers

HDIAC is now accepting abstracts and articles for consideration for future publications. For more information, contact the Publications Team at publications@hdiac.org.

The HDIAC Journal is a quarterly publication, focusing on novel developments and technology in the Alternative Energy, Biometrics, CBRN Defense, Critical Infrastructure Protection, Cultural Studies, Homeland Defense and Security, Medical, and Weapons of Mass Destruction focus areas.

- Articles must be relevant to one of the eight focus areas and relate to Department of Defense applications.
- Articles should be submitted electronically as a Microsoft Word document.
- We require a maximum of 2,500 words.
- All submissions must include graphics or images (300 DPI or higher in JPG or PNG format) to accompany the article. Photo or image credit should be included in the caption.